Residual Chemical Fate and Transport Analysis (Task 2.1.5)

LOTT Clean Water Alliance
Reclaimed Water Infiltration Study

Technical Memorandum

OCTOBER 14, 2021

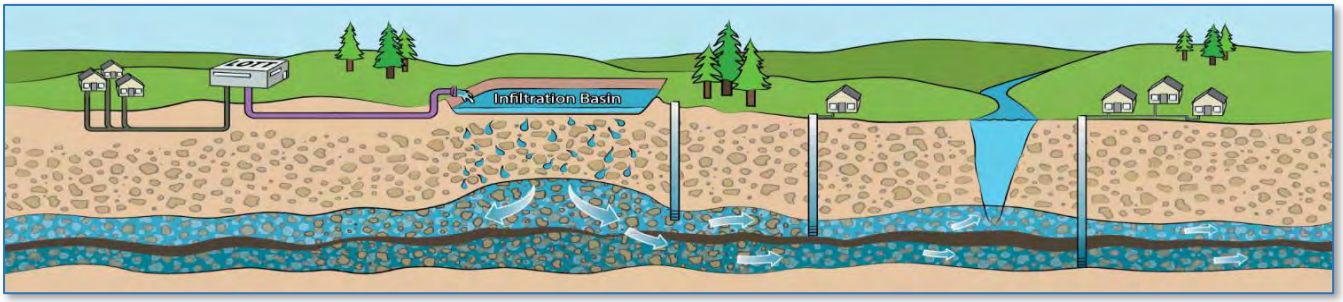

Prepared by

HDR

905 Plum Street SE, Suite 200
Olympia, WA 98501

Prepared for

LOTT Clean Water Alliance
Lacey • Olympia • Tumwater • Thurston County

500 Adams Street NE
Olympia, WA 98501

This page intentionally left blank.

Contents

Tables

Figures

Appendices

Acronyms and Abbreviations

AF	attenuation factor
AMSL	above mean sea level
BDOC	biodegradable dissolved organic carbon
BIRWP	Budd Inlet Reclaimed Water Plant
C/C_0	concentration divided by initial concentration
EPC	exposure point concentration
ft	feet
LOTT	LOTT Clean Water Alliance
MGD	million gallons per day
MGY	million gallons per year
MWRWP	Martin Way Reclaimed Water Plant
RWIS	Reclaimed Water Infiltration Study

SAT	soil aquifer treatment
USACE	United States Army Corp of Engineers
USGS	United States Geological Survey
WAC	Washington Administrative Code

1.0 Introduction

This technical memorandum documents the methodology and results of a fate and transport analysis of residual chemicals present in reclaimed water generated by the LOTT Clean Water Alliance (LOTT). This effort is part of LOTT's ongoing Reclaimed Water Infiltration Study (RWIS).

1.1 Background

LOTT provides services to treat and manage wastewater for the urban areas of Lacey, Olympia, and Tumwater in Thurston County, Washington (at the southern end of Puget Sound). Since 2006, LOTT has also produced reclaimed water at the Budd Inlet Reclaimed Water Plant (BIRWP) and Martin Way Reclaimed Water Plant (MWRWP) for irrigation and other non-drinking purposes. Some of the reclaimed water produced at the MWRWP is used to recharge (replenish) groundwater using rapid-infiltration basins on the LOTT Hawks Prairie Reclaimed Water Ponds and Recharge Basins (Hawks Prairie property). The long-range plan for meeting future wastewater needs includes expanding reclaimed water production and developing additional groundwater recharge facilities.

LOTT is conducting the RWIS to provide local scientific data and community input to help policymakers make informed decisions about future reclaimed water treatment and use. Residual chemicals are the primary focus of the study; these include household chemicals, pesticides/herbicides, pharmaceuticals, personal care products, cooking products, and flame retardants. LOTT is evaluating which of these residual chemicals remain in reclaimed water after treatment, which exist in the local environment, how infiltrated reclaimed water interacts with soils and local groundwater, and what happens to the residual chemicals over time in the environment. LOTT and the wider community will use the findings of the study to make the most appropriate choices for reclaimed water management and protection of public health and the environment.

As described in the RWIS scope of work (HDR 2014a), the study components include (bolded for the current task described in this document):

- Surface water, groundwater, and reclaimed water quality monitoring to determine water quality and evaluate occurrence and concentration of residual chemicals.
- Tracer testing at the LOTT Hawks Prairie property to identify dominant downgradient flow paths and travel times to monitoring wells as reclaimed water infiltrates the vadose zone to the water table and is then transported by groundwater.
- Groundwater flow and particle tracking modeling to estimate flow paths and travel time beyond the spatial and temporal extent identified through tracer testing and at a variety of recharge rates typical of future operational capacity of the reclaimed water recharge facility at Hawks Prairie.
- **Fate and transport groundwater modeling to estimate residual chemical concentrations to downgradient receptors at current and future reclaimed water aquifer recharge rates.**

- Risk assessment to understand potential human health and ecological risks posed by replenishing groundwater with reclaimed water.
- Cost/benefit analysis of various options for reclaimed water treatment.

1.2 Technical Memorandum Contents

The effort described in this technical memorandum is the fate and transport analysis to estimate exposure point concentrations (EPCs) at specific locations within the domain of the groundwater model constructed to support the work. For the most part, this effort followed the scope of services described in *Work Plan Groundwater Modeling Predictive Simulations (Task 2.1.4 continued) and Residual Chemical Fate and Transport (Task 2.1.5), Revised February 20, 2020* (HDR, 2020). However, some deviations from that plan occurred and additional subsurface stratigraphic and groundwater water level data were collected after the completion of Task 2.1.4 prior to completing the fate and transport modeling.

The changes to the modeling approach included:

- Converting the model from a steady state to transient model.
- Using the transient model to simulate historical recharge rates that occurred between 2006 and 2020.
- Simulating the projected recharge rates out to 2120.

Changes to the model itself included:

- Combining Layer 1 and Layer 2 into one layer to reduce instability that was causing long run times and numerical dispersion of simulated concentrations.
- Adjusting the area where the Kitsap Formation is simulated as being sandy.
- Adjusted effective porosity to better match materials identified in borings and geotechnical laboratory testing.
- Checked the model calibration and simulated travel times against the original calibration and to travel times seen during the tracer test.

The changes to the model and modeling approach are described as part of this document rather than updating previous documents.

The results of this work (i.e., the estimated EPCs) serve as inputs to the human health and ecological risk assessments.

2.0 Hydrogeologic Setting and Flow Modeling Refinements

A groundwater model was developed based on the prior investigations at the Hawks Prairie property and existing regional hydrostratigraphic information to simulate LOTT's recharge basins in operation, and ultimately to support fate and transport modeling to estimate EPCs of residual chemicals at specific locations within the model domain. The model development and flow model calibration are described in HDR 2019a. Revisions to the flow model, as described below, were undertaken based on recent (i.e., 2020) monitoring well installation and to facilitate contaminant fate and transport modeling. See Appendix A (provided as a separate document) for details regarding the six new monitoring wells installed in 2020.

The flow modeling uses the United States Geological Survey (USGS) groundwater flow model MODFLOW (Harbaugh, 2005), and the fate and transport modeling uses the USGS/USACE fate and transport model MT3DMS (Zheng, 1999). Originally the model simulated seven layers (HDR, 2019a); however, the upper two layers were mostly dry and, based on initial fate and transport modeling, caused instability resulting in prohibitively long model runtimes (on the order of months) and numerical dispersion problems where concentration above the source concentration were occurring in the model domain. Additionally, field investigations were conducted in the summer of 2020, and the new information from that program was also used in the model revisions. Three adjustments to the model were made to account for model challenges and the new field information:

- The calibrated model was changed from seven to six layers by combining model layers 1 and 2 (Qvr and Qvt). The resulting layer combined the thickness of the two layers and the new hydraulic conductivity was calculated as a thickness-weighted average hydraulic conductivity from the previous layers.
- Effective porosity of the Kitsap formation (layer 4) was increased based on soil sampling and the overall effective porosity was adjusted higher than previously estimated during the 2018 tracer test simulations and original model calibration. As discussed below, the results agree better with the tracer test and model calibration than the original model. Table 1 shows the original effective porosity and the effective porosity used in the current model,
- The Kitsap formation (upper) confining unit hydraulic conductivity was adjusted to account for an area of sandier material proximal to Hawks Prairie that is more permeable than the silt and clay that typically makes up the Kitsap formation. The area where the sandier material occurs was refined based on the new wells installed in 2020. Table 1 shows the original modeled hydraulic conductivity ranges and those used in the current model.

Table 1 - Changes to the Flow Model

Unit	Original Model Layer	Current Model Layer	Initial Effective Porosity	Current Effective Porosity	Original K Range	Current K Range
Qvr	1	1	10%	10%	0.07, 1, 7, 20, 80, 120, 200	2-7, 20, 80, 120, 200
Qvt	2		5%		1, 7, 20, 80, 120, 200	
Qva	3	2	5%	15%	0.07, 1, 3, 7, 10, 15, 20, 30, 50, 60, 80, 100, 120, 140, 200, 225	No Change
Qf	4	3	1%	7%	0.07, 0.2, 0.8, 1, 7, 10, 20, 80	0.05, 0.2, 0.8, **2,** 10, **30,** 80
Qc	5	4	10%	15%	0.5, 3, 10, 30, 80, 120, 500	No Change
TQu (lower confining unit)	6	5	5%	15%	0.07, 0.1, 7	No Change
TQu	7	6	10%	15%	7, 13, 23, 50, 75, 100	No Change

As discussed below, water levels, stream flows and travel times predicted by the revised model were compared to the observed data as well as the output from the original model configuration. The outcome of these comparison shows that the revised six-layer model generally predicts observed data similarly to, and at some locations better than, the original seven-layer model configuration.

2.1 Geologic and Hydrogeologic Setting Summary

The hydrostratigraphy within the model domain is represented by eight identified geologic units which comprise the model's hydrostratigraphy (see Table 2). The upper units are Holocene and Pleistocene glacial and post glacial porous media deposits. The deeper units are Pleistocene and Tertiary glacial and preglacial porous media deposits. The original model set-up details are described in HDR 2019a.

Table 2 - Hydrostratigraphy

Hydrostratigraphic Unit (Model Layer)	Description
Late Vashon Sediments in Woodland Creek Valley Qgof (1)	Sand/silt up to 100 feet thick, which forms an unconfined aquifer within the Woodland Creek Valley.
Alluvium and Vashon Recessional Gravel Outwash, Qvr (1)	Composed of alluvium and recessional glacial outwash sand and gravel which forms the unconfined aquifer.
Vashon Till, Qvt (1)	Dense unsorted silt, clay, sand and gravel ranging in thickness from absent to over 50 ft.

Hydrostratigraphic Unit (Model Layer)	Description
Vashon Advance Outwash, Qva (2)	Regional aquifer (aka Shallow Aquifer) composed of sand and gravel. The depth is generally less than 150 ft bgs..
Upper Confining Unit, Kitsap Formation, Qt (3)	Low-permeability silt, sand, and clay formation that is a regional Upper Confining Unit up to 150 ft thick between the Shallow Aquifer and the Sea-Level Aquifer.
Sea-Level Aquifer, Pre-Vashon Coarse Deposits, Qa (4)	Up to 100 ft thick sequence of coarse stratified sand and gravel forms a regional aquifer.
Lower Confining Unit, Tertiary Unconsolidated and Undifferentiated Sediments, TQu (5)	Unconsolidated and undifferentiated sediments include layers of clay, silt, sand and gravel of glacial and non-glacial.
Deep Aquifer, Tertiary Unconsolidated and Undifferentiated Sediments, TQu (6)	Layers of sand and gravel. The top of the coarse sediments of the deep aquifer between 350 and 530 feet bgs.

2.2 Calibrated Flow Model Summary

The new six-layer model was compared to the same measured water levels as the original seven-layer model. The calibration statistics for both model configurations are shown in Table 3 and the computed versus observed water levels are shown on Figure 1.

Table 3 - Calibration Statistics

Calibration Statistics	7 Layer Model	6 Layer Model
Computed to Observed R^2	0.9834	0.9814
Mean Error	-1.45	-0.06
Mean Absolute Error	4.22	4.07
Root Mean Squared Error	5.71	5.86

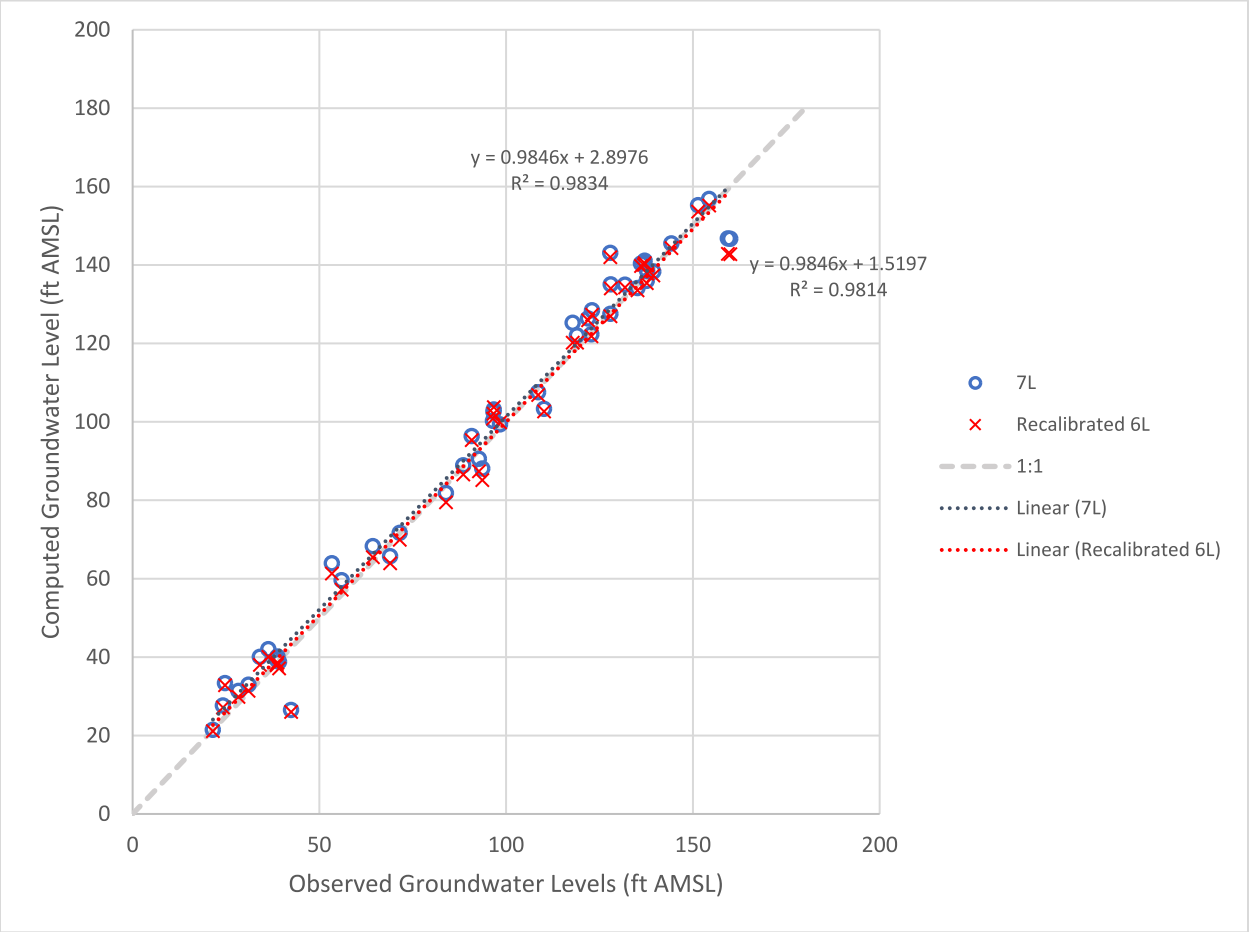

Figure 1 Computed Versus Observed Groundwater Elevations

2.3 Comparison to Tracer Test

Effective porosity was adjusted in the model due to the changes in hydraulic conductivity based on the new field investigation data and re-adjustment of the area of coarser Kitsap confining unit. The final effective porosity values used in the model were 0.1 for layer 1, 0.15 for layer 2, 0.07 for layer 3, and 0.15 for layers 4, 5 and 6. Backward particle tracking using the refined six-layer model was used to estimate the travel time from the water source (recharge) location to monitoring wells that are at and near the Hawks Prairie property where the tracer test was conducted in 2018. The computed travel times are comparable to the travel times identified during the tracer test based on tracer bromide arrivals at the wells. Table 4 shows the computed versus observed travel times.

Table 4 - Computed versus Observed Conservative Tracer Travel Times

Monitoring Well	Observed Travel Time (days)	Predicted Travel Time (days)
MW-3a	27	9
MW-6	ND	253
MW-11	177	110
MW-12	70	873
MW-13	63	59
MW-15	83	2
MW-16	37	1
MW-2	ND	3
MW-20	ND	235
MW-25	37	89
MW-27	32	34
MW-28	ND	426
MW-5	8	9
MW-8	30	26
MW-9	27	32

Shaded entries had computed travel times that were not consistent with the observed. These wells (MW-2, -12, -15 and -16) are within the recharge basin area but did not have arrivals for long periods of time during the tracer test, showing that local small scale heterogeneity influences where recharging water arrives at the water table and local groundwater flow direction. This is not expected to be a factor at locations further away from the recharge facility.

This page intentionally left blank.

3.0 Fate and Transport Modeling

Fate and transport modeling simulates the movement of constituents dissolved in groundwater. While being transported in the groundwater, the constituents are subjected to several processes that affect the concentration and location of the constituent. These processes include:

- *Advection* – transport in the direction of groundwater movement (downgradient).
- *Dispersion* – constituents moving with groundwater must follow complex pathways through the aquifer matrix material which serves to spread the constituent laterally and vertically, lowering the concentration similar to dilution.
- *Diffusion* – concentration gradients cause constituents to move from high concentration to low concentration. This serves to both spread constituents laterally and vertically and to cause constituents to enter dead-end pore spaces in the matrix, slowing downgradient transport.
- *Sorption* – interaction with portions of the aquifer matrix such as organic carbon and clay minerals cause constituents to adhere to the aquifer matrix material, slowing transport downgradient. The amount of sorption is dependent on specific chemicals' affinity to be sorbed to the specific aquifer material and the presence of that material in the aquifer.
- *Decay* – many constituents are subject to biological action from bacteria/archaea in the subsurface or may be altered by geochemical processes (e.g., through changes in oxidation reduction potential and pH). The bacteria metabolize the constituents and geochemical processes transform the constituents into new compounds, reducing the mass of the constituent in the aquifer. Decay is dependent upon the bacteria/archaea's ability to metabolize specific constituents and the presence of those bacteria/archaea in the aquifer or upon changes in the groundwater's geochemistry.

Advection and dispersion are processes that all constituents are subjected to and a constituent that is only subjected to these processes (such as the bromide used in the tracer test) are considered conservative tracers (meaning their movement is the same as the groundwater). Because there were many residual chemicals present in the reclaimed water that needed to be evaluated for consideration in the risk assessment, only advection and dispersion were simulated in the model. Attenuation factors (AFs) were then calculated using empirical data obtained during the 2018 tracer test and model results, as described below. An AF accounts for a residual chemical's specific diffusion, sorption, and decay, as reflected in observed data at the Hawks Prairie property.

3.1 Modeling Approach

The fate and transport modeling was conducted by first using MT3DMS to simulate transport of residual chemicals over the 13 years between the start-up of the Hawks Prairie recharge basins and the collection of quarterly water quality samples from tracer test monitoring wells and reclaimed water in 2018 (2019/2020 was also simulated). This was done using a transient flow model which simulated the average annual reclaimed water recharge volumes for each year between 2006 and 2020. A fate and transport model, which simulated advection and dispersion of a generic constituent modeled as being introduced at the recharge basins at a reclaimed

water concentration of 1.0 (unitless) was tied to the transient flow model of annual average recharge. Downgradient concentrations predicted by the model are reported as concentration divided by initial concentration (C/C_0). Because the model only simulates advection and dispersion of the introduced constituent (i.e., the residual chemicals) in the aquifer, the constituent is treated by the model as a conservative tracer. The C/C_0 value can be seen in two ways, either as the portion of the original constituent remaining in the water after dispersion while being advected with groundwater, or as the portion of the groundwater that is comprised of reclaimed water at any given point and time in the aquifer downgradient of the recharge basins.

Figures presented in the appendix show: a) the model-estimated mound created by recharging reclaimed water to the aquifer (Appendix B); and, b) the model-estimated distribution of reclaimed water (Appendix C) for each year from 2006 to 2020 in both the Q_{va} and the Q_c aquifers. By 2020 the mound created in the Q_{va} (greater than 1-foot increase) extends from Woodland Creek to McAllister Creek in the east-west direction and about half a mile north and a little more than a mile south of the Hawks Prairie facility. At Hawks Prairie, beneath the recharge basins the model indicates the mounding in the Q_{va} will be just less than 100 feet. This is likely an over estimation and not the case due to more transmissive materials in the vadose zone that are not represented in the model which would reduce the mounding beneath the recharge basins (and agree more with the observed conditions at Hawks Prairie).In the Qc the mounding greater than 1 foot extends from Woodland Creek to McAllister Creek in the east west direction and about a mile north and a to the model boundary more than 2 miles to the south of the Hawks Prairie facility. The mounding beneath Hawks Prairie in the Qc is about 20 feet.

The model estimated distribution of reclaimed water in the Q_{va} in 2020 is approximately 2,500 feet towards the west, 1,000 feet to the east (with a low-level finger extending another 2,000 feet), 2,000 feet to the south and 200 feet to the north. In the Q_c, the reclaimed water extends west about 2,500 feet and eastward to McAllister Creek, to the north about 2,000 feet and to little more than a mile to the south.

The predicted C/C_0 were multiplied by the concentrations of different residual chemicals detected in the reclaimed water at the downgradient monitoring wells and these concentrations were compared to the actual concentrations detected in the wells. The travel times between the recharge basins and the monitoring wells estimated during the tracer test were used to plot the model predicted concentrations and the observed concentrations against travel time. The difference between the observed and predicted was used to estimate the AF for each residual chemical that had sufficient data and a usable downgradient decreasing concentration trend. The AFs calculated from the difference between the observed and predicted approximate the other processes that act on constituents when being transported through the environment (e.g., sorption to organic material in the aquifer matrix and degradation by biological processes).

After the average annual recharge between 2006 and 2020 was simulated and the AFs for the residual chemicals were estimated, a 100-year simulation was conducted to predict C/C_0 concentrations into the future and at peak concentration locations at specific distances from the recharge facility (given broad conservative conditions and assumptions). The 100-year transient flow was based on estimates of future recharge rates that reflect the trends of past infiltration rates while also accounting for growth in LOTT's service area that will result in expanded use of

the Hawks Prairie infiltration site. Once the transient flow model was completed, a dispersion/advection simulation of C/C_0 was conducted for the 100-year period (the actual model includes a 16-year lead up and then 100 years of predictive simulation, see Section 3.2 below). The highest C/C_0 values at specific distances from the recharge basins in both the Shallow Aquifer (Qva) and the Sea Level Aquifer (Qc), and at Woodland and McAllister Creeks, were identified in the model. These C/C_0 values were used to estimate EPCs for each residual chemical by multiplying the reclaimed water concentration then subtracting the constituent specific AF multiplied by the travel time to the peak locations. A more detailed discussion of the method and equation used to calculate EPCs is presented in Section 4.0 Estimated Residual Chemical Exposure Point Concentrations.

3.2 Transient Flow Modeling

Modeling the fate and transport of constituents in groundwater requires an underlying flow model to simulate the advective forces. If the advective forces/stresses are constant throughout the fate and transport period, then a steady state flow model such as the calibrated flow model (HDR, 2019b) is sufficient to simulate the advective movement. However, if there are changes to the advective forces over the duration of the fate and transport simulation, such as changes in recharges rates at the Hawks Prairie facility, then the flow model must be converted to a transient model that simulates these changes. As discussed above, two transient simulations were conducted to provide the advective forces for the fate and transport modeling, one of the average annual operational recharge rate of the Hawks Prairie recharge basins between 2006 and 2020, and the other of the estimated changes in flow over the next 100 years.

3.2.1 Historical Annual Average Recharge Rates Flow Model

The simulation of reclaimed water that has already been recharged to the aquifers was done as a starting point for the constituent fate and transport modeling. This simulation used the average annual recharge rates recorded at Hawks Prairie. Table 5 shows the recharge rates simulated.

Table 5 - Simulated Average Annual Recharge Rates

Year	Total Amount of Reclaimed Water (in MGY)	Average Daily Recharge (MGD)
2006	72	0.2
2007	189	0.52
2008	196	0.54
2009	319	0.87
2010	361	0.99
2011	237	0.65
2012	134	0.37
2013	0	0
2014	190	0.52
2015	171	0.49
2016	192	0.53
2017	125	0.34
2018	251	0.69
2019	253	0.69
2020	217	0.59

3.2.2 100-Year Projected Recharge Rates Flow Model

The schedule of recharge rates for the 100-year future transient modeling were provided by LOTT and reflect the trends of past infiltration rates while also accounting for growth in LOTT's service area that will result in expanded use of the Hawks Prairie infiltration site. Table 6 summarizes the recharge rate schedule simulated in the 100-year simulation.

Table 6 - Estimated Future Recharge Rates used for Predictive Fate and Transport Modeling

Start Year	End Year	Duration	Recharge Rate (MGD)
2006	2022	16	0.5
2023	2038	16	1.1
2039	2042	4	1.8
2043	2049	7	2.6
2050	2067	18	3.4
2068	2120	53	4.2

3.3 Simulation of C/C_0 using Advection and Dispersion

As discussed in 3.1 above, the fate and transport modeling simulated a source term value of 1.0 representing C_0 for the recharging water (reclaimed water being recharged) at the Hawks Prairie recharge basins. The model simulates the movement of the constituent with advection downgradient and the dispersion caused by the tortuosity of the aquifer's pore system (complex flow path). Horizontal dispersion (in the direction of flow) was calculated from the tracer test results to be 14 feet (HDR, 2019b), with an assumed transverse to horizontal ratio of 0.1 and a vertical to horizontal ratio 0.01.

3.3.1 Historical Annual Average Recharge Rates Fate and Transport Model

The transient flow model that simulated average annual recharge rates was used to simulate the fate and transport of a conservative tracer originating with the recharge water at the Hawks Prairie facility. The C/C_0 concentration was estimated at downgradient locations (see Figure 2 for the breakthrough curves at selected monitoring wells). As expected, arrivals at locations occurred later at locations further downgradient and the maximum predicted C/C_0 was also less at locations further downgradient. Note that recharge did not occur in 2013 (see Table 5), so C/C_0 decreased slightly for a short period after that year. Figures showing the model estimated mounding in the Q_{va} and the Q_c aquifers created by the historic recharge are found in Appendix B. Figures showing the movement and distribution of the recharged reclaimed water in the Q_{va} and the Q_c aquifers are found in Appendix C.

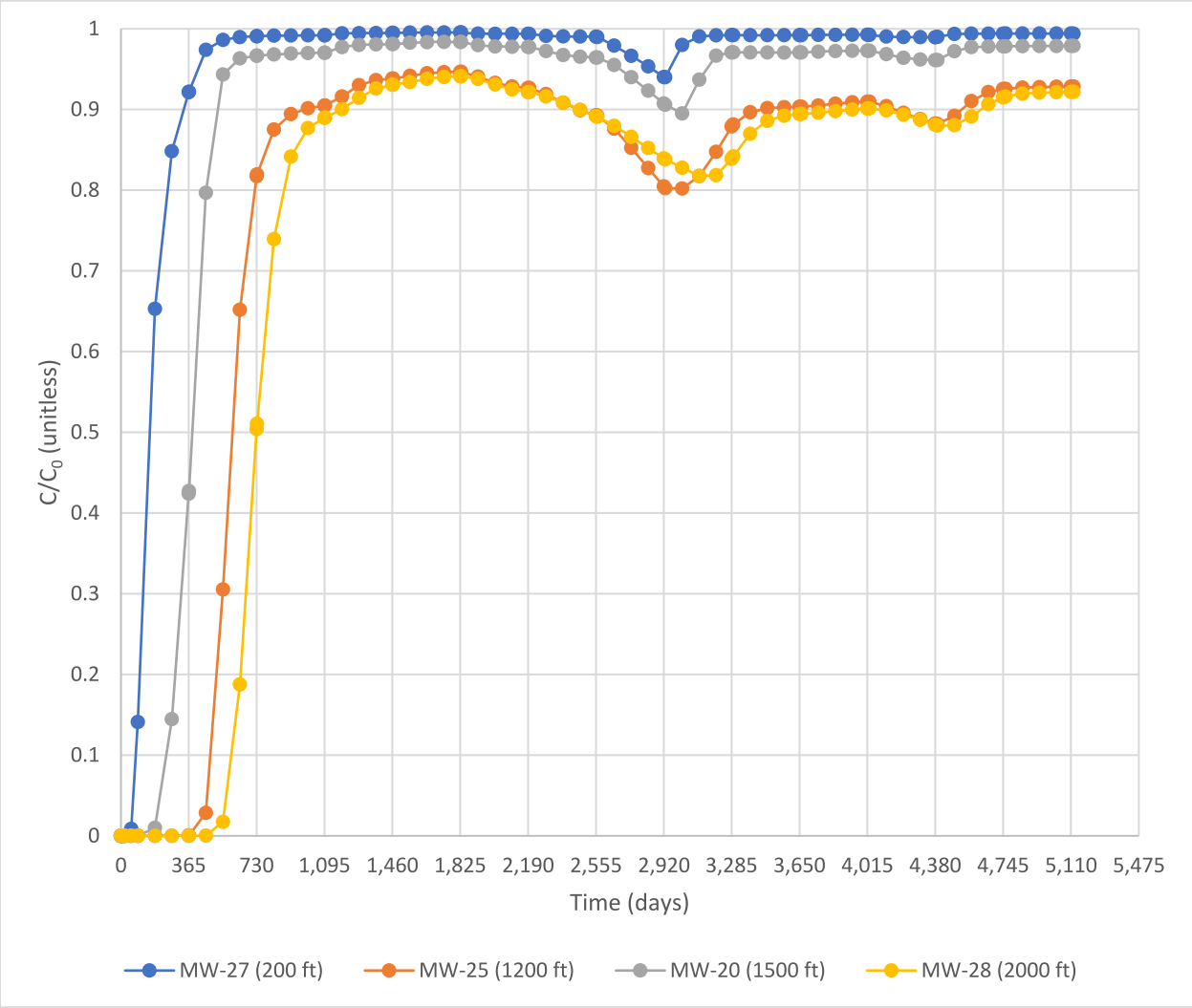

Figure 2 Model Estimated C/C_0 at Select Downgradient Monitoring Wells Based on Average Annual Recharge Rates Simulation

3.3.2 100-Year Projected Recharge Rates Fate and Transport Model

The 100-year projected recharge rates transient model was used as the advective engine for a fate and transport model to estimate C/C_0 of a conservative tracer at specific locations over the next 100 years (given conservative conditions and assumptions). Figure 3 shows the predicted C/C_0 concentration distribution at 100 years in the Shallow Aquifer and Figure 4 shows the predicted C/C_0 concentration distribution at 100 years in the Sea Level Aquifer. Figures showing the model estimated mounding in the Q_{va} and the Q_c aquifers created over the next 100 years of recharge are found in Appendix D. Figures showing the movement and distribution of the recharged reclaimed water in the Q_{va} and the Q_c aquifers over the next 100 years of recharge are found in Appendix E.

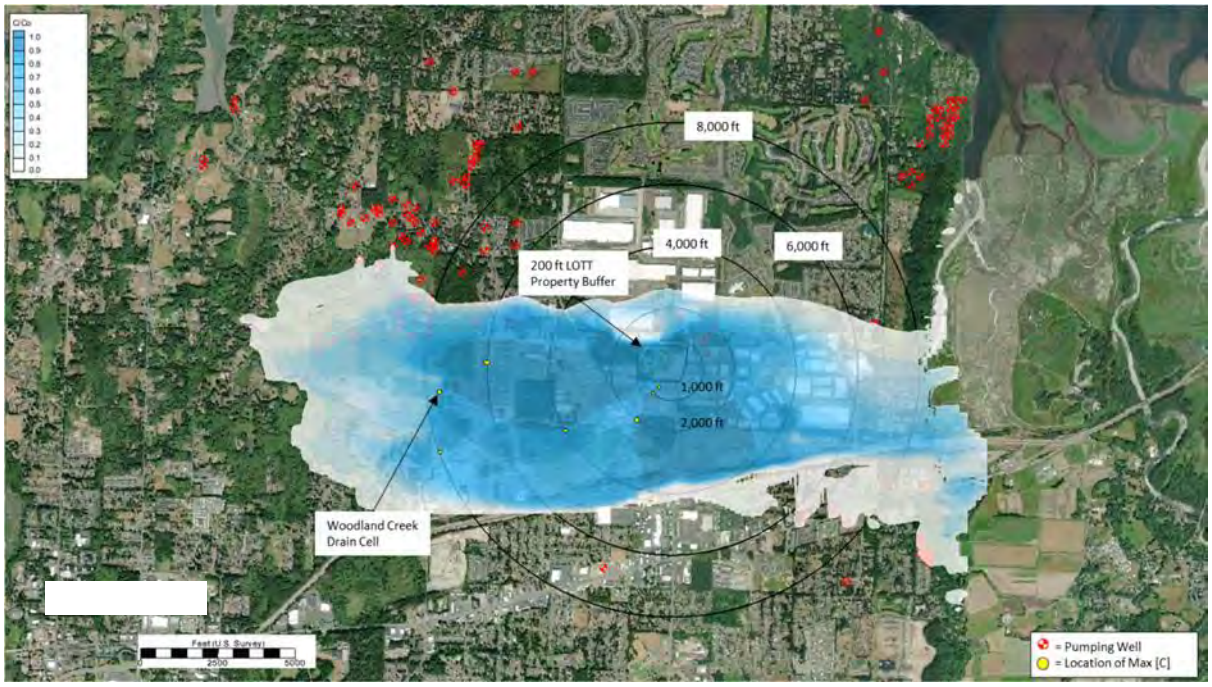

Figure 3 C/C_0 Distribution in the Shallow Aquifer after 100 years

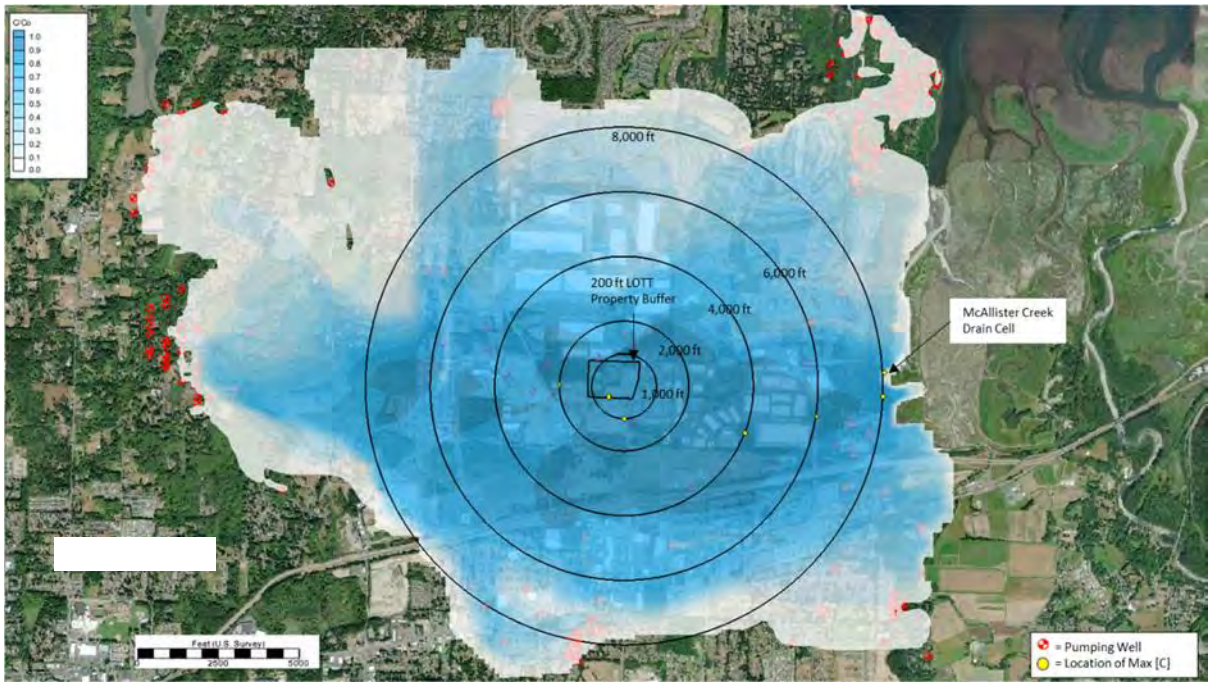

Figure 4 C/C_0 Distribution in the Sea Level Aquifer after 100 Years

3.4 Estimated Attenuation Factors for Residual Chemicals

For those residual chemicals that passed the screening level risk assessment and for which data obtained during the 2018 tracer test were sufficient to do so, an AF was estimated to represent the additional attenuation beyond advection and dispersion reflected in observations at the Hawks Prairie site. This was done by comparing the model predicted C/C_0 for 2018 (i.e., twelve years after the Hawks Prairie recharge basins began recharging reclaimed water to the aquifer) at downgradient monitoring wells resulting from the annual average recharge to measured concentrations of residual chemicals in the same wells, divided by the average concentration in reclaimed water. The two were plotted by tracer test travel times to identify the difference between computed and observed transport. Figure 5 is an example of the difference between model predicted C/C_0 and measured concentrations/reclaimed water concentration for 1,4-dioxane.

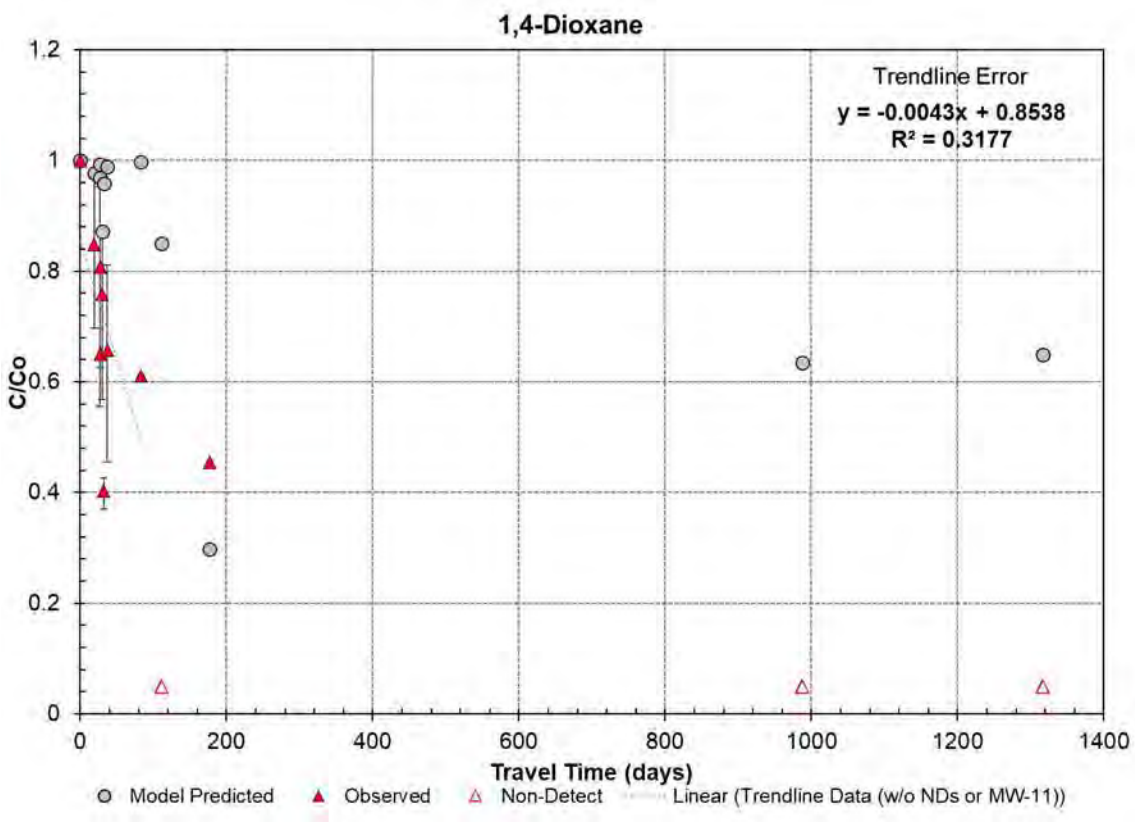

Figure 5 Modeled and Observed C/C_0 for 1,4-dioxane Compared to Travel Time

The difference between modeled C/C_0 and observed C/C_0 (summarized in HDR 2019a) for each point is assumed to be a result of the processes not simulated in the model. The model simulates changes in C/C_0 due to advective transport and dispersion in the aquifer, which were determined based on the results of the 2018 tracer study. The differences between predicted C/C_0 and observed C/C_0 can be explained by four processes:

- Decay or degradation of the residual chemicals as they are transported.

- Sorption of the residual chemicals to the aquifer matrix.
- Diffusion of the residual chemicals into pore spaces in the aquifer matrix (especially into low-hydraulic conductivity materials such as silts and clays).
- Variability of the source concentration.

These processes are collectively empirically captured by the calculated AF. The first three are processes at work as residual chemicals are transported in the aquifer while the fourth is a source of uncertainty in the AF. The AFs were calculated based on average concentrations of samples collected over a year which reduces the uncertainty associated with the variability of source concentrations.

The slope of a trendline through the difference (or fraction attenuated) plotted against travel time represents the AF, which collectively accounts for these processes. Figure 6 shows an example of the slope determination for 1,4-dioxane. The AF for 1,4-dioxane based on this analysis is 0.007/day. The charts for each residual chemical where an AF was calculated are presented in Appendix F.

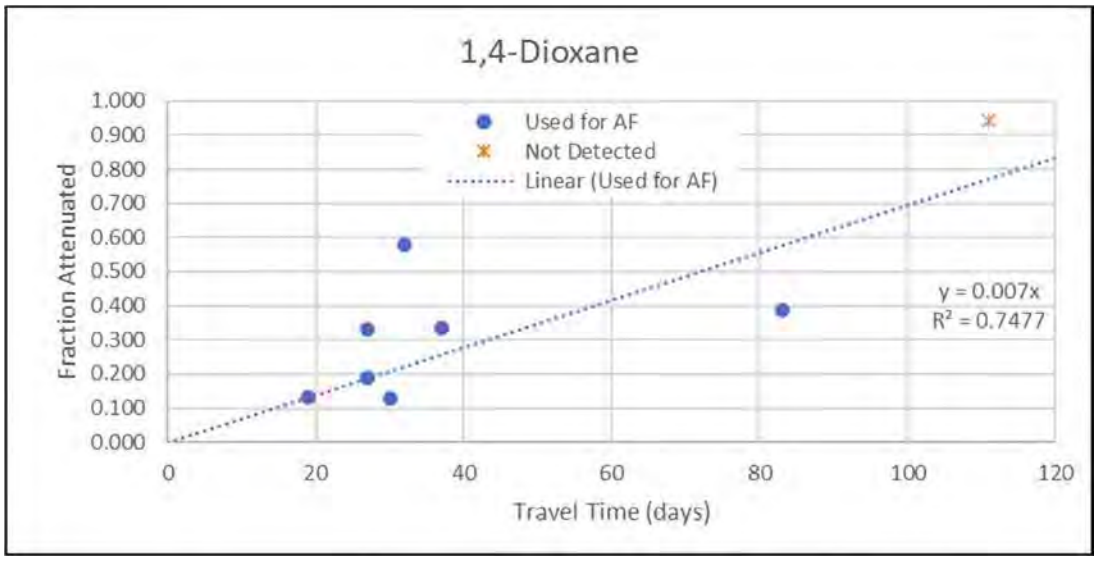

Figure 6 Determination of AF for 1,4-dioxane

It is noted that the AFs are calculated based on data after a little more than a decade of recharge operations at a rate of just less than 1 MGD, and therefore represent reclaimed water transport on a decadal scale and at the lower end of possible future recharge rates. The modeling and estimations of residual chemical concentrations is for the next 100 years and at rates of up to 4.2 MGD. Sorption and matrix diffusion can be overwhelmed when concentrations increase and when the mass of residual chemicals sorbed exceeds the capacity of the matrix. When this happens, chemicals can be transported further than expected. However, the concentrations of residual chemicals in the reclaimed water are comparatively small which means they are unlikely to overwhelm both sorption and matrix diffusion; and further, decay/degradation depletes chemical mass in the aquifer over time as well, reducing the mass sorbed or diffused into the matrix. For these reasons, such effects were not estimated as their overall influence on the AF is likely to be negligible.

4.0 Estimated Residual Chemical Exposure Point Concentrations

Exposure point concentrations (EPCs) were derived for the 50 residual chemicals that passed through the screening level human health and ecological risk evaluations. These EPCs then are used as inputs to the human health and ecological risk assessments. EPCs were calculated for select locations using the following formula:

$$EPC = (C_{ochem} * C/C_o) * (1-(AF*T_{loc}))$$

Where:
C_{ochem} = the concentration of the residual chemical in reclaimed water
C/C_o = the model predicted maximum C/C_0 at the exposure point (see Section 3.3 for detail)
AF = the calculated attenuation factor (see Section 3.4 for detail)
T_{loc} = the model predicted travel time to the exposure point

The sections below describe the locations where EPCs were estimated, the determination of reclaimed water concentrations, and summarize the resultant EPCs.

4.1 Locations for Estimation of Exposure Point Concentrations

In order to inform the human health and ecological risk assessments, maximum concentration points were identified as potential or theoretical exposure points at various distances from the infiltration basins and where groundwater discharges to surface water based on the 100-year groundwater model.

Evaluated distances include a 200-foot buffer around the perimeter of the LOTT Hawks Prairie property and five concentric circles centered at the midpoint between infiltration basins 4 and 5. The 200-foot property buffer was chosen as the most conservative point of exposure for the human health risk assessment, as that is the closest downgradient location that is off-site (i.e., not on LOTT property) where it would be legal to install a domestic water supply well in the shallow aquifer. Per the state's Reclaimed Water Rule (WAC 173-219-360 [Table 3]), this would be a minimum of 200 feet away from the infiltrations basins (e.g., if an individual, permit-exempt well were drilled in this location). While this is unlikely, because the area immediately surrounding the Hawks Prairie property is within the City of Lacey's retail water service area, this is taken as a conservative approach to the human health risk assessment based on potential future permitting since 200 feet is the minimum buffer required to install a new groundwater supply well in proximity to an infiltration basin. The radii of the concentric circles beyond this were chosen to adequately describe the model predicted distribution of C/C_0 over the 100-year simulation and range from 1,000, 2,000, 4,000, 6,000, and 8,000 feet.

For the five concentric circles and LOTT property buffer, concentrations were compared along the circle or buffer perimeters in both the Shallow and Sea-Level Aquifers to identify a maximum at each location (twelve points). For the surface water intercepts, which represent the most

conservative points of exposure for the ecological risk assessment, concentrations were compared at drain cells, model-defined locations where water is removed from the aquifer, corresponding with McAllister Creek to the east and Eagle Creek, a tributary of Woodland Creek, to the west. One maximum concentration point was identified for each creek. The locations of the maximum concentration points for both the Shallow and the Sea Level Aquifers and for Woodland and McAllister Creeks are shown on Figure 3 and Figure 4. The maximum concentration points were based on the entire 100-year model simulation. While most maximum concentrations take place at or near the end of the modeled period, some maximums occur at earlier time steps and decrease some over time after the maximum. The variability in arrival time maximum concentrations is due to the changes in recharge resulting in changes in groundwater flow direction over the modeled period. A total of fourteen maximum concentration points were identified as bases for the EPCs. Table 7 shows the time of travel to each point and the time of the highest concentration at each point.

Table 7 - Times of Maximum Concentration and Travel Times to EPC Locations

Distance (ft)	Qva		Qc	
	Time to Max Conc. (days)	Time to First Arrival (days)	Time to Max Conc. (days)	Time to First Arrival (days)
200	900	30	12,000	250
1000	1,100	90	13,000	570
2000	7,000	880	15,000	1,000
4000	20,000	14,000	43,000	6,600
6000	25,000	15,500	46,000	4,800
8000	28,000	20,500	43,000	4,400
Woodland Creek (~7,700)	27,000	16,800	NA	NA
McAllister Creek (~8,200)	NA	NA	38,000	4,800

Travel times to the EPC locations were also determined from the model by identifying the time of first arrival at each of the points. The flow paths are three-dimensional and given the strong downward gradient between the Shallow Aquifer and the Sea Level Aquifer that occurs where the Kitsap confining unit is more hydraulically conductive, reclaimed water moves further faster in the Sea Level Aquifer than in the Surficial Aquifer. For this reason, reclaimed water arrival times at 4,000, 6,000 and 8,000 feet are faster in the Sea Level Aquifer than in the Shallow Aquifer.

4.2 Reclaimed Water Concentrations

The reclaimed water concentration of each assessed residual chemical was determined based on all reclaimed water monitoring data obtained during the course of the RWIS. This includes 2014/2015 data from both the BIRWP and MWRWP (HDR 2017b) and MWRWP data from the 2018 tracer test (HDR 2019b). For the purpose of calculating EPCs for subsequent use in the risk assessments, the following approach was taken for reclaimed water concentration estimation:

- Calculation of the 95% upper confidence limit (UCL) of the arithmetic mean, using USEPA's ProUCL statistical software, version 5.1. This approach is taken where ProUCL has sufficient data to produce this metric, which typically requires a minimum of six detection.
- Use of the observed maximum reclaimed water concentration where the number of detections were not sufficient to support calculation of the 95% UCL.
- Use of the minimum reporting limit (MRL) in those cases where the residual chemical was not detected in reclaimed water.

The reclaimed water concentrations used in the EPC calculations are summarized in Table 6. In summary, of the 50 residual chemicals for which EPCs were generated, 27 had sufficient data by which to calculate the 95% UCL for the reclaimed water concentration, whereas 10 required use of the maximum detected concentration and 13 required use of the MRL.

4.3 Exposure Point Concentrations

Table 8 summarizes the calculated EPCs for the 50 chemicals being considered in the risk assessments, based on the EPC equation presented earlier in this section. These results can be organized into the following groups (as is also indicated on the table):

1. Not detected in offsite wells; no AF calculated (32 chemicals). These residual chemicals are being considered in the risk assessments because of their observed maximum concentration in reclaimed water or pore water (i.e., in the unsaturated vadose zone). However, these chemicals were not detected in offsite monitoring wells. It is reasonable to assume therefore that these chemicals attenuate and are not predicted to be present above the MRL beyond the footprint of the Hawks Prairie facility. That said, a conservative approach was taken and potential EPCs have been calculated without the use of an AF. This was expressly for the purpose of supporting a conservative approach to the risk assessment, if the risk assessors elect to make use of such information. Otherwise, concentrations for these chemicals at locations away from the Hawks Prairie site are assumed to be zero for these chemicals.
2. Detected in offsite wells; no AF calculated (9 chemicals). These residual chemicals were detected in offsite monitoring wells, but AFs were not calculated due to insufficient data by which to arrive at an AF (given the methodology described in Section 3.4; category 2a), or the data indicate strong persistence (category 2b).
3. Detected in offsite wells; AF calculated (9 chemicals). These chemicals comprise the subset for which AFs have been calculated based on data sufficient to support their derivation.

Literature review of residual chemical attenuation factors found that some of the residual chemicals that did not have sufficient data to calculate an AF are known to degrade in the environment. The literature review for these residual chemicals is found in Section 5.0 Literature Review of Residual Chemical Attenuation. For those compounds where fate and transport properties are described in the literature, such as fipronil, literature-based AFs were estimated, and EPCs calculated based on the literature values.

The EPCs in Table 8 are provided at all locations described in Section 4.1. These values have been advanced for use in the human health and ecological risk assessments.

4.4 Mass Flux to Surface Water Calculations

Mass flux to surface water was calculated based on the results from the fate and transport groundwater model. Mass flux is the contaminant mass moving across the aquifer perpendicular to the groundwater flow direction and mass flux into cells simulating surface water represents the load of residual chemicals mixing with the water already in the surface water body. At each cell location where a constant head or drain cell representing either Woodland Creek McAllister Creek, or the springs along McAllister Creek, the calculated mass output from the MT3DMS simulation was summed for each timestep. The resulting calculated masses were then compiled into a total mass by year at each of the surface water locations. These mass fluxes were provided as inputs to the risk assessments, for use in mixing calculations for residual chemicals that potentially arrive at surface water.

October 14, 2021

Table 8 - Exposure Point Concentrations

				Calculated Exposure Point Concentrations (EPCs, in ng/L) [Note 2]													
				Qva (Model Layer 2; Shallow Aquifer)							Qc (Model Layer 4; Deep, Sea-Level Aquifer)						
Location (distance away from infiltration basin center, ft):				200 ft	1,000 ft	2,000 ft	4,000 ft	6,000 ft	8,000 ft	Woodland Creek	200 ft	1,000 ft	2,000 ft	4,000 ft	6,000 ft	8,000 ft	McAllister Creek
Modeled First Arrival Time (days):				30	90	880	14000	15500	20500	16800	250	570	1000	6600	4800	4400	4800
Dispersion-Modeled Max Unit Concentration (C/C_o):				1.00	1.00	1.00	1.00	0.99	0.95	0.75	0.99	0.99	0.99	0.96	0.93	0.88	0.32
	Reclaimed Water Concentration (ng/L) [Note 1]		EPC Category [Note 3]	Attenuation Factor (AF)													
1,4-Dioxane	689		3	0.007		544	255	0	0	0	0	0	0	0	0	0	0	0	0
4-Nonylphenol	1,221		2a	0		1,221	1,221	1,221	1,221	1,209	1,160	916	1,209	1,209	1,209	1,172	1,136	1,074	391
Acesulfame-K	8,395		3	0.0072		6,582	2,955	0	0	0	0	0	0	0	0	0	0	0	0
Albuterol	10		1	0		10	10	10	10	10	10	8	10	10	10	10	9	9	3
Amoxicillin	80		1	0		80	80	80	80	79	76	60	79	79	79	77	74	70	26
Androstenedione	10		1	0		10	10	10	10	10	10	8	10	10	10	10	9	9	3
Atenolol	166		1	0		166	166	166	166	164	157	124	164	164	164	159	154	146	53
Carbamazepine	428		3	0.0115		280	0	0	0	0	0	0	0	0	0	0	0	0	0
Chloramphenicol	24		1	0		24	24	24	24	24	23	18	24	24	24	23	22	21	8
Cotinine	51		1	0		51	51	51	51	51	49	38	51	51	51	49	48	45	16
Diazepam	9		1	0		9	9	9	9	9	9	7	9	9	9	9	9	8	3
Diclofenac	52		1	0		52	52	52	52	52	50	39	52	52	52	50	48	46	17
Dilantin	84		1	0		84	84	84	84	83	80	63	83	83	83	81	78	74	27
Estradiol - 17 beta	5		1	0		5	5	5	5	5	5	4	5	5	5	5	5	4	2
Estriol	10		1	0		10	10	10	10	10	10	8	10	10	10	10	9	9	3
Estrone	0.91		1	0		0.91	0.91	0.91	0.91	0.90	0.86	0.68	0.90	0.90	0.90	0.87	0.85	0.80	0.29
Ethinyl Estradiol - 17 alpha	64		1	0		64	64	64	64	63	61	48	63	63	63	61	60	56	20
Fipronil (Note 4)	51		2a	0		25	12	0	0	0	0	0	0.2	0	0	0	0	0	0
Fluoxetine	152		1	0		152	152	152	152	151	145	114	151	151	151	146	142	134	49
Gemfibrozil	316		1	0		316	316	316	316	313	300	237	313	313	313	303	294	278	101
Lopressor	495		1	0		495	495	495	495	490	470	371	490	490	490	475	460	435	158
Meclofenamic Acid	300		1	0		300	300	300	300	297	285	225	297	297	297	288	279	264	96
N-Nitroso dimethylamine (NDMA)	3		2a	0		3	3	3	3	3	3	2	3	3	3	3	3	3	1
Norethisterone	5.9		1	0		5.9	5.9	5.9	5.9	5.8	5.6	4.4	5.8	5.8	5.8	5.7	5.5	5.2	1.9
Perfluoro butanoic acid (PFBA)	10		1	0		10	10	10	10	10	10	8	10	10	10	10	9	9	3
Perfluoro octanesulfonate (PFOS)	5		1	0		5	5	5	5	5	5	4	5	5	5	5	5	4	2
Perfluoro octanesulfonic acid (PFOS)	5		1	0		5	5	5	5	5	5	4	5	5	5	5	5	4	2

					Calculated Exposure Point Concentrations (EPCs, in ng/L) [Note 2]													
					Qva (Model Layer 2; Shallow Aquifer)							Qc (Model Layer 4; Deep, Sea-Level Aquifer)						
Location (distance away from infiltration basin center, ft):					200 ft	1,000 ft	2,000 ft	4,000 ft	6,000 ft	8,000 ft	Woodland Creek	200 ft	1,000 ft	2,000 ft	4,000 ft	6,000 ft	8,000 ft	McAllister Creek
Modeled First Arrival Time (days):					30	90	880	14000	15500	20500	16800	250	570	1000	6600	4800	4400	4800
Dispersion-Modeled Max Unit Concentration (C/C_o):					1.00	1.00	1.00	1.00	0.99	0.95	0.75	0.99	0.99	0.99	0.96	0.93	0.88	0.32
	Reclaimed Water Concentration (ng/L) [Note 1]		EPC Category [Note 3]	Attenuation Factor (AF)														
Perfluoro octanoic acid (PFOA)	15		2b	0	15	15	15	15	15	14	11	15	15	15	14	14	13	5
Perfluoro-1-butanesulfonate	9		2b	0	9	9	9	9	9	8	7	9	9	9	9	8	8	3
Perfluoro-1-butanesulfonic acid	9		2b	0	9	9	9	9	9	8	7	9	9	9	8	8	8	3
Perfluoro-1-hexanesulfonate	5		1	0	5	5	5	5	5	5	4	5	5	5	5	5	4	2
Perfluoro-1-hexanesulfonic acid	5		1	0	5	5	5	5	5	5	4	5	5	5	5	5	4	2
Perfluoro-n-decanoic acid	5		1	0	5	5	5	5	5	5	4	5	5	5	5	5	4	2
Perfluoro-n-heptanoic acid	5		1	0	5	5	5	5	5	5	4	5	5	5	5	5	4	2
Perfluoro-n-hexanoic acid	46		2b	0	46	46	46	46	45	44	34	45	45	45	44	43	40	15
Perfluoro-n-nonanoic acid (PFNA)	5		1	0	5	5	5	5	5	5	4	5	5	5	5	5	4	2
Perfluoropentanoic acid	79		2b	0	79	79	79	79	78	75	59	78	78	78	76	74	70	25
Primidone	377		3	0.0176	178	0	0	0	0	0	0	0	0	0	0	0	0	0
Progesterone	5		1	0	5	5	5	5	5	5	4	5	5	5	5	5	4	2
Quinoline	12		3	0.0059	10	6	0	0	0	0	0	0	0	0	0	0	0	0
Sucralose	58,531		3	0.0072	45,888	20,603	0	0	0	0	0	0	0	0	0	0	0	0
Sulfamethoxazole	146		2a	0	146	146	146	146	144	138	109	144	144	144	140	135	128	47
Testosterone	6.6		1	0	6.6	6.6	6.6	6.6	6.5	6.3	5.0	6.5	6.5	6.5	6.3	6.1	5.8	2.1
TCEP	142		3	0.0323	4	0	0	0	0	0	0	0	0	0	0	0	0	0
TCPP	662		1	0	662	662	662	662	655	629	496	655	655	655	635	615	582	212
TDCPP	978		3	0.0317	48	0	0	0	0	0	0	0	0	0	0	0	0	0
Theobromine	30		1	0	30	30	30	30	30	29	23	30	30	30	29	28	26	10
Theophylline	95		1	0	95	95	95	95	94	90	71	94	94	94	91	88	84	30
Thiabendazole	50		1	0	50	50	50	50	50	48	38	50	50	50	48	47	44	16
Triclosan	83		3	0.024	23	0	0	0	0	0	0	0	0	0	0	0	0	0

October 14, 2021

Notes:

Light green cells are EPCs at various locations in the Shallow Aquifer.

Light blue cells are EPCs at various locations in the Deep Aquifer.

1. Reclaimed water concentration input into EPC model (Cochem). Basis:

Green cells based on 95% UCL.

Yellow cells based on maximum reclaimed water concentration.

Red cells indicate non-detects in reclaimed water; MRL taken as concentration.

2. EPC = (Cochem*C/Co) * (1-(AF*Tloc))

3. EPC category, based on calculation approach:

1 - Not detected in offsite wells; no AF calculated. Offsite concentration assumed to be zero, but a conservative upper bound is provided, assuming no AF.

2a - Detected in offsite wells, insufficient data; no AF calculated.

2b - Detected in offsite wells, strong persistence; no AF calculated

3 - Detected in offsite wells; AF calculated.

4. See Section 5 for additional detail on attenuation of fipronil, based on literature review.

This page intentionally left blank.

5.0 Literature Review of Residual Chemical Attenuation

The analysis of attenuation factors and estimation of exposure point concentrations presented in this technical memorandum is based on empirical data reflective of the conditions observed at the LOTT Hawks Prairie facility. A high-level comparison of these results has been made with published results from other similar studies.

A literature review of the effectiveness of soil aquifer treatment (SAT) on residual chemical removal was conducted during Phase 1 of the RWIS and is documented in the *State of the Science* technical memorandum (HDR 2013a) and a series of reclaimed water infiltration case studies that are summarized in the *Case Study Summary* technical memorandum (HDR 2013b). The general finding of that review was that SAT has been observed in other studies to have a percent removal of more than 90% for most residual chemicals, with specific compounds persisting for longer times in SAT systems. Figure 7 provides a high-level summary (USEPA 2012).

Table 6-5 Indicative percent removals of organic chemicals during various stages of wastewater treatment

Treatment	Target Compounds										
			Pharmaceuticals					Hormones			
	Blain-	Antibiotics[1]	DZP	CBZ	DCF	IBP	PCT	Steroid[2]	Anabolic[3]	Fragrance	NDMA
Secondary (activated sludge)	nd	10–50	nd	–	10–50	>90	nd	>90	nd	50–90	–
Soil aquifer treatment	nd	nd	nd	25–50	>90	>90	>90	>90	nd	>90	>90
Aquifer storage	nd	50–90	10–50	–	50–90	50–90	Nd	>90	nd	–	–
Microfiltration	nd	<20	<20	<20	<20	<20	<20	<20	nd	<20	
Ultrafiltration/ powdered activated carbon (PAC)	nd	>90	>90	>90	>90	>90	nd	>90	nd	>90	>90
Nanofiltration	>80	50–80	50–80	50–80	50–80	50–80	50–80	50–80	50–80	50–80	
Reverse osmosis	>80	>95	>95	>95	>95	>95	>95	>95	>95	>95	25–50
PAC	>80	20–>80	50–80	50–80	20–50	<20	50–80	50–80	50–80	50–80	
Granular activated carbon		>90	>90	>90	>90	>90		>90		>90	>90
Ozonation	>80	>95	50–80	50–80	>95	50–80	>95	>95	>80	50–90	50–90
Advanced oxidation		50–80	50–80	>80	>80	>80	>80	>80	>80	50–80	>90
High-level ultraviolet		20–>80	<20	20–50	>80	20–50	>80	>80	20–50	nd	>90
Chlorination	>80	>80	20–50	–<20	>80	<20	>80	>80	<20	20–>80	–
Chloramination	50–80	<20	<20	<20	50–80	<20	>80	>80	<20	<20	

(Sources: Ternes and Joss, 2006; Snyder et al., 2010)

B(a)p = benz(a)pyrene; CBZ = carbamazepine, DBP = disinfection by-product; DCF = diclofenac; DZP = diazepam; IBP = ibuprofen; NDMA=N-nitrosodimethylamine; nd = no data; PAC = powdered activated carbon; PCT = paracetamol.

[1] erythromycin, sulfamethoxazole, triclosan, trimethoprim

[2] ethynylestradiol; estrone, estradiol and estriol

[3] progesterone, testosterone

Figure 7 Summary of Residual Chemical Removal Efficiencies (USEPA 2012)

A comparison of the literature findings in these prior summaries against the approach taken in this analysis with respect to EPC determination finds similarities with respect to most of the residual chemicals (i.e., chemicals for which this effort suggest significant attenuation are depicted similarly in the literature). However, key observations worth noting are:

- Estrogenic hormones (e.g., ethinyl estradiol-17 alpha). The literature consistently shows rapid attenuation of these hormones through SAT. Monitoring of offsite wells during the 2018 tracer test suggest a consistent finding in this study. Furthermore, detections in LOTT's reclaimed water are few (e.g., two detections out of 12 sampling events for ethinyl estradiol-17 alpha), indicating inconsistent presence above the MRL in reclaimed water. However, to provide a conservative "upper bound" of potential EPC for use in the risk assessment, if/as applicable, EPCs were generate assuming conservative transport with groundwater (i.e., EPC category 1 in Table 8).
- Fluoxetine and gemfibrozil. Similar to the estrongenic hormones, these residual chemicals have been extensively studied in reclaimed water infiltration applications, with significant attenuation observed, as seen in Figure 8 (Laws, et al 2011). And as with the hormones, these chemicals were not detected in offsite wells, but to remain conservative, EPCs were calculated.
- Carbamazepine and primidone. Many studies have shown these residual chemicals to be highly recalcitrant through SAT. Laws et al (2011) showed negligible attenuation during travel times of up to 60 days. By contrast, empirical data at the LOTT site suggest some level of attenuation beyond a timeframe of 60 days. A deeper look at the literature indicates that under some highly oxic and low biodegradable dissolved organic carbon (BDOC) conditions, observed in practice and replicated in the laboratory setting, degradation of these chemicals can occur in the subsurface. This has been observed in studies associated with the Prairie Waters riverbank filtration and aquifer recharge project in Colorado (Hellauer, et al 2017). Such studies have found that the microbial population that develops during SAT under these conditions is more diverse than at other SAT sites (i.e., where BDOC is higher). This supports the hypothesis that a more diverse microbial population develops when bacteria are only exposed to refractory compounds and aerobic conditions allow for more growth under what would typically be viewed as "low" growth conditions. The reclaimed water produced by the MWRWP has consistently low BDOC (i.e., typically less than 0.6 mg/L). With conditions similar to those studied at sites like Prairie Waters, and data from the 2018 tracer test and water quality sampling effort indicating attenuation, AFs were derived for carbamazepine and primidone, as opposed to relying on data from the more generally cited literature, which would have resulted in higher estimated EPCs.
- NDMA. Many studies of NDMA show attenuation through SAT (see Figure 7). However, the data for the Hawks Prairie site were limited and indicated persistence in the wells sampled. There are instances in other locations where NDMA has been observed to be persistent in groundwater settings. This has been most notable in data reviewed regarding direct injection of reclaimed water treated by reverse osmosis (and therefore with very low BDOC) into sweater intrusion barriers in southern California[1]. The same conditions that may support degradation of carbamazepine and primidone, as noted above, can limit NDMA degradation, due to the lack of more readily degradable organic carbon. Because the Hawks Prairie site

[1] Personal communication, Dr. Peter Fox, Arizona State University, October 2021. As noted by Dr. Fox, the referenced data regarding seawater intrusion barriers has not yet been published in peer-reviewed journals, but has been reviewed and discussed in academic settings.

reflects these conditions, no AF was calculated and the resulting EPCs calculated for locations further downgradient are likely estimated conservatively high.

- Fipronil. Fipronil was only analyzed in reclaimed water and not in the groundwater monitoring wells, for this reason an AF could not be calculated for it. EPA and others have published information on the fate and transport of fipronil in the environment which indicate that it has a high organic partitioning coefficient (Koc) and has a relatively short half life (Tang, Z. and T.S. Ramanarayanan. 2006; Odenkirken and Wente, 2011; Bowers and Tjeerrdema, 2017). These sources generally agree on the biodegradation of fipronil in aerobic water environments (e.g., reclaimed water being recharged to the groundwater through the vadose zone). Table 9 summarizes the half-lives and K_{oc} of fipronil presented in the literature. Figure 9 (graph below) is based on the longest decay rate in an aqueous presented in these references. Based on the aerobic aqueous half-life, fipronil concentration decreases three orders of magnitude within 300 days of travel time. Given decay alone, the furthest detectable concentrations of fipronil will be approximately 1,000 feet downgradient in the Shallow Aquifer (Q_{va}). If sorption is also considered, the downgradient limits of fipronil's transport distances are shorter. This information was used to refine the EPC for fipronil, as depicted in Table 8.

Table 3
Removal of trace organic contaminants detected in the basin and selected bulk water quality parameters based on: concentrations at WP Z (travel time = 12 h), the average concentrations in the upper aquifer (MLS 8–PR 11, travel time < 3 days), and the average concentrations in the lower aquifer (PR 8, PR 10, travel time = 60 days). Removal of less than 20% was considered negligible and ≥ indicates removal below the minimum reporting level (MRL).

			% Removal (WP Z, travel time = 12 h)	% Removal (average MLS 8-PR 11, travel time < 3 days)	% Removal (average PR 8, PR 10, travel time = 60 days)	
					With dilution	Without dilution[a]
CEC						
Attenuation ranking	1	Atenolol	98	96	≥99.9	≥99.9
	2	Iopromide	97	98	97	95
	3	Fluoxetine	94	≥97	≥97	≥97
	4	Gemfibrozil	97	92	96	94
	5	Naproxen	74	63	93	88
	6	Diclofenac	55	55	≥99	≥99
	8	Trimethoprim	52	Negligible	94	90
	10	Triclosan	Negligible	Negligible	≥86	≥86
	9	TCPP	Negligible	Negligible	89	82
	7	Ibuprofen	Negligible	47	84	74
	11	DEET	27	24	84	75
	12	Meprobamate	Negligible	Negligible	69	50
	13	TCEP	Negligible	Negligible	54	49
	14	Sulfamethoxazole	Negligible	Negligible	42	26
	15	Phenytoin	38	36	47	Negligible
	16	Carbamazepine	Negligible	Negligible	49	Negligible
	17	Primidone	Negligible	Negligible	69	Negligible
Bulk water quality parameters						
		DOC	45	52	78	–
		UVA_{254}	18	26	58	–

[a] Removal estimated using 62% reclaimed and 58% native groundwater (assumed to be absent of trace organic chemicals).

Figure 8 Removal of Select Residual Chemical During Infiltration and SAT (Laws et al. 2011)

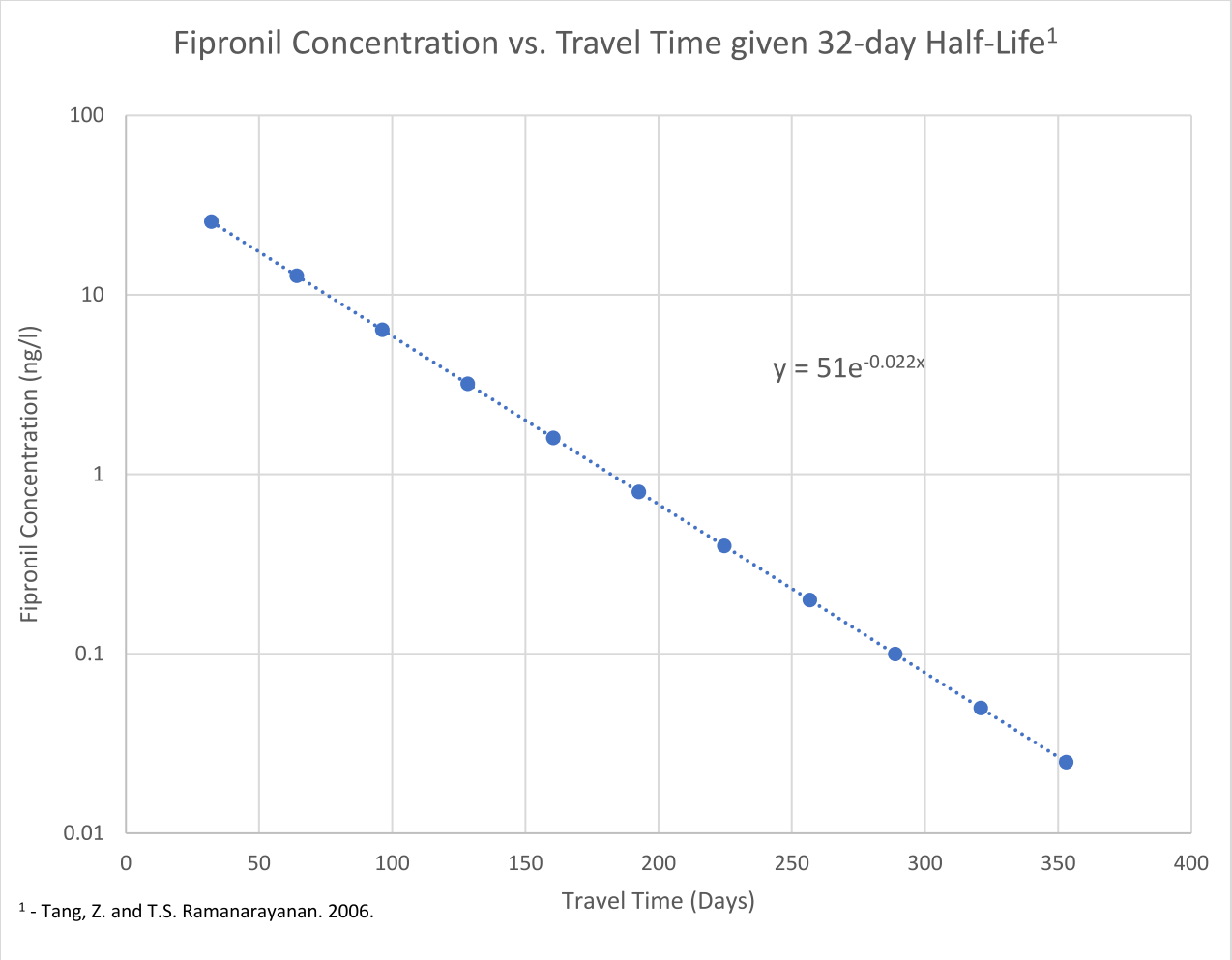

Figure 9 Fipronil Concentration vs. Travel Time

Table 9 - Fipronil Fate and Transport Parameters from Liturature

Reference	K_{oc} Range	Aerobic Aquatic Half-Life Range
Tang, Z. and T.S. Ramanarayanan. 2006	427 – 1248 L/Kg	15-32 days
Odenkirken and Wente, 2011	427 – 1248 L/Kg	14.5 – 35.5
Bowers and Tjeerrdema, 2017	396 – 37,154 L/Kg	5.85 – 74.8

6.0 Sensitivity Analyses

This section describes the approach to sensitivity analyses conducted upon the groundwater model and related results.

6.1 Sensitivity Analyses Approach

A sensitivity analysis of the calibrated MT3DMS model was performed to help bound the results of the fate and transport modeling. When simulating the fate and transport of residual chemicals, the model includes dispersion, porosity, and recharge. These parameters were varied to assess the sensitivity of the model results to each parameter. The results of this analysis provide ranges of outcomes which identify the most likely and the most conservative results based on the three parameters' constraints by either field data or literature-derived values.

There are two primary drivers of conservative transport in the aquifer: dispersion and advection. Dispersion accounts for the effects of tortuous flow path and the heterogeneity of the aquifer materials at scales smaller than the model grid cells. Dispersion is controlled by the parameter dispersivity. The range of dispersivity used in the initial fate and transport model was derived from the tracer test conducted at the Hawks Prairie Recharge Facility in 2018 (HDR, revised February 2020). The model was run using a low, average (baseline) and high dispersivity value based on the tracer test analyses. Table 10 describes the sensitivity analysis scenario and the corresponding description. For all scenarios the low and high are a multiplier based on the baseline simulation. The low dispersivity uses the baseline dispersivity and multiplies that value by 0.5 and the high dispersivity uses the baseline simulation and multiplies it by 2.0.

Advection is the subject of the flow model calibration and was tested through several sensitivity analyses of hydraulic conductivity and pumping rates of simulated wells during calibration and the effective porosity calculated from the tracer test. The calibrated model is the best fit simulation to the data (groundwater levels and stream base-flow) given the reasonable constraints on regional groundwater recharge and understanding of the aquifer properties. Effective porosity is constrained by the tracer test data and geotechnical testing of soil samples collected in 2020. Increasing and decreasing effective porosity alters flow velocity and hence the timing of the contaminant transport in the model. Low porosity and high porosity runs were conducted to bound arrival times and are described as baseline porosity multiplied by 0.5 and 2.0, respectively.

Due to the potential for climate change and development, recharge was the third parameter analyzed in the sensitivity analysis. Recharge is increased (baseline recharge multiplied by 1.25) to simulated changes toward a wetter climate and decreased (baseline recharge multiplied by 0.75) to simulate changes toward a drier climate.

The different sensitivity analyses scenarios are presented in Table 10.

Table 10 - Sensitivity Analyses Scenarios

Scenarios	Description
Baseline	Condition for all variables used in the calibrated model
Low Dispersivity	Baseline dispersivity multiplied by 0.5
High Dispersivity	Baseline dispersivity multiplied by 2.0
Low Effective Porosity	Baseline effective porosity multiplied by 0.5
High Effective Porosity	Baseline effective porosity multiplied by 2.0
Low Recharge	Baseline recharge multiplied by 0.75
High Recharge	Baseline recharge multiplied by 1.25

6.2 Sensitivity Analyses Evaluations

In the same manner as the estimation of EPCs, concentric circles at different distances from the recharge basins were created to evaluate the effects of the sensitivity scenarios. These locations were chosen to show where the highest modeled concentration appears at a radial distance from the discharge area of 200, 1,000, 2,000, 4,000, 6,000, 8,000 feet in both the Q_{va} and Q_c (model layers 2 and 4), as well as the highest concentration in drain cells for Woodland and McAllister Creeks (these are the same locations as used for the EPC calculations discussed in Section 3). The baseline scenario was then used by finding the grid cell along the concentric circles (and McAllister creek for Q_c and Woodland Creek for Q_{va}) that has the maximum concentration, time to the maximum concentration and time of the first arrival for the plume. Those cell locations (see Figure 3 and Figure 4) are the locations where the different sensitivity scenarios were compared to the baseline scenario to determine the overall effect dispersivity, effective porosity and recharge have on the fate and transport model. This analysis was performed for the Qva (layer 2) and Qc (layer 4) of the model.

Dispersivity quantifies how movement around aquifer matrix material causes constituents to spread while being transported downgradient (e.g., the water carrying the constituent is divided as it flows around a grain of sand causing lateral dispersion). Pores in the matrix material are the conduits where water flows and constituents are transported; however, some pores are dead-ended, some are too small for water to flow through, and there is some portion of the pore that is occupied by water that is adhered to the matrix material. These factors reduce the total porosity, so effective porosity is the portion of the porosity available for water and constituents to move through. Effective porosity affects the rate that water moves through the aquifer in the same way water flowing in a river is affected by the river's width and depth: where a river is wide and deep, water moves slowly and where it is narrow and shallow, it moves more quickly. In the same way, the lower the effective porosity, the faster the water moves through the aquifer. Dispersivity and effective porosity were estimated based on the 2018 tracer test. Total porosity was measured in aquifer matrix material that was retrieved during the 2020 monitoring well drilling. The total porosity values represent an upper bound to the effective porosity.

Table 11 shows the results from the analysis for the Q_{va} (layer 2) and Table 12 shows the results for Q_c (layer 4). The distance column shows the distance from the recharge basins that

the analysis was performed, Max Conc. is the maximum concentration at the distance, Time to Max Conc. is the number of days it took to reach the max concentration at that distance and the Time to First Arrival is the number of days it took for the plume to first reach that distance.

Table 11 - Changes in Model Results due to Sensitivity Analyses, Q_{va} Aquifer

		Q_{va}						
Distance	**Stats**	**Baseline**	**Low Porosity**	**High Porosity**	**Low Dispersivity**	**High Dispersivity**	**Low Recharge**	**High Recharge**
200 ft	**Max Conc.**	**1.00**	1.00	1.00	1.00	1.00	1.00	0.99
	Time to Max Conc. (d)	**900**	470	1,900	790	1,500	1,500	2,400
	Time to First Arrival (d)	**30**	20	50	30	30	30	30
1,000 ft	**Max Conc.**	**1.00**	1.00	1.00	1.00	1.00	1.00	0.99
	Time to Max Conc. (d)	**1,100**	1,500	4,800	1,500	2,900	5,900	4,800
	Time to First Arrival (d)	**90**	40	160	90	80	100	80
2,000 ft	**Max Conc.**	**1.00**	1.00	1.00	1.00	1.01	1.00	0.98
	Time to Max Conc. (d)	**7,000**	7,000	10,600	6,600	8,000	10,600	7,700
	Time to First Arrival (d)	**880**	440	1,900	900	820	1,100	710
4,000 ft	**Max Conc.**	**1.00**	1.00	0.99	1.00	0.99	1.00	0.92
	Time to Max Conc. (d)	**20,000**	19,400	24,800	21,100	23,700	21,500	13,900
	Time to First Arrival (d)	**14,000**	13,200	15,300	13,900	13,900	14,000	12,400
6,000 ft	**Max Conc.**	**0.99**	0.99	0.98	0.99	0.98	0.99	0.91
	Time to Max Conc. (d)	**25,000**	25,200	27,700	24,800	25,900	26,300	16,800
	Time to First Arrival (d)	**15,500**	13,900	17,900	15,300	15,000	15,000	13,100
8,000 ft	**Max Conc.**	**0.95**	0.97	0.91	0.96	0.93	0.95	0.55
	Time to Max Conc. (d)	**28,000**	26,300	33,200	28,100	28,400	28,400	21,100
	Time to First Arrival (d)	**20,500**	17,200	25,200	20,800	20,400	20,500	16,400
Woodland Creek Drain	**Max Conc.**	**0.75**	0.78	0.71	0.69	0.79	0.75	0.57
	Time to Max Conc. (d)	**27,000**	25,900	30,300	24,800	27,000	27,000	17,500
	Time to First Arrival (d)	**16,800**	14,700	21,900	16,800	16,400	16,500	13,900

Table 12 - Changes in Model Results due to Sensitivity Analyses, Q_c Aquifer

		Q_c						
Distance	**Stats**	**Baseline**	**Low Porosity**	**High Porosity**	**Low Dispersivity**	**High Dispersivity**	**Low Recharge**	**High Recharge**
200 ft	**Max Conc.**	**0.99**	0.99	0.98	0.99	0.99	0.99	0.96
	Time to Max Conc. (d)	**12,000**	23,000	21,900	21,100	12,400	20,400	9,200
	Time to First Arrival (d)	**250**	130	490	260	230	260	240
1,000 ft	**Max Conc.**	**0.99**	0.99	0.99	1.00	0.99	0.99	0.97
	Time to Max Conc. (d)	**13,000**	12,800	20,800	19,300	18,600	20,000	22,600
	Time to First Arrival (d)	**570**	290	1,150	590	540	620	540
2,000 ft	**Max Conc.**	**0.99**	0.99	0.99	0.99	0.99	0.99	0.93
	Time to Max Conc. (d)	**15,000**	18,600	21,500	19,700	22,200	23,700	12,400
	Time to First Arrival (d)	**1,000**	500	2,250	1,030	970	1,030	970
4,000 ft	**Max Conc.**	**0.96**	0.97	0.90	0.96	0.95	0.96	0.92
	Time to Max Conc. (d)	**43,000**	32,000	42,700	39,800	41,600	42,300	39,000
	Time to First Arrival (d)	**6,600**	2,250	7,300	4,400	4,000	5,100	3,700
6,000 ft	**Max Conc.**	**0.93**	0.94	0.86	0.94	0.91	0.93	0.89
	Time to Max Conc. (d)	**43,000**	25,600	42,700	40,500	40,800	41,200	41,200
	Time to First Arrival (d)	**4,800**	2,250	8,500	4,800	4,400	5,800	4,000
8,000 ft	**Max Conc.**	**0.88**	0.89	0.81	0.89	0.85	0.88	0.84
	Time to Max Conc. (d)	**43,000**	25,200	42,700	40,100	41,600	40,900	36,800
	Time to First Arrival (d)	**4,400**	2,250	8,500	4,400	4,400	5,100	4,000
McAllister Creek Drain	**Max Conc.**	**0.32**	0.36	0.25	0.33	0.30	0.32	0.29
	Time to Max Conc. (d)	**38,000**	11,700	42,700	38,300	38,300	38,300	25,500
	Time to First Arrival (d)	**4,800**	2,250	9,200	4,800	4,800	5,100	4,400

As shown on Table 11, at a distance of 200 feet the baseline maximum concentration of 1.0 was changed to 0.99 by the high recharge scenario. It took 900 days to reach the maximum concentration for the baseline scenario. The low effective porosity and low dispersivity have shorter time to maximum concentrations of 470 days and 790 days, respectively. High effective porosity, high dispersivity, low recharge and high recharge have a higher time to maximum concentration with recharge high having the largest time of 2,400 days. The time to first arrival remained relatively similar to the baseline simulation of 30 days with the exception of the low porosity simulation which took 20 days and the high porosity simulation which took 50 days.

The baseline maximum concentration at a distance of 1,000 ft was 1.00 with all scenarios having the same result except high recharge which had a maximum concentration of 0.99. The time to maximum concentration was greater for all scenarios than the baseline of 1,100 days with the low recharge taking the longest at 5,900 days. Low dispersivity and baseline scenarios have the same time to first arrival of 90 days. Low porosity, high dispersivity and high recharge have the lowest time to first arrival with low porosity having the lowest at 40 days. High porosity and low recharge have higher time to first arrival with 160 days and 100 days, respectively.

The baseline scenario maximum concentration at 2,000 feet is 1.00 with only high dispersivity and high recharge scenarios being different with 1.01 and 0.98, respectively (note 1.01 is likely due to numerical dispersion since concentrations cannot increase). The baseline and low porosity scenarios take 7,000 days to reach their maximum concentration. High porosity, high dispersivity, low recharge and high recharge all take longer with low recharge and high porosity taking the longest at 10,600 days. Low dispersivity takes less time at 6,600 days. Low porosity, high dispersivity and high recharge take less time to reach first arrival than the 880 days the baseline scenario needs and high porosity, low dispersivity and low recharge taking longer. High porosity takes more than twice as long to reach first arrival at 1,900 days.

The baseline scenario maximum concentration at a distance of 4,000 ft is 1.00. High porosity, high dispersivity and high recharge have lower maximum concentrations with high recharge having the lowest at 0.92. The baseline scenario time to maximum concentration is 20,000 days. Low porosity and high recharge both have lower times with high recharge having the lowest at 13,900 days. High porosity, low dispersivity, high dispersivity and low recharge scenarios take longer to reach the maximum concentration with high porosity taking the longest at 24,800 days. The baseline and low recharge scenarios take the same time for first arrival at 14,000 days. The high porosity scenario takes longer for the first arrival at 15,300 days and low porosity, low dispersivity, high dispersivity, and high recharge take less time with high recharge taking the least time at 12,400 days.

The baseline scenario maximum concentration for low porosity, low dispersivity, and low recharge at 6,000 ft is 0.99. High porosity, high dispersivity and high recharge take less time to reach maximum concentration at 0.98, 0.98 and 0.91, respectively. Low porosity, high porosity, high dispersivity and low recharge all take longer to reach maximum concentration than the baseline scenario of 25,000 days. Low dispersivity and high recharge scenarios take less time with high recharge taking the least amount of time at 16,800 days. All the scenarios except for high porosity take less time than the baseline of 15,500 days to reach first arrival with high recharge taking the least at 13,100 days. The high porosity scenario takes 17,900 days which is just over 2,000 days longer than the baseline.

The maximum concentration of the baseline and low recharge scenario at a distance of 8,000 ft is 0.95. the low porosity and low dispersivity scenarios are 0.97 and 0.96, respectively. The high porosity, high dispersivity and high recharge scenarios maximum concentrations are all less with high recharge being significantly less at 0.55. The time to maximum concentration for the baseline scenario is 28,000 days. The low porosity and high recharge scenarios take less time at 26,300 and 21,100, respectively. The high porosity, low dispersivity, high dispersivity and low recharge scenarios take longer to reach the maximum concentrations with high porosity taking the longest at 33,200 days. Low porosity and high recharge scenarios take less time to the first arrival than the baseline and low recharge scenarios with the baseline taking 20,500 days and the low porosity and high recharge taking 17,200 and 16,400, respectively. High porosity and low dispersivity scenarios take more time at 25,200 and 20,800 respectively.

Figure 3 shows the location on Woodland Creek where the sensitivity analysis was performed. At this location the baseline and low recharge scenarios maximum concentration is 0.75. The low porosity and high dispersivity have higher maximum concentrations at 0.78 and 0.79, respectively. High porosity, low dispersivity and high recharge have lower maximum concentrations with high recharge having the least at 0.57. The time to reach the maximum concentration for the baseline, high dispersivity and low recharge scenarios is 27,000 days. Low porosity, low dispersivity and high recharge scenarios take less time with high recharge taking the least time at 17,500 days. The high porosity scenario takes more time to reach the maximum concentration at 30,300 days. The time to the first arrival for the baseline and low dispersivity is 16,800 days. Low porosity, high dispersivity, low recharge and high recharge scenarios take less time to reach first arrival at 14,700, 16,400, 16,500 and 13,900, respectively. The high porosity scenario takes more time to reach first arrival at 21,900 days.

As shown on Table 12 at a distance of 200 feet the high recharge and high porosity was changed from baseline maximum concentration of 1.00 to 0.96 and 0.98, respectively. It took 12,000 days to reach the maximum concentration for the baseline scenario. The high recharge scenario has a shorter time to maximum concentrations of 9,200 days. Low porosity, high porosity, low dispersivity, high dispersivity and low recharge take a longer time to reach the maximum concentration with high porosity taking the largest time of 23,000 days. The time to first arrival for the baseline scenario is 250 days. Low dispersivity, high dispersivity, low recharge and high recharge remain similar to the baseline scenario at 260, 230,260 and 240 days, respectively. The low porosity and high porosity scenarios had the largest change taking 130 and 490, days respectively.

The baseline maximum concentration at a distance of 1,000 ft and 2,000 ft was 0.99 with all scenarios having the same result except low dispersivity and high recharge which had a maximum concentration of 1.00 and 0.97, respectively for 1,000 ft and high recharge having 0.93 for 2,000 ft. The time to maximum concentration was greater for all scenarios than the baseline of 13,000 days for the 1,000 ft with the high porosity taking the longest at 20,800 days. The baseline for the 2,000 ft time of maximum arrival is 15,000 ft with only the high recharge being less than the baseline scenario at 12,400 days. The time to first arrival for the baseline scenario is 570 days for the 1,000 ft and 1,000 days for the 2,000 ft. Low dispersivity, high dispersivity, low recharge and high recharge remain similar to the baseline scenario for both

distances. Low porosity and high porosity scenarios had the largest change taking 290 and 1,150 days, respectively for the 1,000 ft and 500 and 2,250 ft, respectively for the 2,000 ft.

The baseline scenario maximum concentration at a distance of 4,000 ft is 0.96. High porosity, high dispersivity and high recharge have lower maximum concentrations with high porosity having the lowest at 0.90. The baseline scenario time to maximum concentration is 43,000 days. All scenarios have lower times with low porosity having the lowest at 32,000 days. The baseline scenario takes 6,000 days for the first arrival. The high porosity scenario takes longer for the first arrival at 7,300 days and low porosity, low dispersivity, high dispersivity, and high recharge take less time with the low porosity taking the least time at 2,250 days.

The maximum concentration for the baseline and low recharge scenarios at 6,000 ft is 0.93. High porosity, high dispersivity and high recharge take less time to reach maximum concentration at 0.86, 0.91 and 0.89, respectively. The baseline time to max concentration is 43,000 days. All other scenarios take less time to reach the max concentration with low porosity taking almost 20,000 days less than the baseline at 25,600 days. The time to first arrival for the baseline and low dispersivity scenarios is 4,800 days. High dispersivity and low recharge all take longer to for the first concentration to reach at 8,500 and 5,100 days. Low porosity, high dispersivity and high recharge all take less time for the first arrival to reach with low porosity taking the least amount of time at 2,250 days.

The maximum concentration of the baseline and low recharge scenario at a distance of 8,000 ft is 0.88. The low porosity and low dispersivity scenarios are both slightly above the baseline at 0.89. The high porosity, high dispersivity and high recharge scenarios maximum concentrations are all less with high porosity being at 0.81. The time to maximum concentration for the baseline scenario is 43,000 days. All of the scenarios take less time than the baseline to reach the maximum concentration with the low porosity scenario taking significantly less time at 25,200 days. The baseline, low dispersivity and high dispersivity scenarios all have a time to first arrival of 4,400 days. Low porosity and high recharge scenarios take less time to the first arrival than the baseline at 2,250 and 4,000 days, respectively. High porosity and low recharge scenarios take more time at 8,500 and 5,100 days, respectively.

Figure 4 shows the location on McAllister Creek where the sensitivity analysis was performed (the location where EPCs were calculated as discussed in Section 3). At this location the baseline and low recharge scenarios maximum concentration is 0.32. The low porosity and low dispersivity have higher maximum concentrations at 0.36 and 0.33, respectively. High porosity, high dispersivity and high recharge have lower maximum concentrations with high porosity having the least at 0.25. The time to reach the maximum concentration for the baseline scenario is 38,000 days. Low porosity and high recharge scenarios take less time with low porosity taking the least time at 11,700 days. The high porosity, low dispersivity, high dispersivity and low recharge scenarios takes more time to reach the maximum concentration 42,7000, 38,300, 38,300 and 38,300 days, respectively. The time to the first arrival for the baseline, high dispersivity and low dispersivity is 4,800 days. Low porosity and high recharge scenarios take less time to reach first arrival at 2,250 and 4,400 days, respectively. The high porosity and low recharge scenarios take more time to reach first arrival at 9,200 and 5,100 days respectively.

The high recharge scenario for both the Q_{va} and Q_c result in a decrease in overall maximum concentration, time to maximum concentration and time to first arrival. Low recharge scenario for the Q_{va} tends to have similar results with the baseline scenario with the exception of the time to maximum concentration which has increased slightly. The low recharge Q_c is also similar to the baseline however the time to maximum concentration fluctuates between longer and shorter than the baseline at different distance. Low dispersivity for both the Q_v and Q_c have generally similar results with all values being close the baseline scenario results. The low dispersivity Qva seems to take less time at short distances to reach the maximum concentration but then at 6,000 ft switch to taking longer. There is a similar trend in the Qc but reversed. The high dispersivity in both the Qva and Qc are similar to the baseline scenarios with the exception of the higher dispersivity in the Qc at longer distances (6,000 ft and 8,000 ft) where the maximum concentration, time to reach the maximum concentration and first arrival time are all less than the baseline scenario. Low porosity in the Qva and Qc generally take less time to reach the maximum concentration and time to first arrival. The maximum concentration for both layers are similar to the baseline. The high porosity scenarios in the Qv and Qc tend to take more time in reaching the time to maximum concentration and time to first arrival.

Figures G 1 (a and b) to G-6 (a and b) in Appendix G are breakthrough curves for each of the parameters (porosity, dispersivity and recharge) at each distance represented in Table 11 and Table 12. The breakthrough curves are a visual representation of the data above, which help to see trends in the different scenarios by layer. The blue line is the Baseline run (Calibrated run), the orange line is the low run (a decrease in the baseline parameter) and the grey line is the high run (an increase in the baseline parameter).

6.3 Sensitivity Analyses Results Discussion

Based on the breakthrough curves at concentric circle locations and the creeks of interest, the changes to porosity resulted in differences in first arrival times. The lower porosity simulation allowed faster movement of concentration relative to the baseline and higher porosity simulations. The difference in arrival times is more drastic at further distances from the recharge location as the effect on travel time compounds. The porosity change affected the arrival times as well as overall trend of the breakthrough curves for the Q_C more than the Q_{va}.

The changes to modeled dispersion (Figures G-3a, G-3b, G-4a and G-4b) did not have a significant effect on the arrival times for initial or max concentration. The magnitude of concentrations decreased with higher dispersion and increased from lower dispersion. The larger discrepancies occur farther from the discharge point and in the Q_C more than the Q_{va}.

The baseline scenario and the low recharge scenario are nearly identical in breakthrough curve trend, with some minor differences in Q_C that do not significantly affect the timing or concentrations. The high recharge scenario results in earlier first arrivals and initial peaks in nearly every location for both aquifers. Aside from the spike of decreased concentration due to numerical dispersion from changing model simulations around 18,000 days, many of the curves show a concentration drop in the 12,000-25,000-day range. In nearly every location, the concentration trending to the end of the simulated time is less than both the baseline and low-recharge scenarios.

The results of the sensitivity analyses show that in general, variability in porosity, dispersivity and recharge could change the time of first arrival and time of maximum concentration at each of the locations used to estimate EPC; however, the ultimate maximum concentrations at these locations will be similar. This is especially true at the locations that are closer to the Hawks Prairie recharge facility. For the most part, increases in these parameters lengthen the travel times, so any attenuation would be increased if the parameters are underestimated. Based on the sensitivity analyses, the biggest concern would be if effective porosity is overestimated, as the travel times to the closer EPC locations will be shorter, so there would be less time for attenuation to occur. First arrivals at 200 and 1,000 feet are roughly one third to one half shorter for the scenario assuming 0.5 times the calibrated effective porosity.

Given the faster travel times with lower effective porosity it is more likely that residual chemicals would not attenuate as much before arriving at the nearby EPC locations (200 and 1,000 feet in both the Q_{va} and the Q_c). While arrivals are also shorter at the further points, the attenuation will still have sufficient time to occur (for those parameters where attenuation factors have been calculated; otherwise, the maximum concentration is essentially the same, with only the timing being different). Given the reduced travel time for the scenario assuming 0.5 times the effective porosity, those residual chemicals with AFs would increase in concentration at the 200 and potentially 1,000 foot EPC locations by roughly one half to double. However, it is important to note that the baseline, calibrated effective porosity is based on empirical data from the tracer test, so there is low probability that it is overestimated. Because these data were collected mostly from the Q_{va}, effective porosity in the Q_c is more uncertain. However, the range of total porosity from aquifer matrix samples analyzed in 2020 shows that the Q_{va} and the Q_c have similar total porosity ranges, suggesting they would likely have similar effective porosity. Figure 10 shows the total porosity ranges for the Qva, Qf, and Qc.

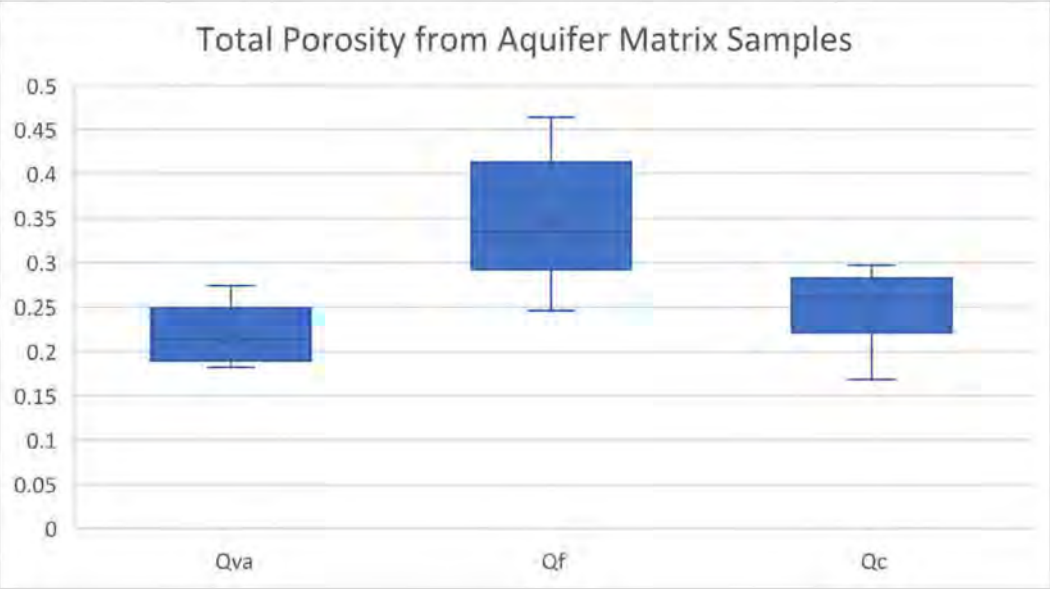

Figure 10 Total Porosity from Aquifer Matrix Samples

7.0 Model Limitations

All models necessarily generalize the dynamic and heterogeneous conditions which they simulate. In doing so, uncertainty is introduced; therefore, the results of modeling must be viewed as a tool to help inform decision making by showing the possible outcomes of educated decisions and not as absolute conditions. Several factors are known to produce uncertainty in the RWIS model that should be acknowledged when reviewing and using the model results:

- Model limitations and assumptions associated with the calibrated steady state flow model and listed in Section 8 of HDR 2019b.
- While annual average recharge values were used for portions of the transient flow modeling, flows to the recharge basins varied throughout the year which could affect groundwater movement in a time frame of days, weeks and months instead of years. The importance of the variability of recharge rates at smaller time frames has not been evaluated.
- The 100-year modeling used current estimates of future recharge rates. The recharge rates that occur in the future will vary from those simulated by the model.
- Pumping that occurs in the model domain was simulated to be constant across the flow simulations (the pumping rates used in the calibrated flow model were used in the transient models). In reality, pumping rates vary based on use and are not constant through time. Changes in pumping will affect groundwater flow direction and potentially the transport of residual chemicals in the groundwater.
- Modeling and calculations involving C/C_0 assumes that the source concentration, C_0 is constant and that the downgradient concentration, C, is a function of the current C_0. The data show us that residual chemical concentrations in the reclaimed water vary over time. The data gathered to characterize C_0 were concurrent with the groundwater samples so are not directly linked to the C in the wells (which would have been introduced at the recharge basin sometime prior to sampling). Note that all uncertainties associated with collecting and analyzing water samples will also affect the uncertainty of the model.
- Similarly, the suite of residual chemicals in the reclaimed water was assumed to be constant; however, the residual chemicals will change through time both because of changes in the use of those chemicals in general and because of changes in treatment processes.

This page intentionally left blank.

8.0 References

Bower, J. C. and R. S. Tjeerdema. 2017. Water and Sediment Quality Criteria Report for Fipronil; Phase III: Application of the pesticide water and sediment quality criteria methodologies. Department of Environmental Toxicology University of California, Davis. Prepared for the Central Valley Regional Water Quality Control Board

Harbaugh, A.W., 2005. MODFLOW-2005, the U.S. Geological Survey modular ground-water model -- the Ground-Water Flow Process: U.S. Geological Survey Techniques and Methods 6-A16.

Hellauer, K., Mergel, D., Ruhl, A., Filter, J., Hubner, Uwe, Jekel, M., Drewes, J.E., 2017. Advancing Sequential Managed Aquifer Recharge Technology Using Different Intermediate Oxidation Processes. Water (Special Issue: Water Quality Considerations for Managed Aquifer Recharge Systems), March 17, 2017.

HDR 2013a. Technical Memorandum – “State of the Science”, LOTT Clean Water Alliance Reclaimed Water Infiltration Study, May 31, 2013.

HDR 2013b. Technical Memorandum – Case Study Summary, LOTT Clean Water Alliance Reclaimed Water Infiltration Study, July 26, 2013.

HDR 2017a. Groundwater Quality Characterization (Task 1.1), LOTT Clean Water Alliance Reclaimed Water Infiltration Study Technical Memorandum, February 7, 2017.

HDR 2017b. Wastewater and Reclaimed Water Quality Characterization (Task 1.3), LOTT Clean Water Alliance Reclaimed Water Infiltration Study Technical Memorandum, February 7, 2017.

HDR 2019a. Draft Technical Memorandum Steady-State Groundwater Development and Calibration (Task 2.1.4), LOTT Clean Water Alliance Reclaimed Water Infiltration Study, July 10, 2019.

HDR 2019b. Tracer Test and Water Quality Monitoring (Task 2.1.3), LOTT Clean Water Alliance Reclaimed Water Infiltration Study, October 30, 2019.

Laws, B.V., Dickenson, E.R.V., Johnson, T.A., Snyder, S.A., Drewes, J.E., 2011. Attenuation of contaminants of emerging concern during surface-spreading aquifer recharge. Science of the Total Environment 409, 1087-1094.

Odenkirken, E. and S. Wente. 2011. Problem Formulation for the Environmental Fate and Ecological Risk, Endangered Species, and Drinking Water Assessments in Support of the Registration Review of Fipronil. U. S. Environmental Protection Agency Office of Pesticide Programs, Environmental Fate and Effects Division, Environmental Risk Branch I.

Tang, Z. and T.S. Ramanarayanan. 2006. Modeling Fate and Transport of Fipronil and Its Metabolites in Surface Water Following Application of Chipco Topchoice@ to Turf. Sponsored by Bayer Crop Science, RTP, NC. Performed by Bayer Crop Science, Stillwell, KS, MRID 46936103.

U.S. Environmental Protection Agrency (USEPA) 2012. *Guidelines for Water Reuse*. 600/R-12/618.

Zheng, Chunmiao and Wang, P. Patrick, 1999. MT3DMS, A Modular Three A Modular Three-Dimensional Multispecies Transport Model Dimensional Multispecies Transport Model, US Army Corp of Engineers.

Appendix A: 2020 Field Investigation Report (separate document)

This page intentionally left blank.

Appendix B: Model Results: Mounding (2006-2020)

This page intentionally left blank.

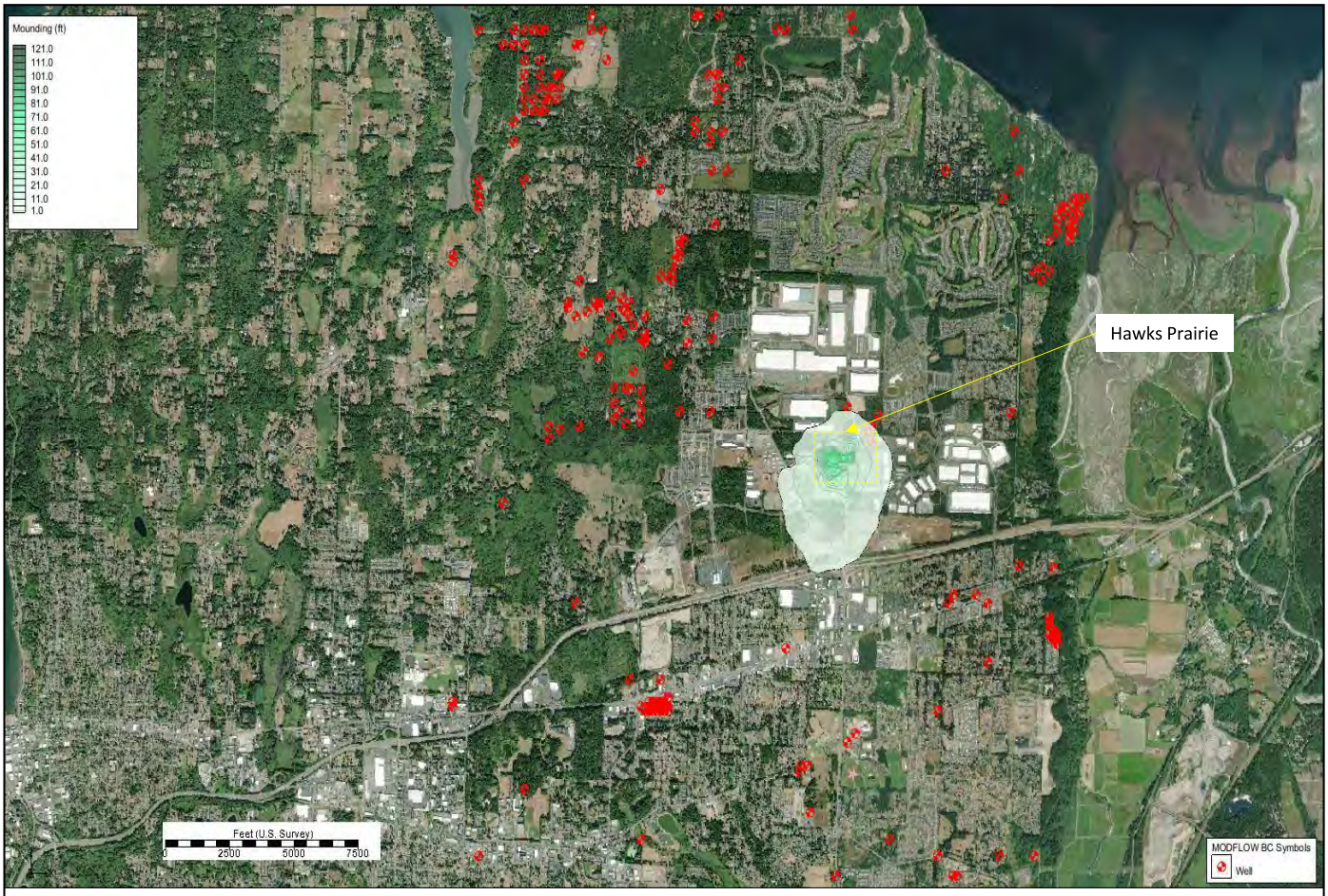

Figure B-1 Q_{va} Groundwater Mounding 2007

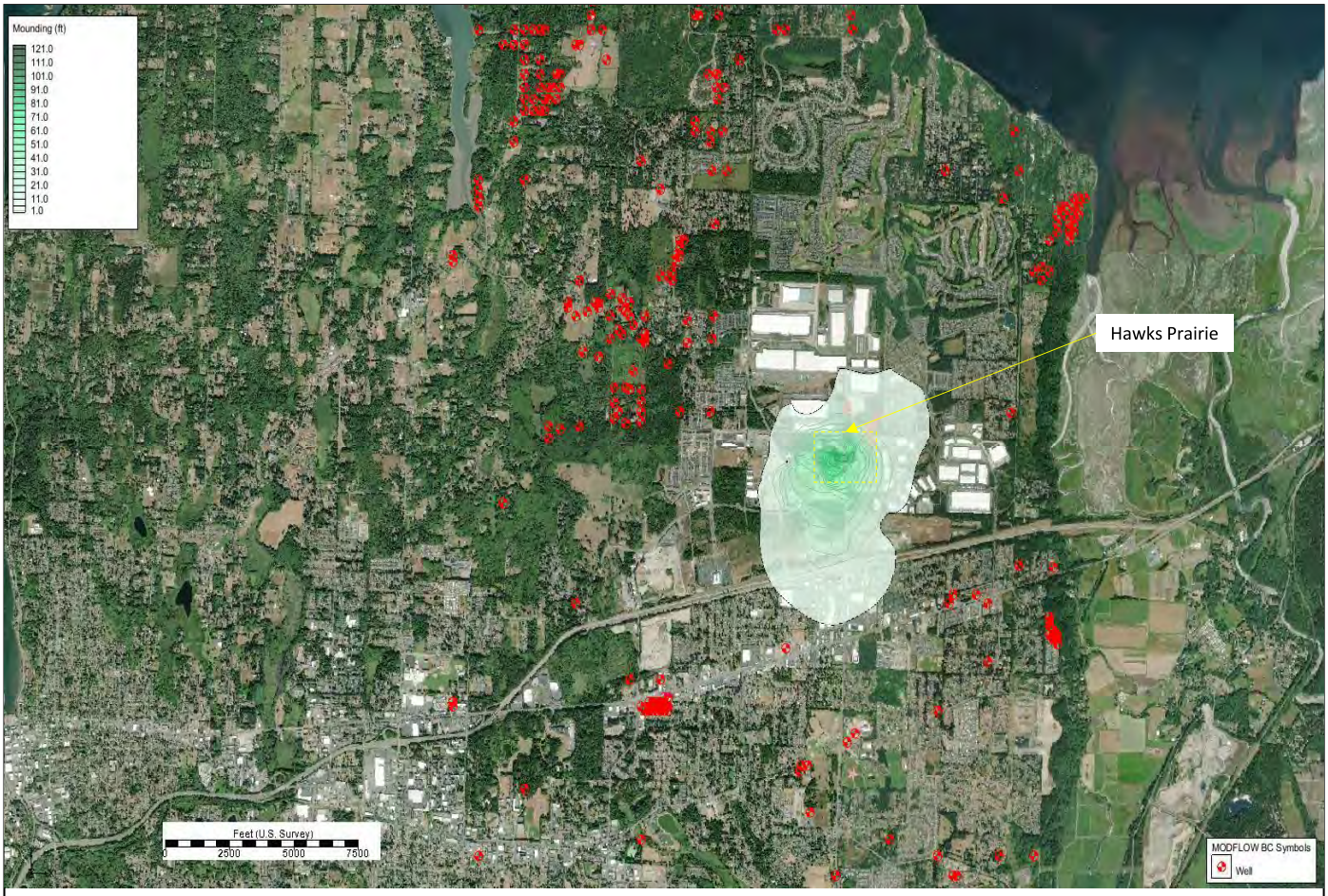

Figure B-2 Q_{va} Groundwater Mounding 2008

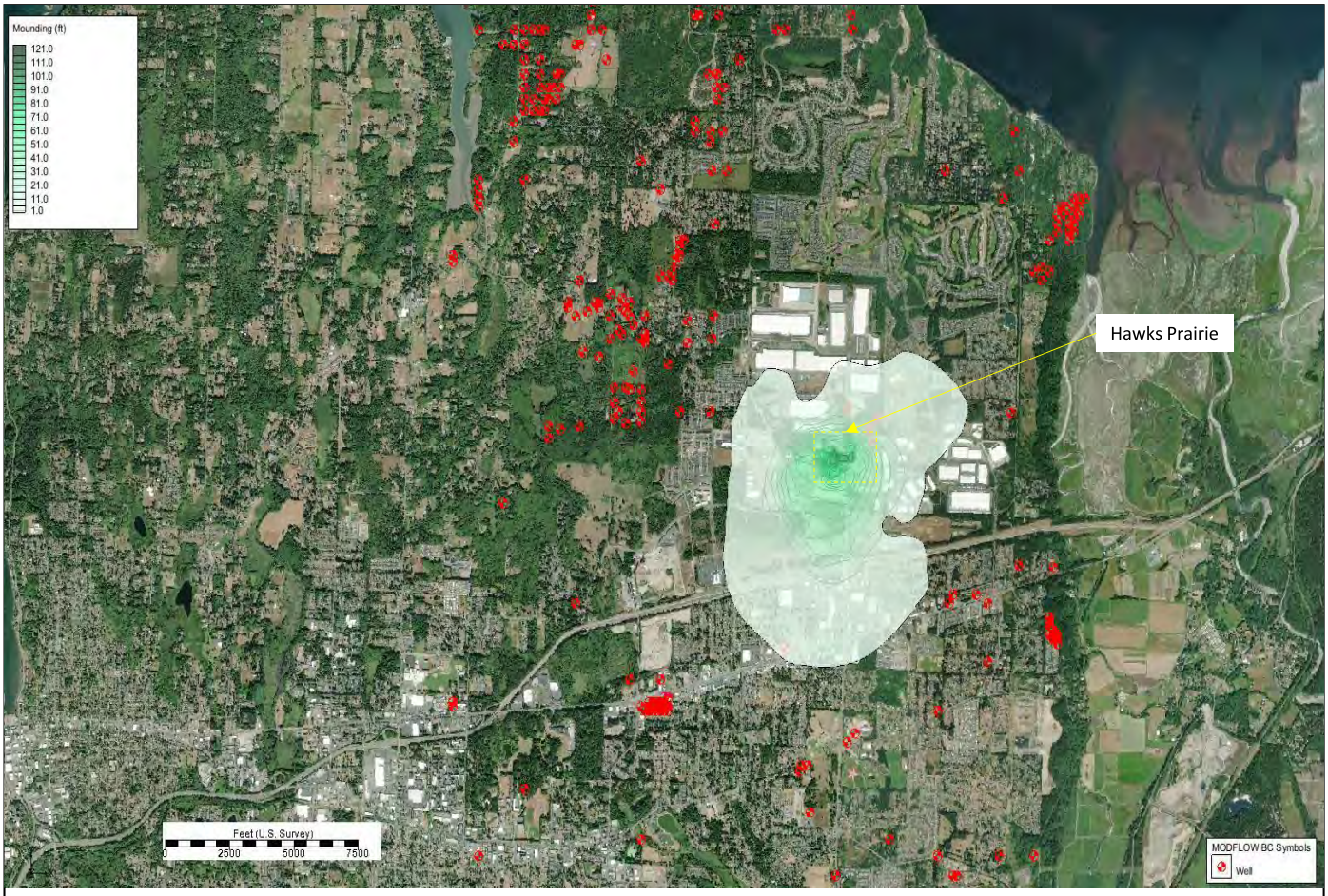

Figure B-3 Q_{va} Groundwater Mounding 2009

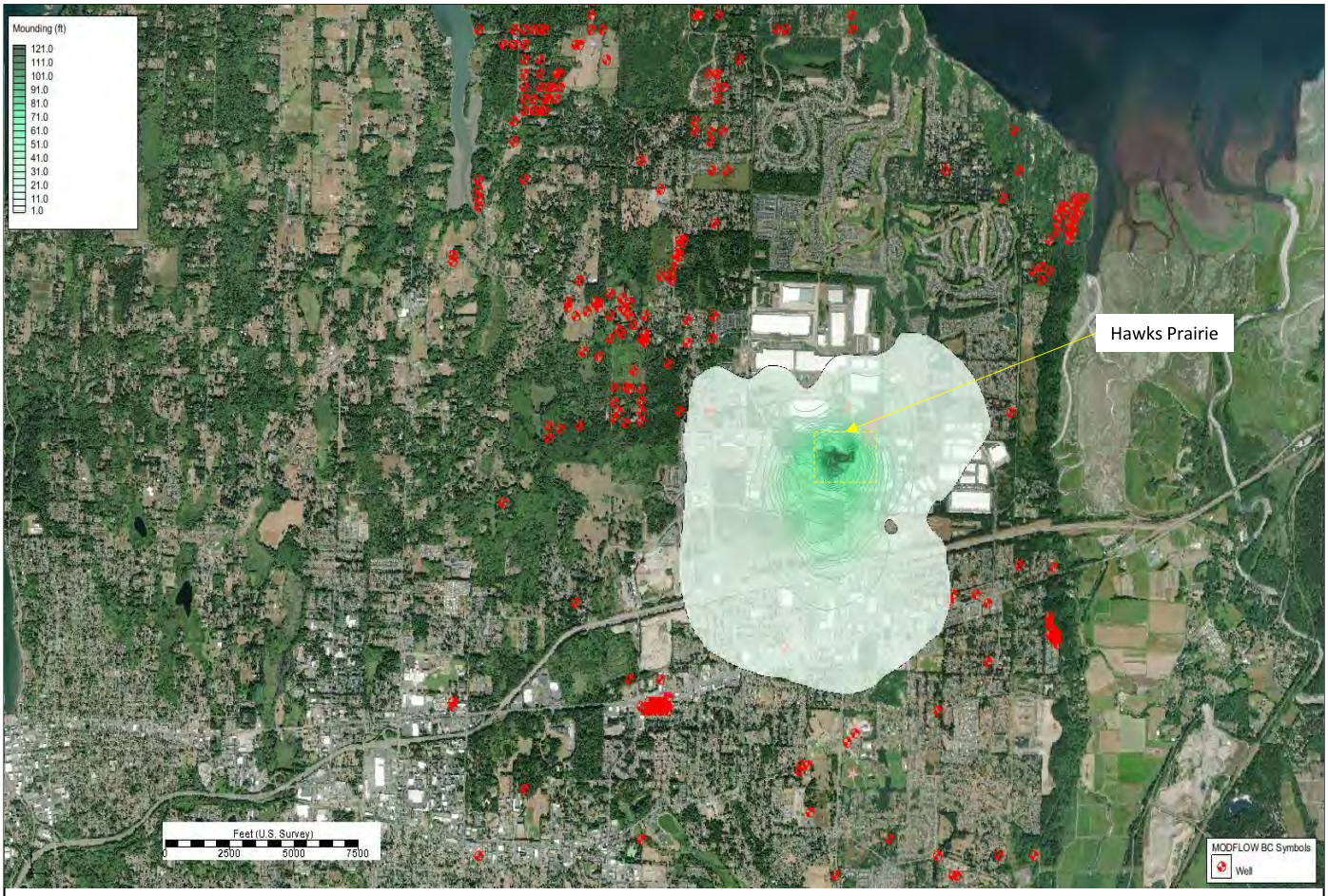

Figure B-4 Q_{va} Groundwater Mounding 2010

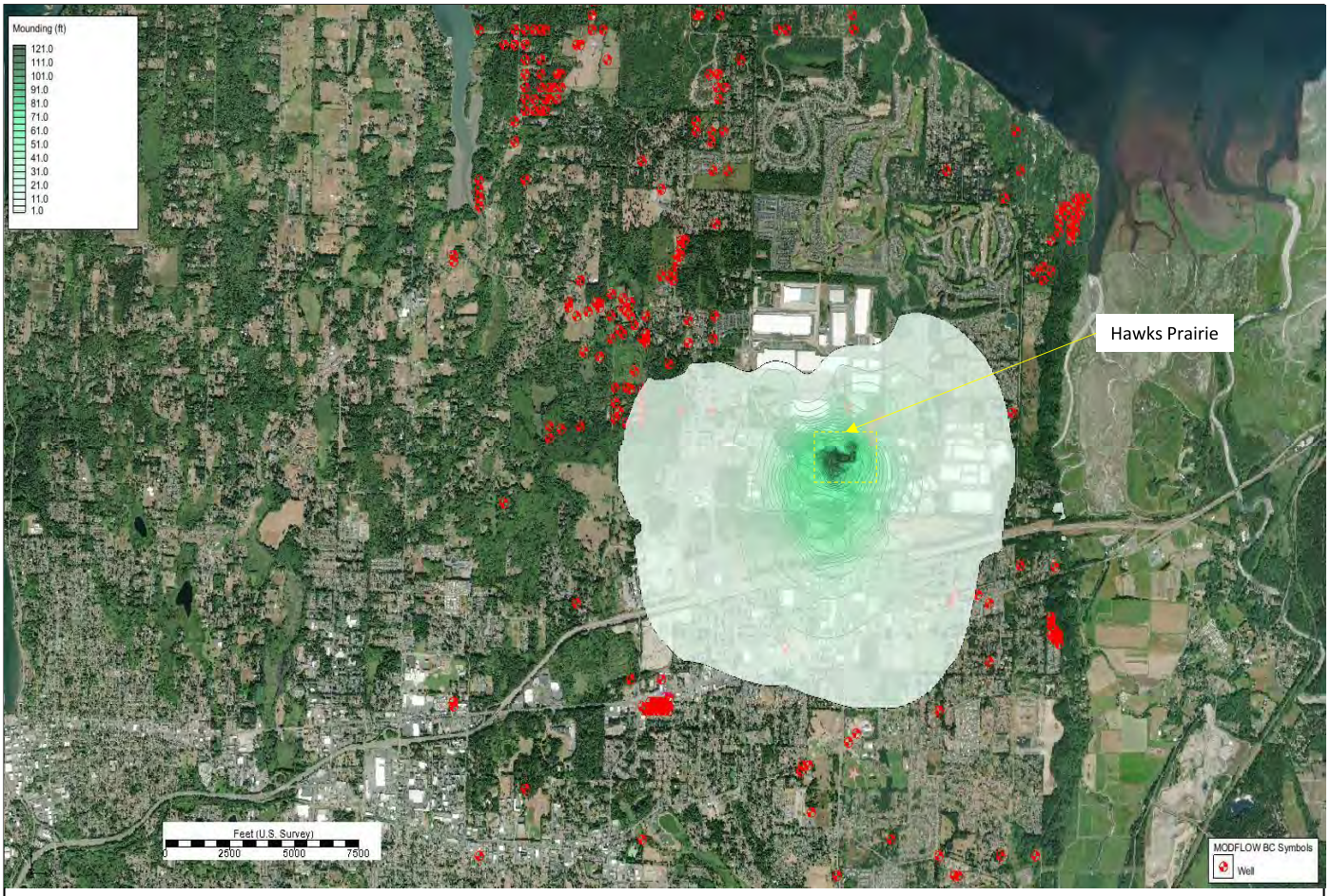

Figure B-5 Q_{va} Groundwater Mounding 2011

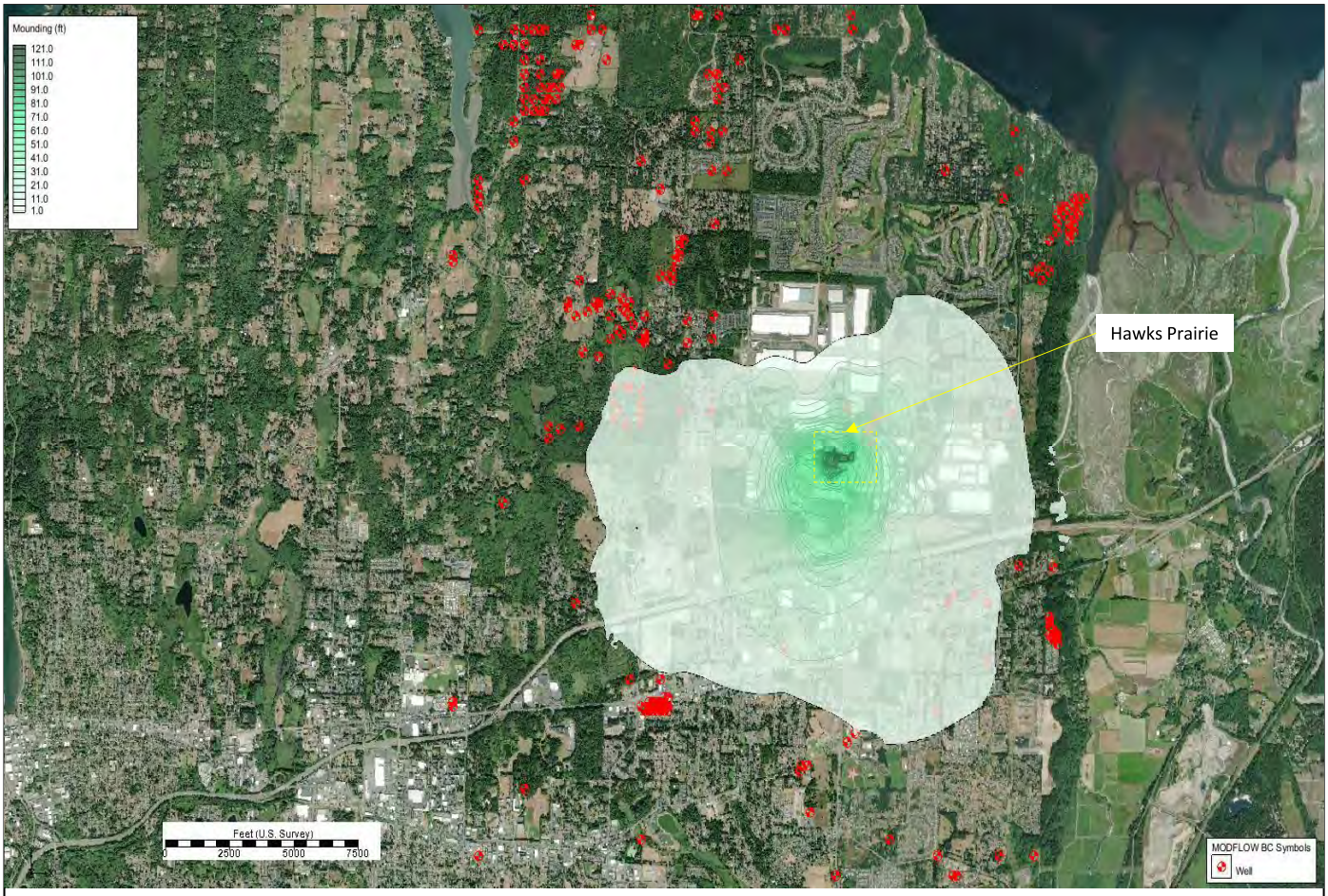

Figure B-6 Q_{va} Groundwater Mounding 2012

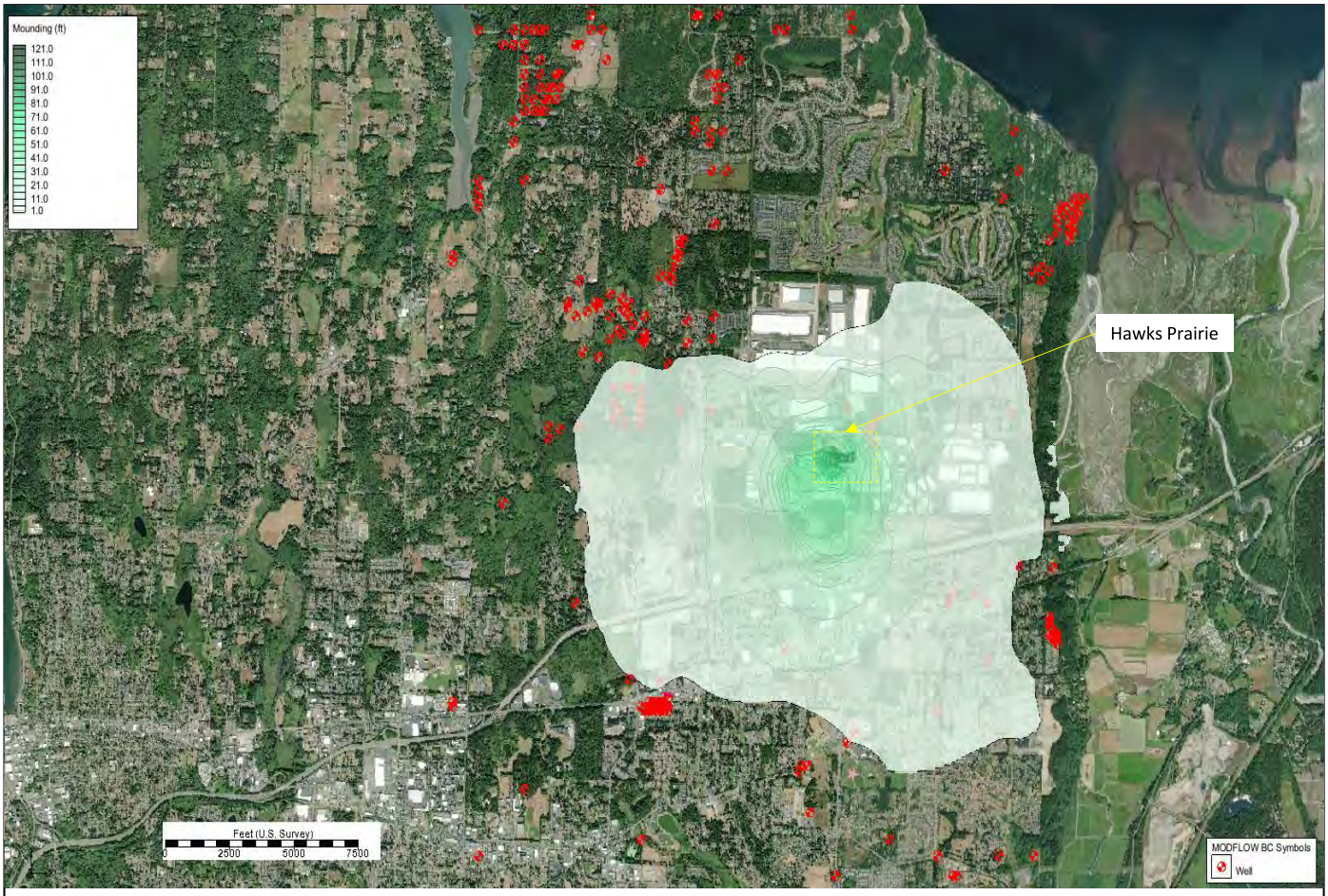

Figure B-7 Q_{va} Groundwater Mounding 2013

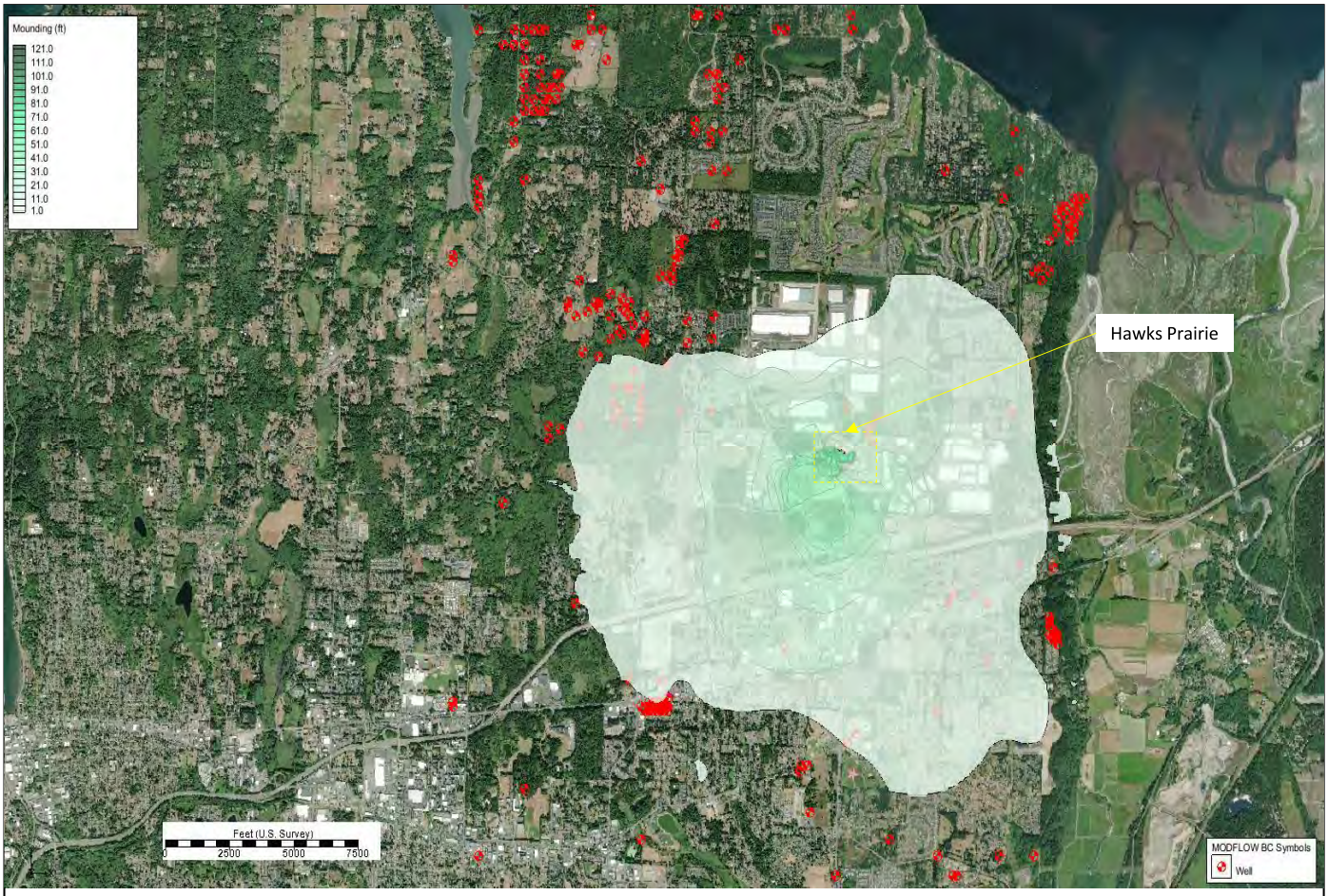

Figure B-8 Q_{va} Groundwater Mounding 2014

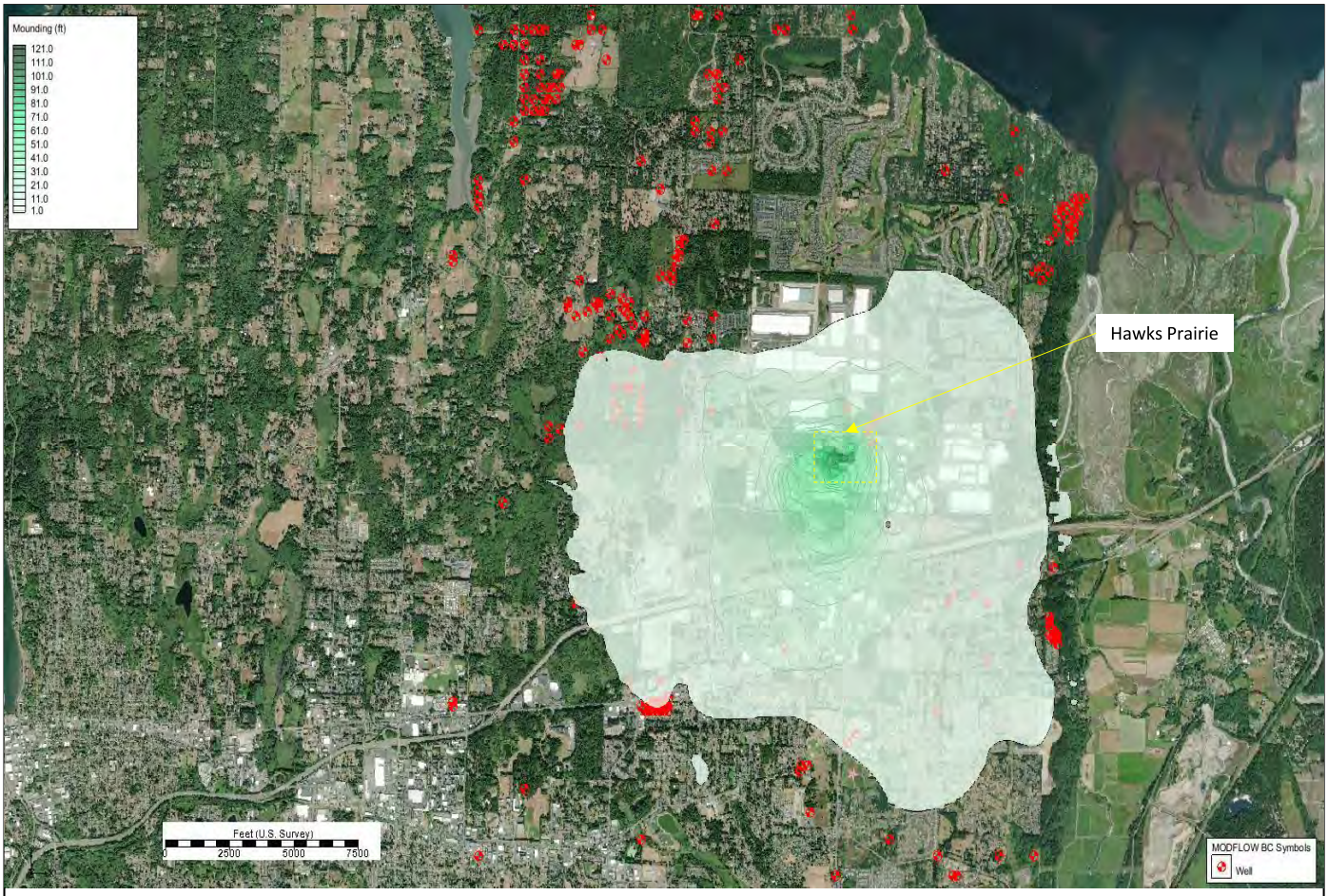

Figure B-9 Q_{va} Groundwater Mounding 2015

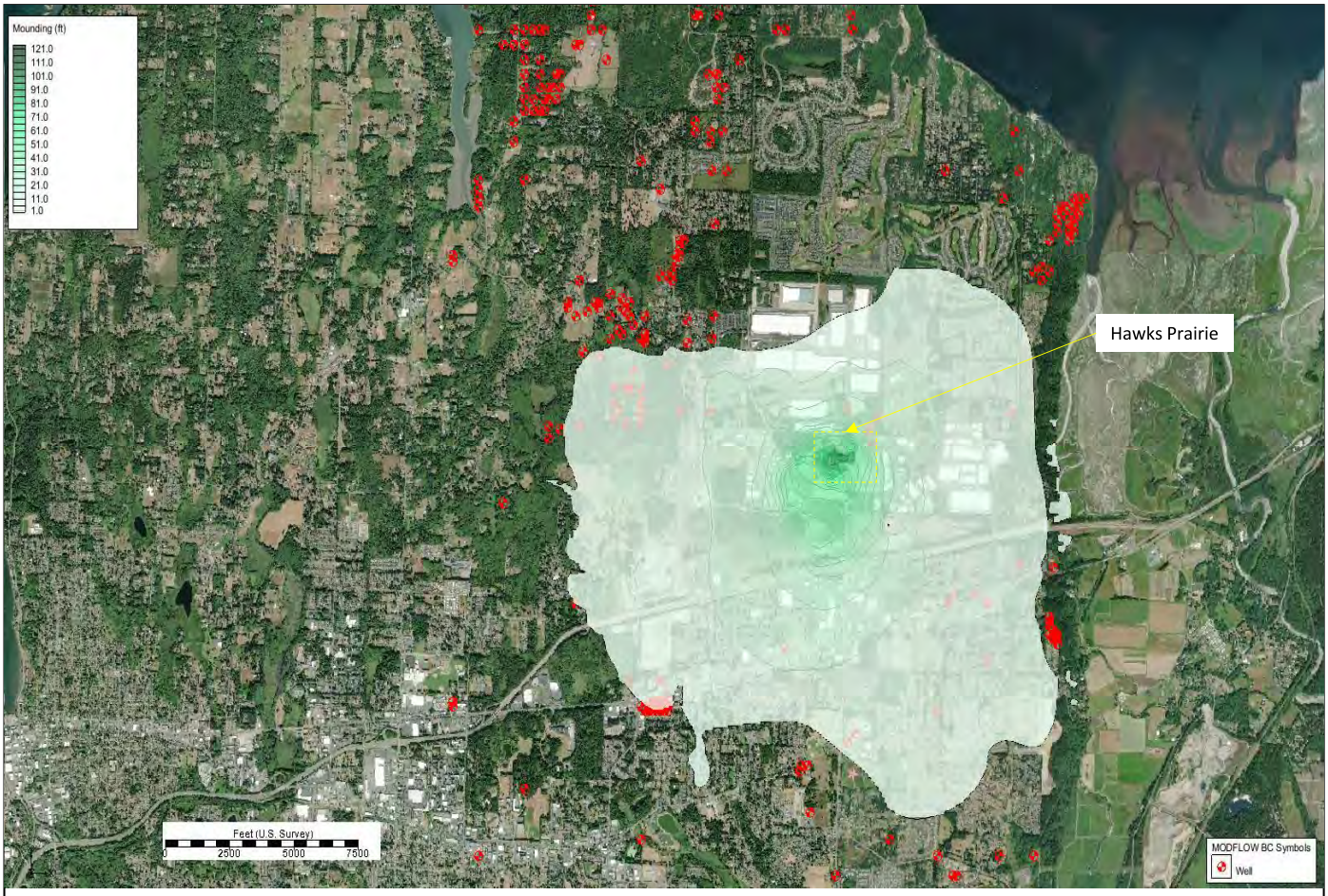

Figure B-10 Q_{va} Groundwater Mounding 2016

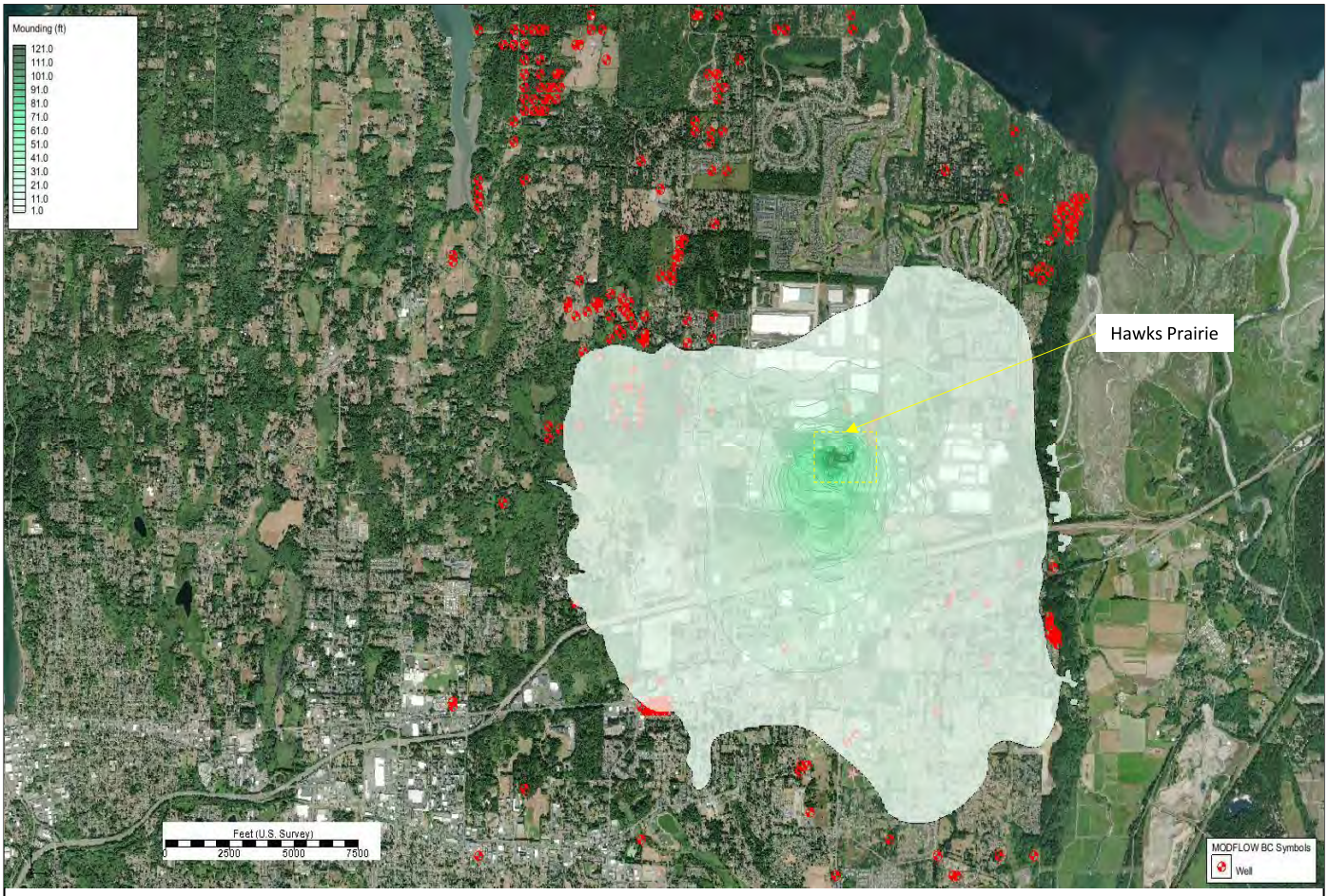

Figure B-11 Q_{va} Groundwater Mounding 2017

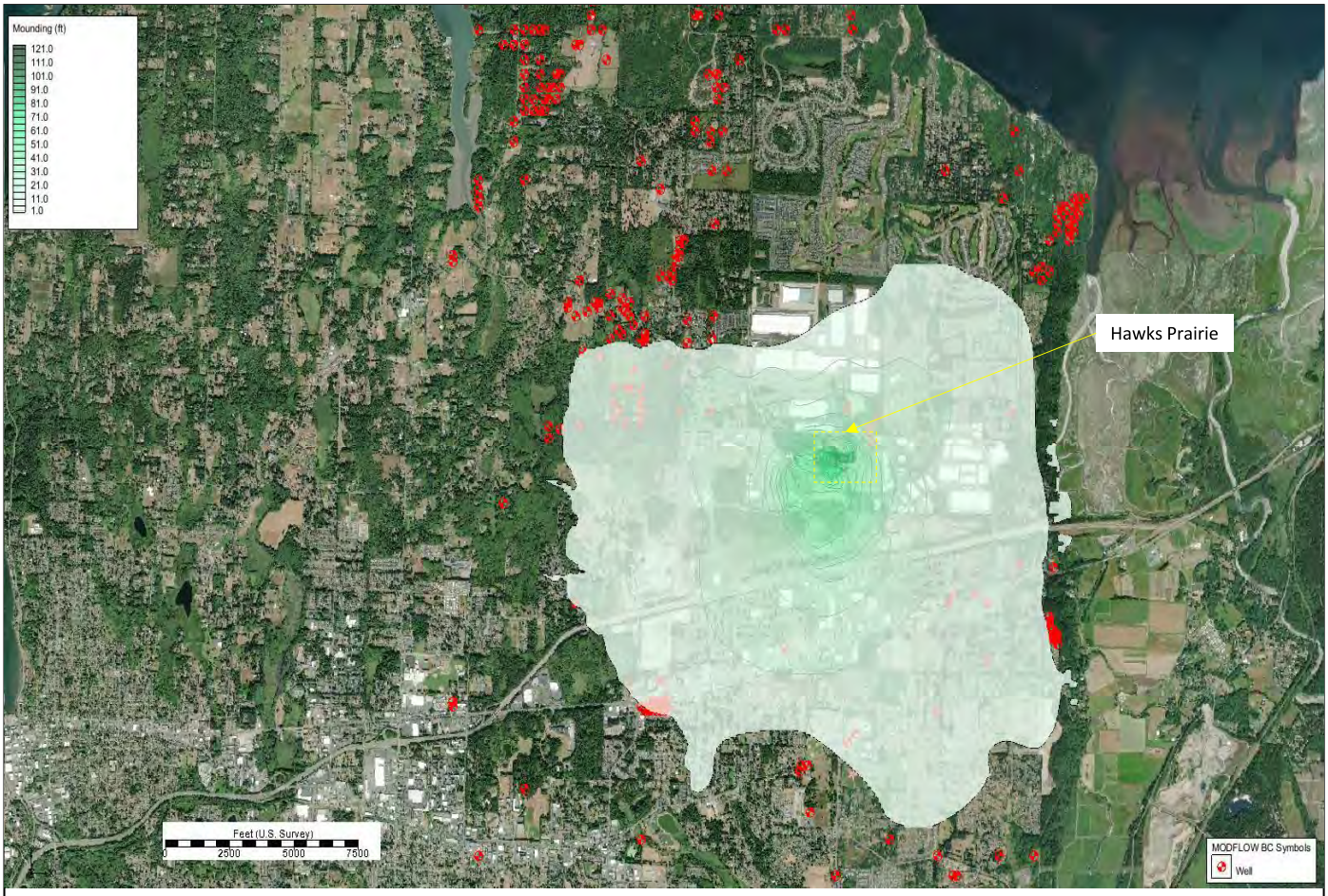

Figure B-12 Q_{va} Groundwater Mounding 2018

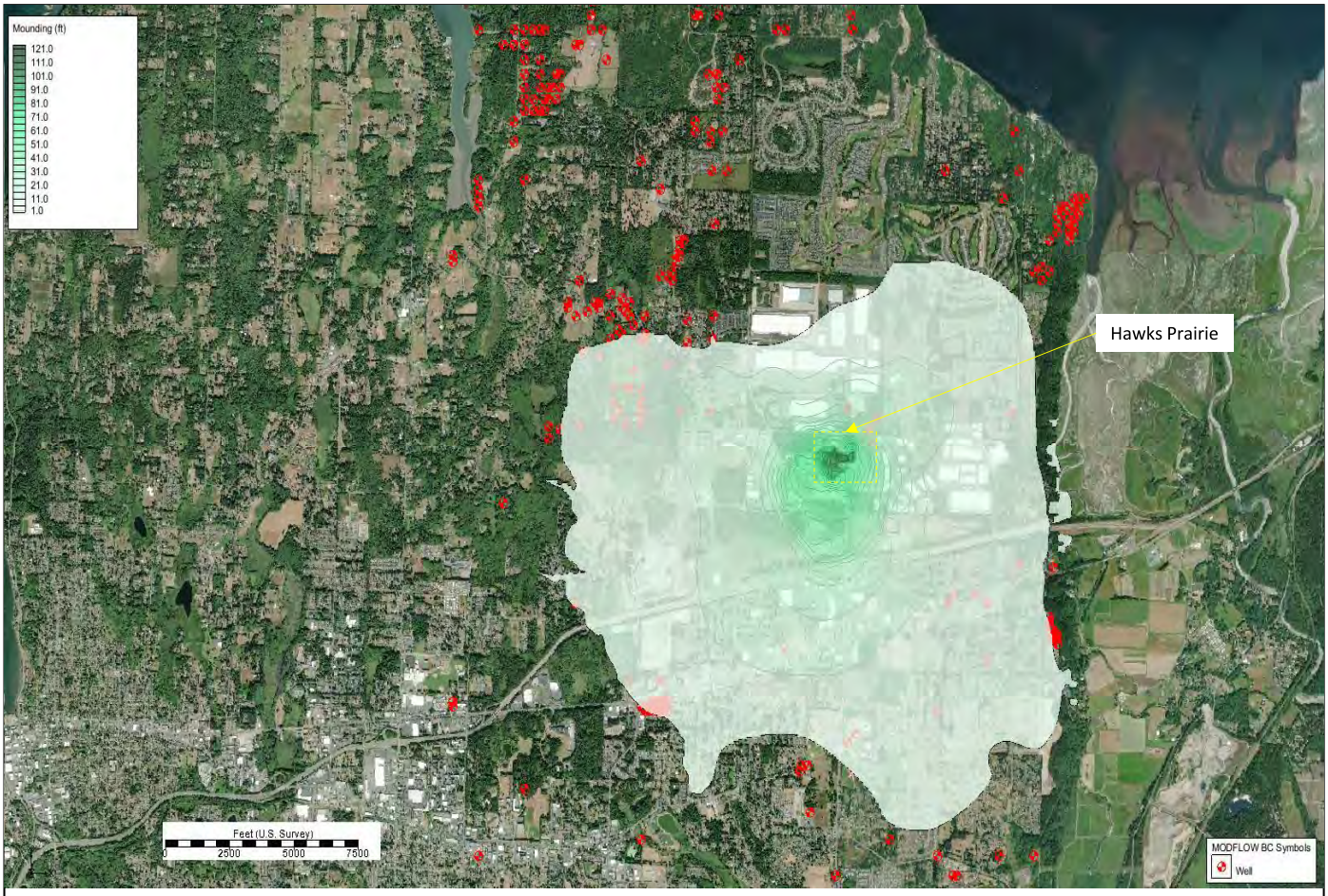

Figure B-13 Q_{va} Groundwater Mounding 2019

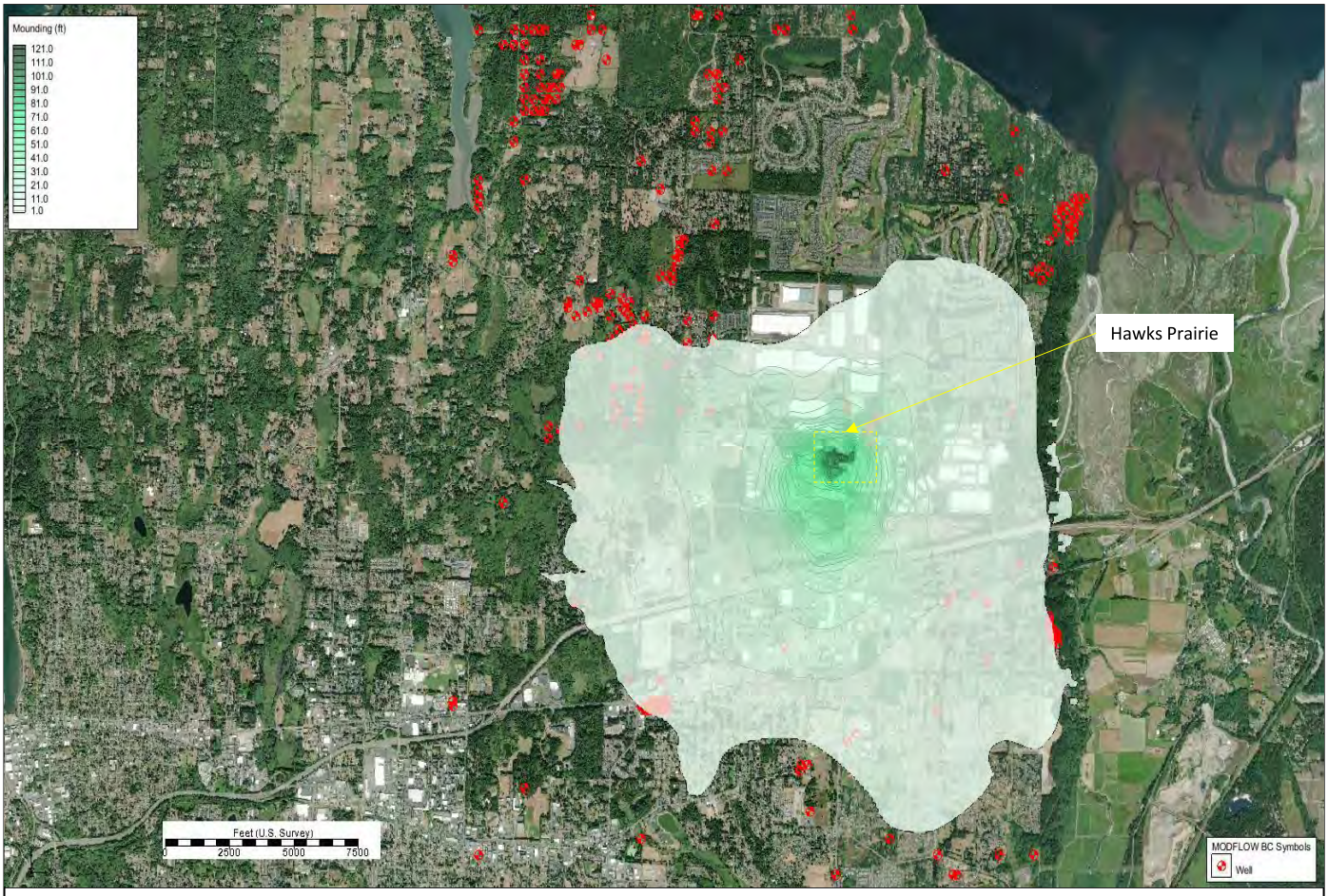

Figure B-14 Q_{va} Groundwater Mounding 2020

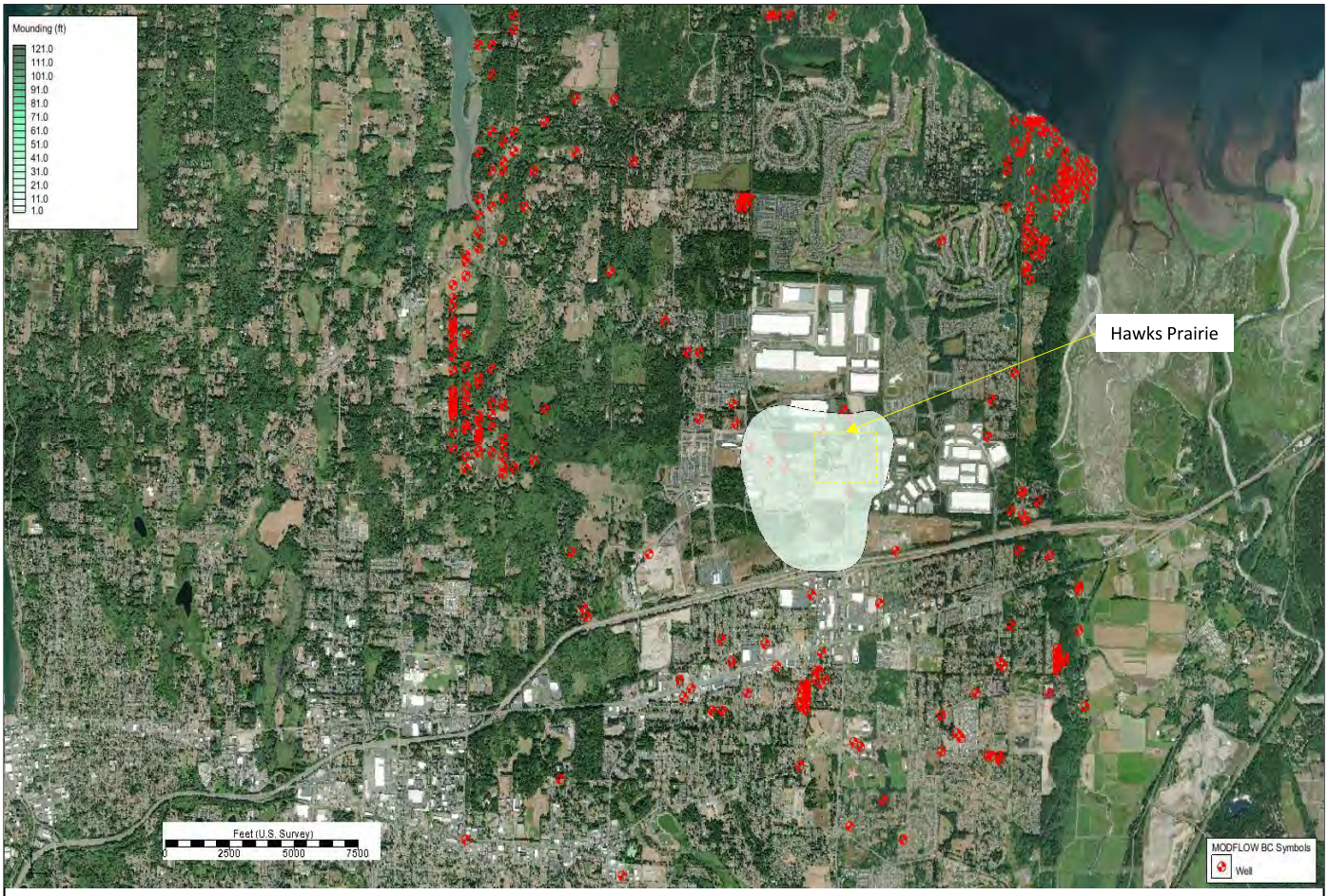

Figure B-15 Q_c Groundwater Mounding 2007

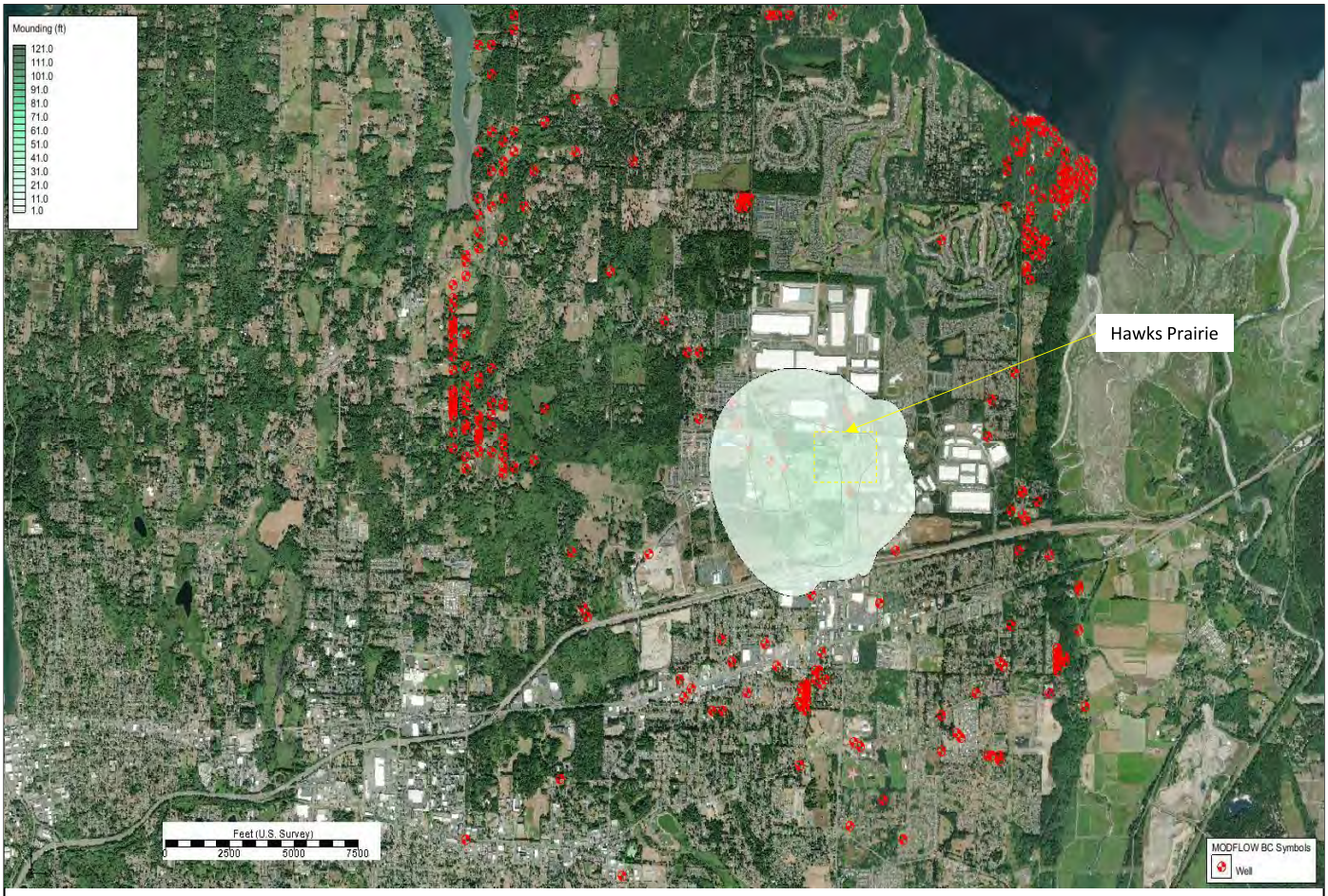

Figure B-16 Q_c Groundwater Mounding 2008

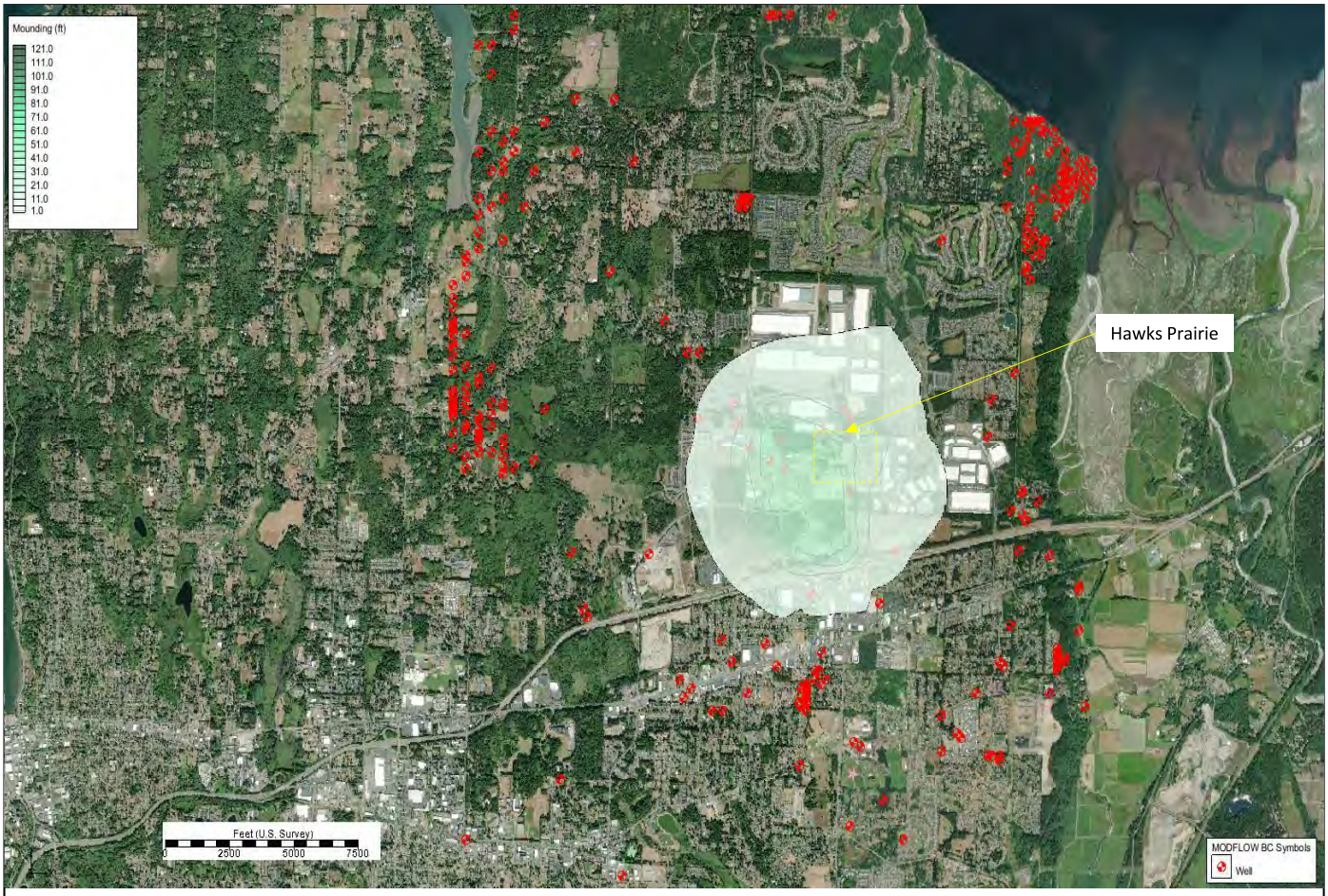

Figure B-17 Q_c Groundwater Mounding 2009

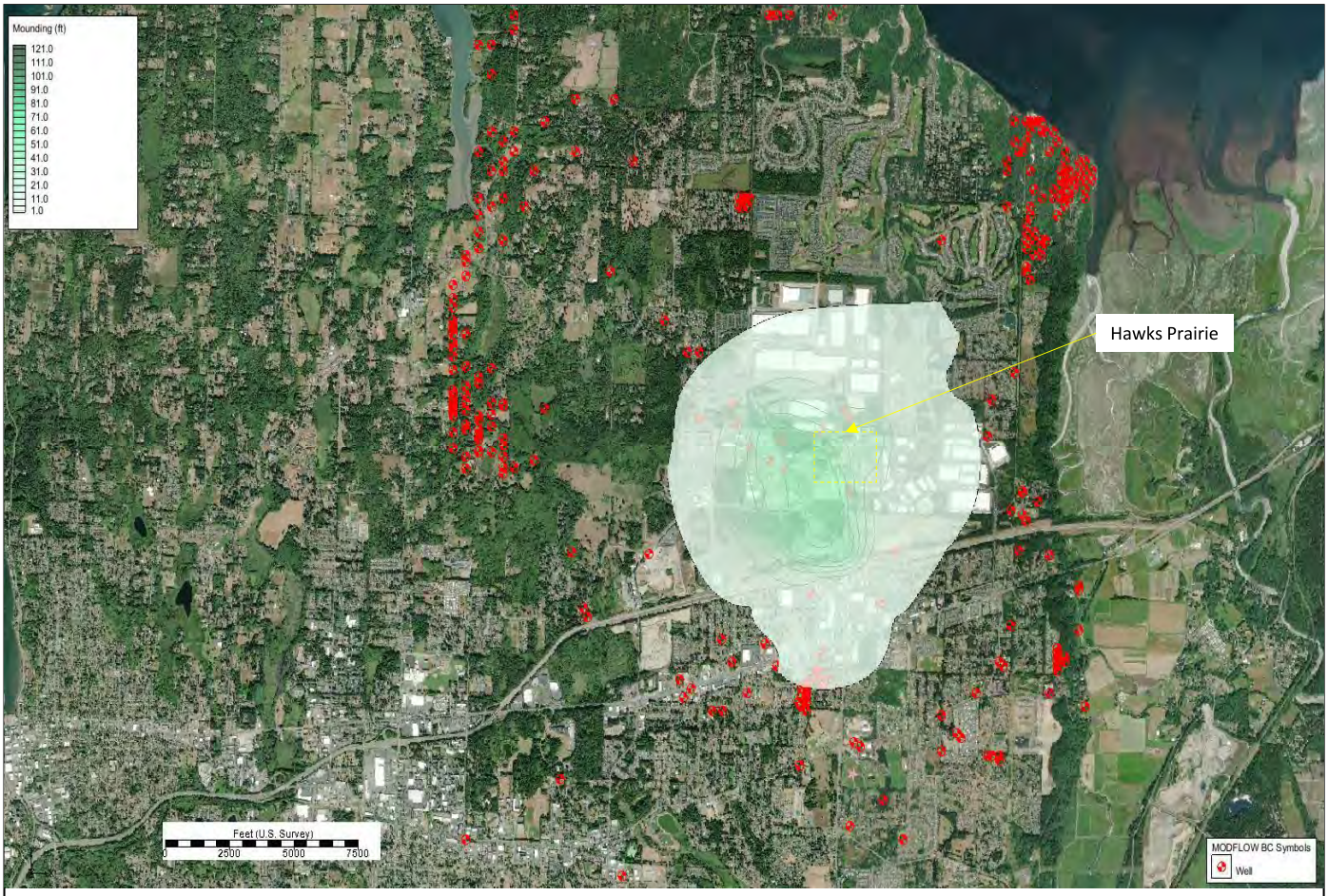

Figure B-18 Q_c Groundwater Mounding 2010

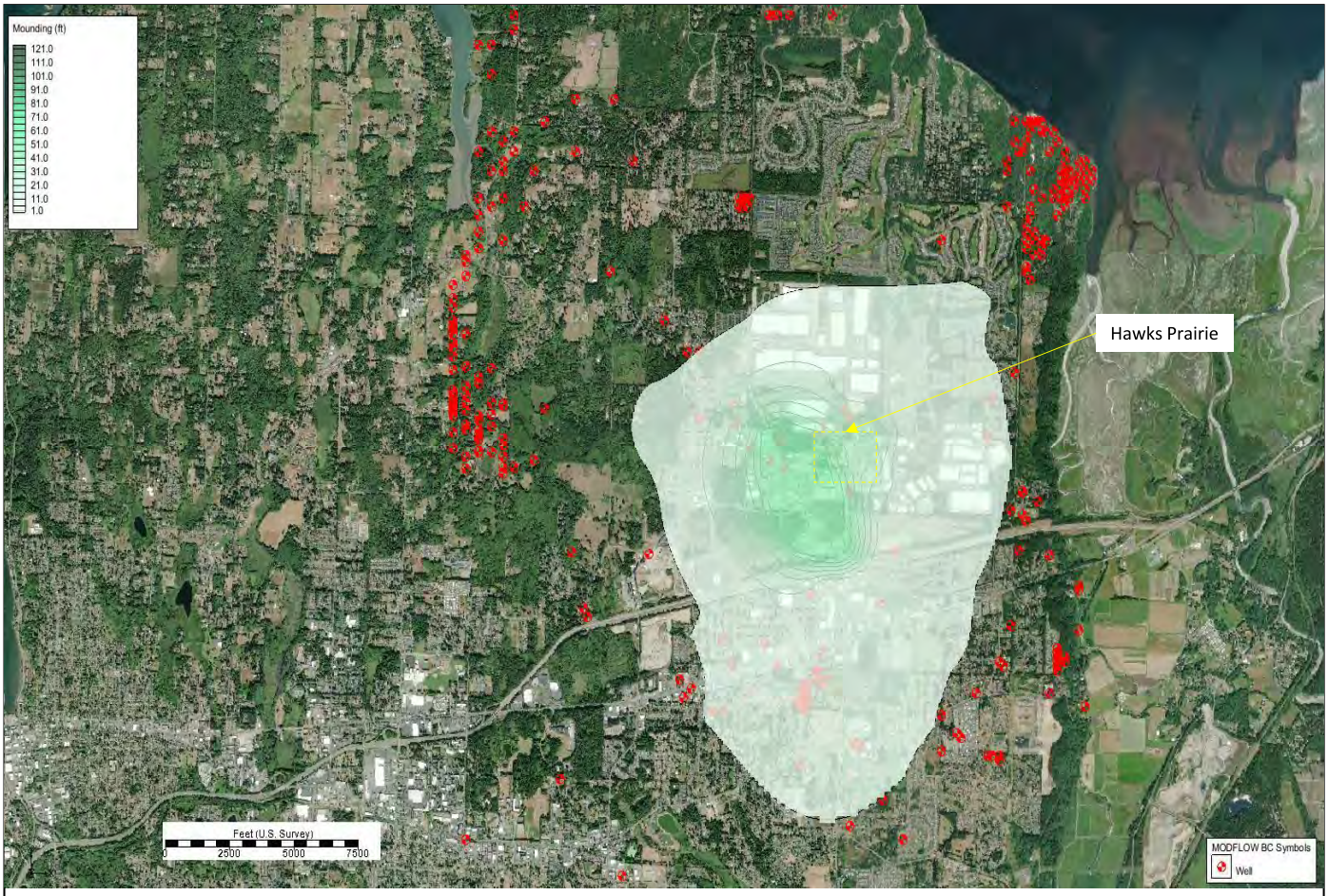

Figure B-19 Q_c Groundwater Mounding 2011

Figure B-20 Q_c Groundwater Mounding 2012

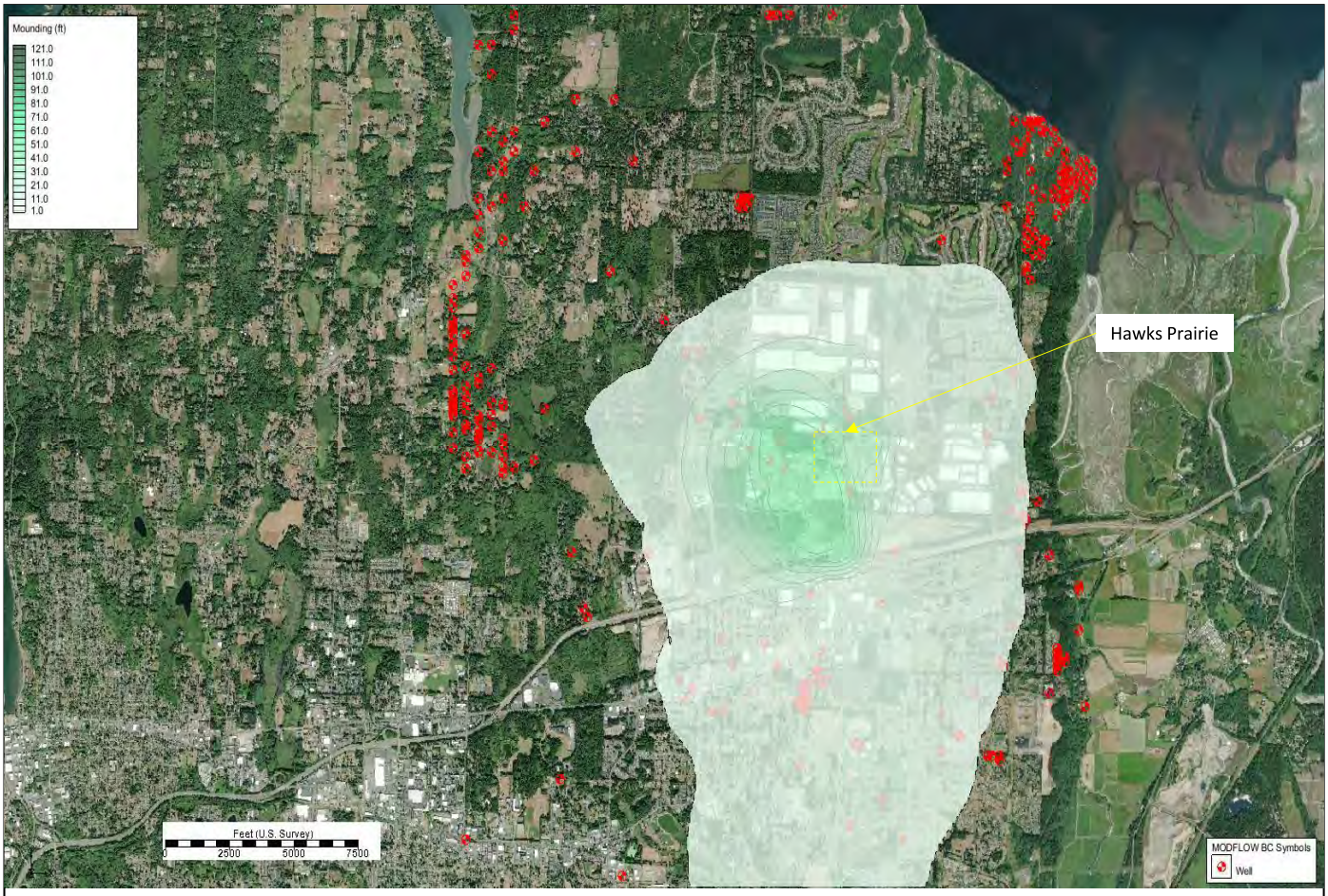

Figure B-21 Q_c Groundwater Mounding 2013

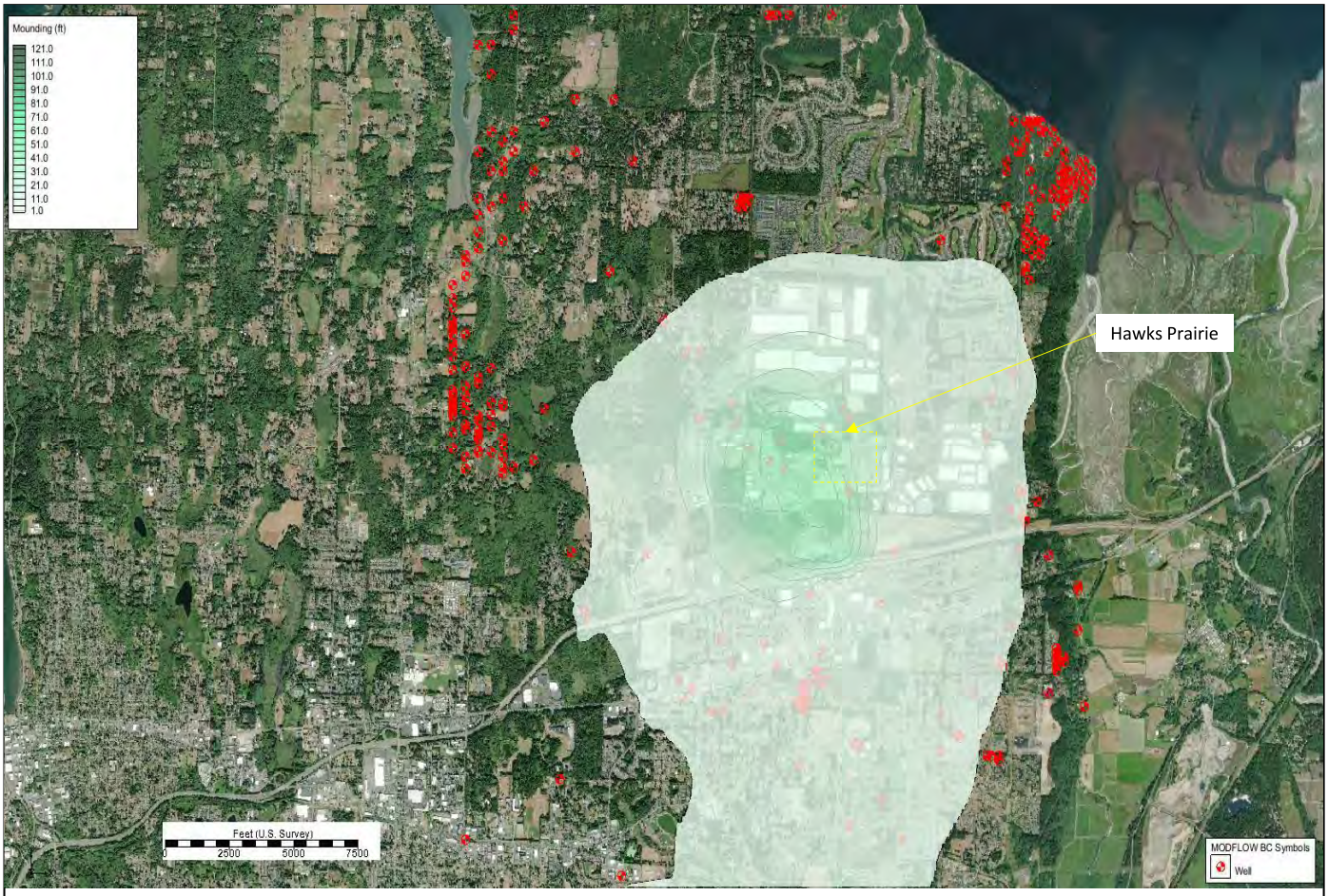

Figure B-22 Q_c Groundwater Mounding 2014

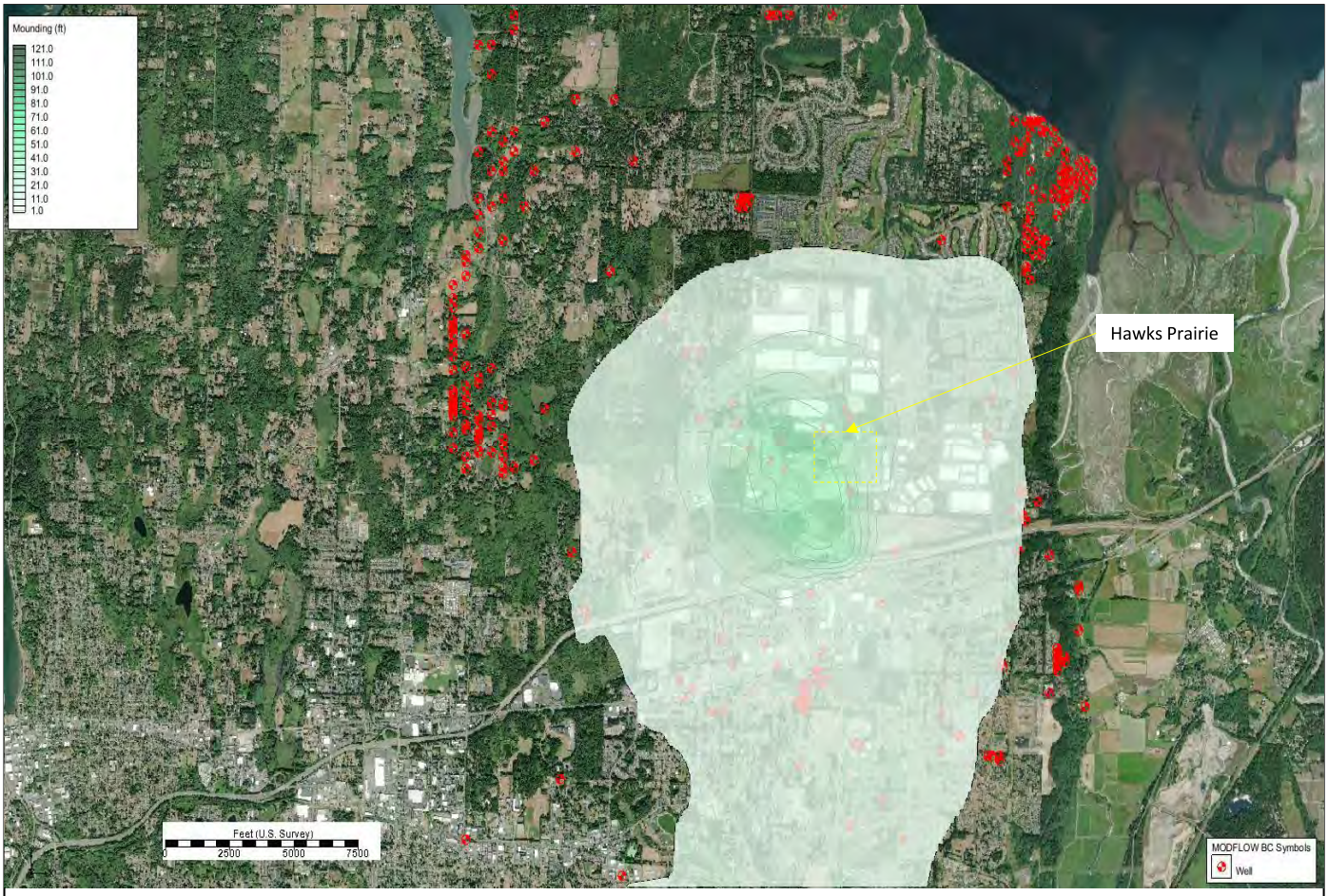

Figure B-23 Q_c Groundwater Mounding 2015

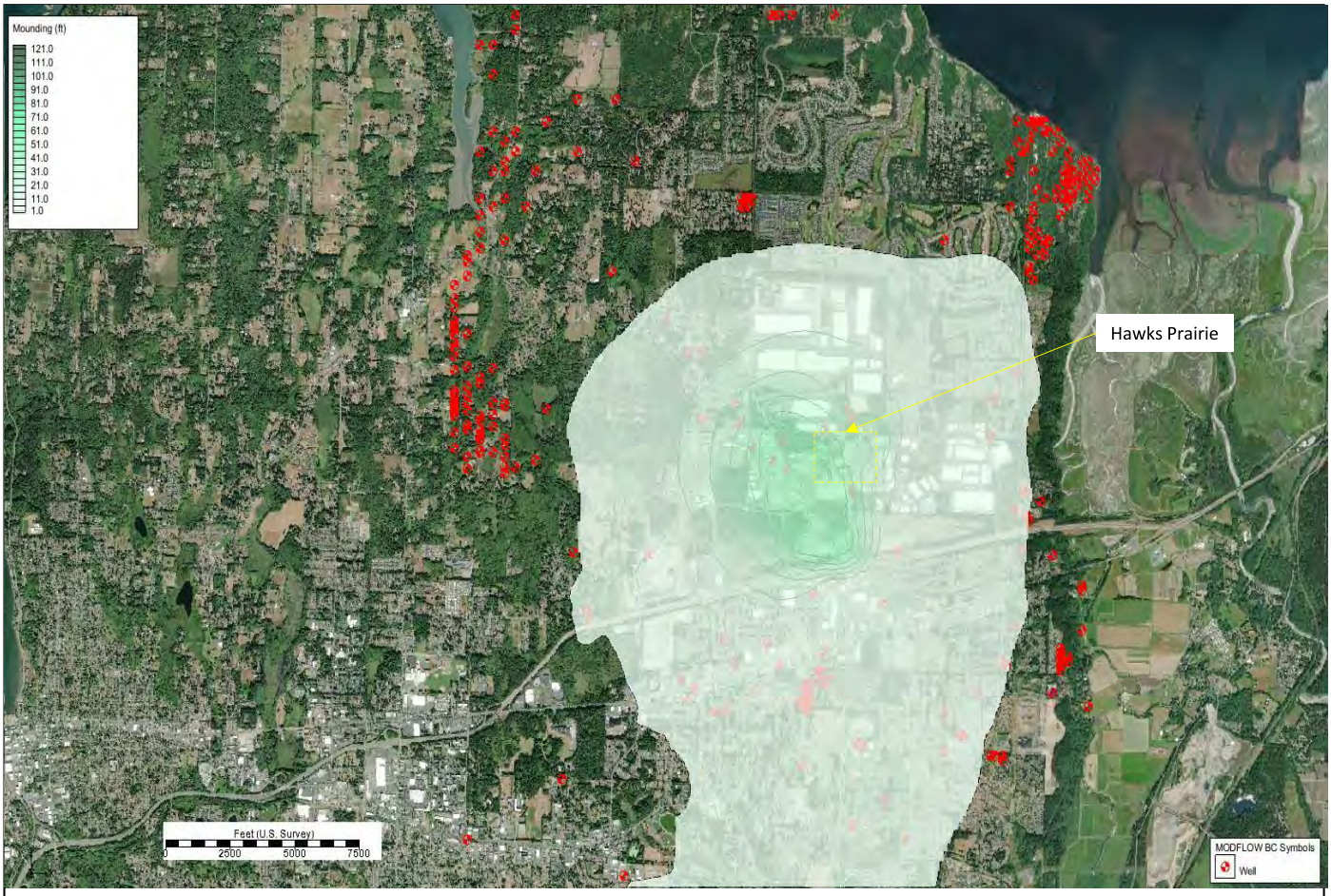

Figure B-24 Q_c Groundwater Mounding 2016

Figure B-25 Q_c Groundwater Mounding 2017

Figure B-26 Q_c Groundwater Mounding 2018

Figure B-27 Q_c Groundwater Mounding 2019

Figure B-28 Q_c Groundwater Mounding 2020

Appendix C: Model Results: Reclaimed Water Extent (2006-2020)

This page intentionally left blank.

Figure C-1 Q_{va} C/C_0 Concentration 2007

Figure C-2 Q_{va} C/C_0 Concentration 2008

Figure C-3 Q_{va} C/C_0 Concentration 2009

Figure C-4 Q_{va} C/C_0 Concentration 2010

Figure C-5 Q_{va} C/C_0 Concentration 2011

Figure C-6 Q_{va} C/C_0 Concentration 2012

Figure C-7 Q_{va} C/C_0 Concentration 2013

Figure C-8 Q_{va} C/C_0 Concentration 2014

Figure C-9 Q_{va} C/C_0 Concentration 2015

Figure C-10 Q_{va} C/C_0 Concentration 2016

Figure C-11 Q_{va} C/C_0 Concentration 2017

Figure C-12 Q_{va} C/C_0 Concentration 2018

Figure C-13 Q_{va} C/C_0 Concentration 2019

Figure C-14 Q_{va} C/C_0 Concentration 2020

Figure C-15 Q_c C/C_0 Concentration 2007

Figure C-16 Q_c C/C_0 Concentration 2008

Figure C-17 Q_c C/C_0 Concentration 2009

Figure C-18 Q_c C/C_0 Concentration 2010

Figure C-19 Q_c C/C_0 Concentration 2011

Figure C-20 Q_c C/C_0 Concentration 2012

Figure C-21 Q_c C/C_0 Concentration 2013

Figure C-22 Q_c C/C_0 Concentration 2014

Figure C-23 Q_c C/C_0 Concentration 2015

Figure C-24 Q_c C/C_0 Concentration 2016

Figure C-25 Q_c C/C_0 Concentration 2017

Figure C-26 Q_c C/C_0 Concentration 2018

Figure C-27 Q_c C/C_0 Concentration 2019

Figure C-28 Q_c C/C_0 Concentration 2020

Appendix D: Model Results: Mounding (2020-2120)

This page intentionally left blank.

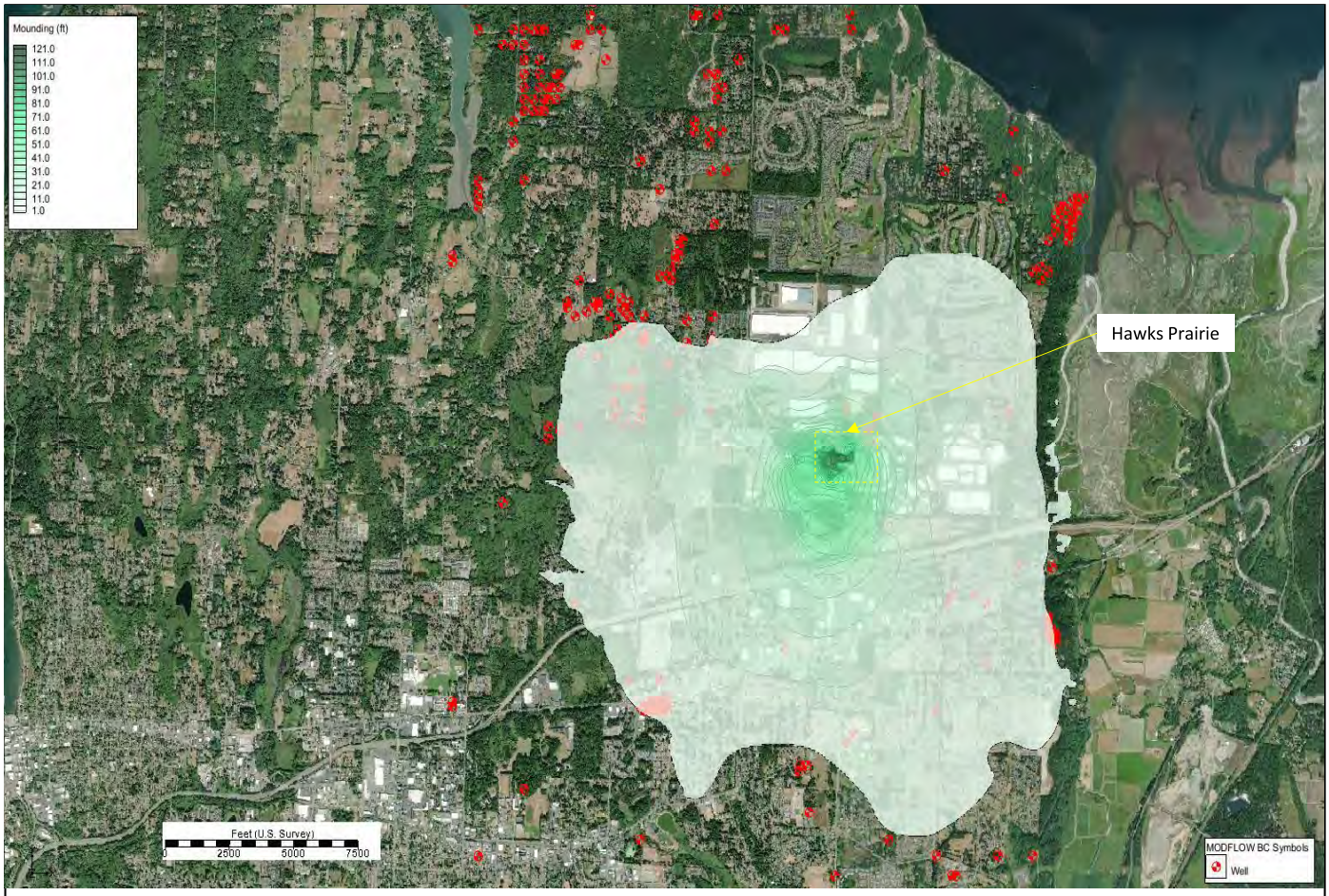

Figure D-1 Q_{va} Groundwater Mounding 2022

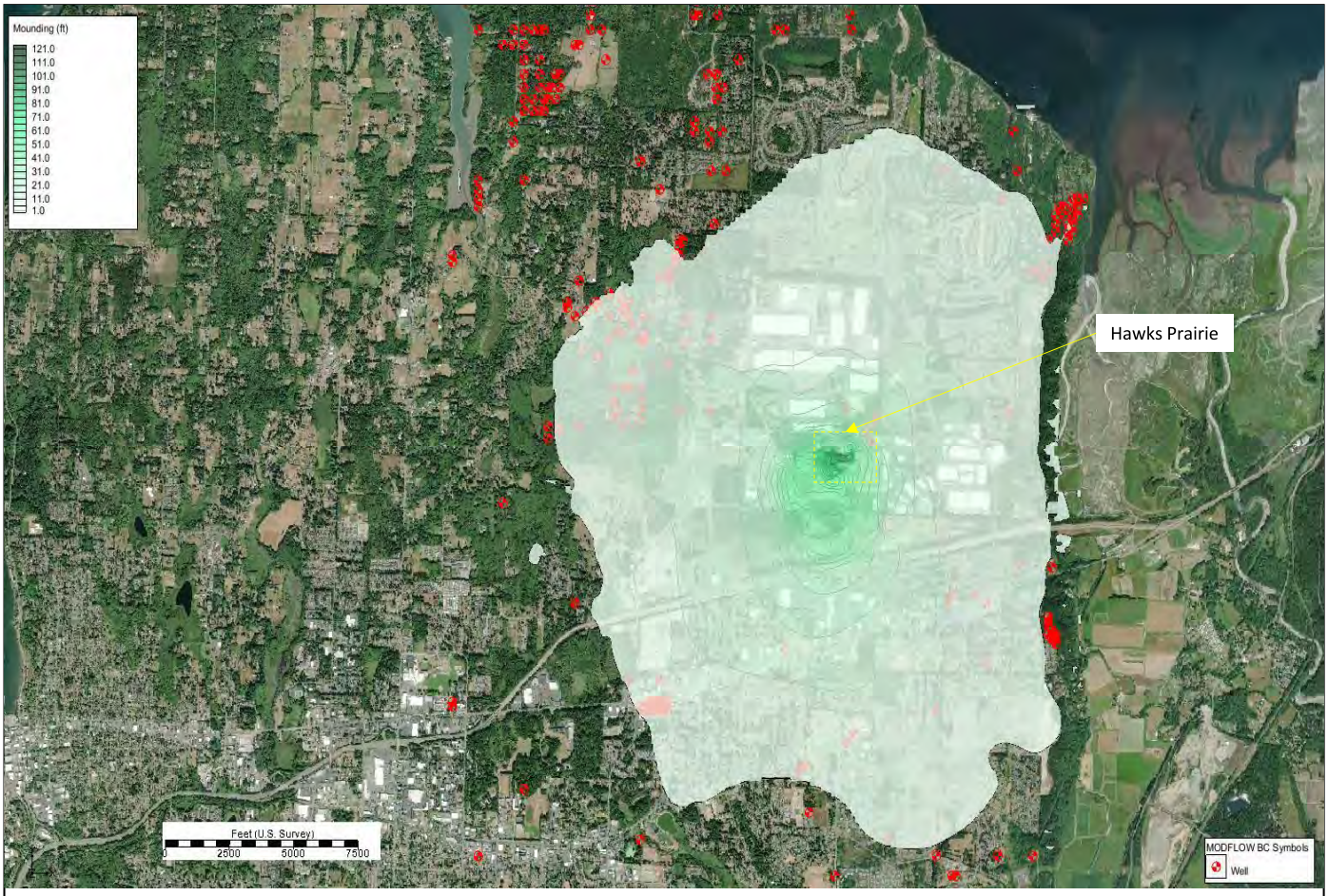

Figure D-2 Q_{va} Groundwater Mounding 2032

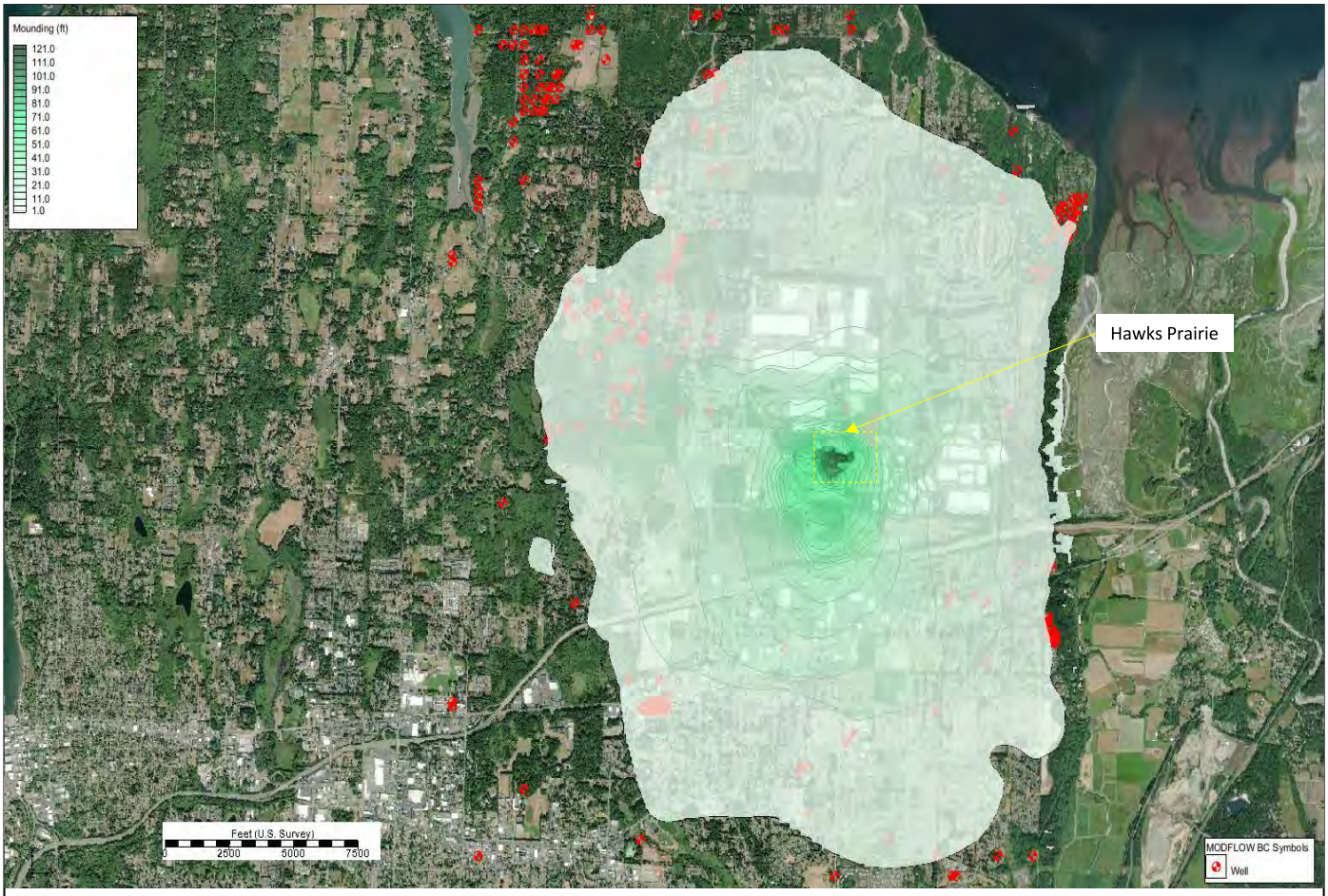

Figure D-3 Q_{va} Groundwater Mounding 2038

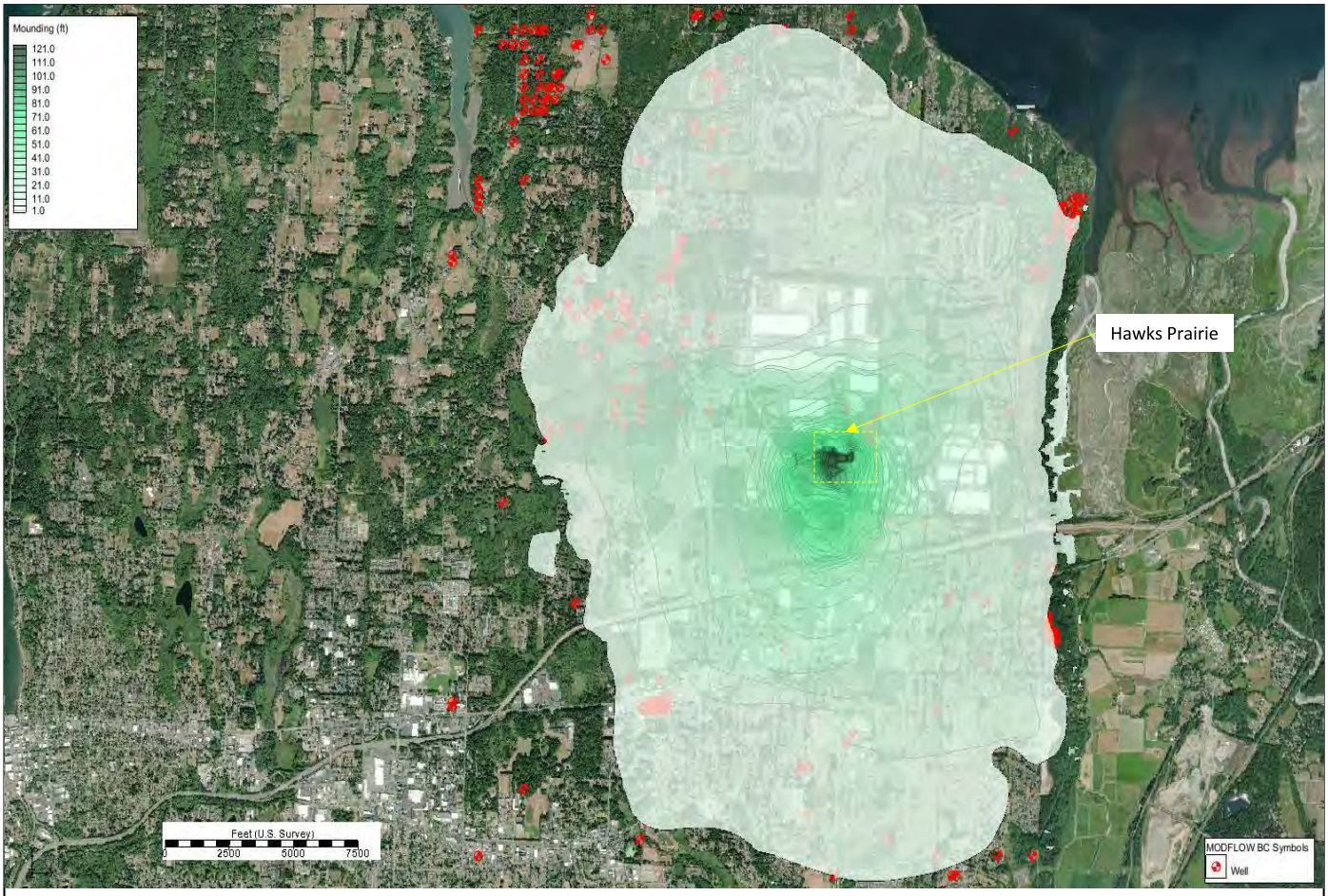

Figure D-4 Q_{va} Groundwater Mounding 2042

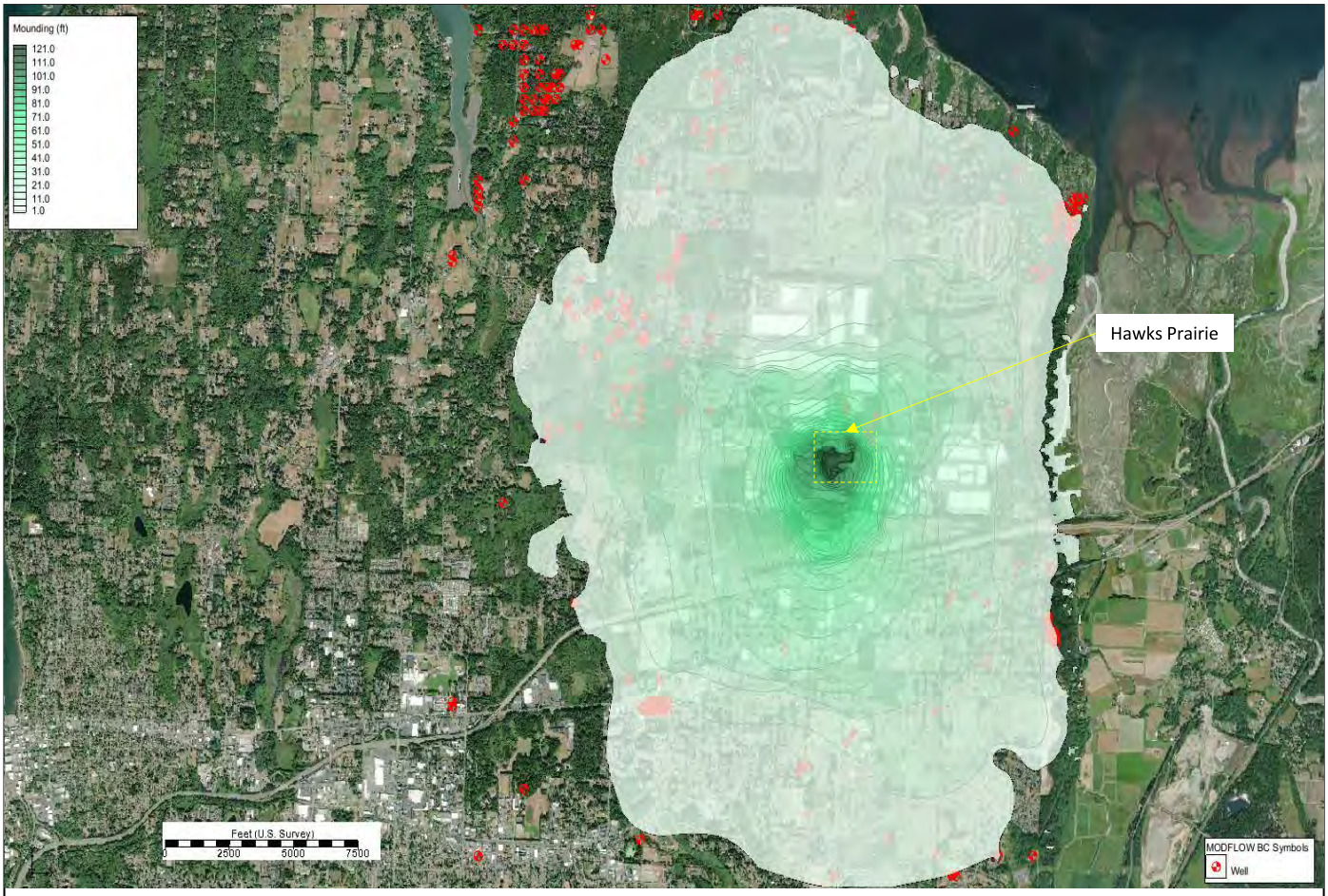

Figure D-5 Q_{va} Groundwater Mounding 2049

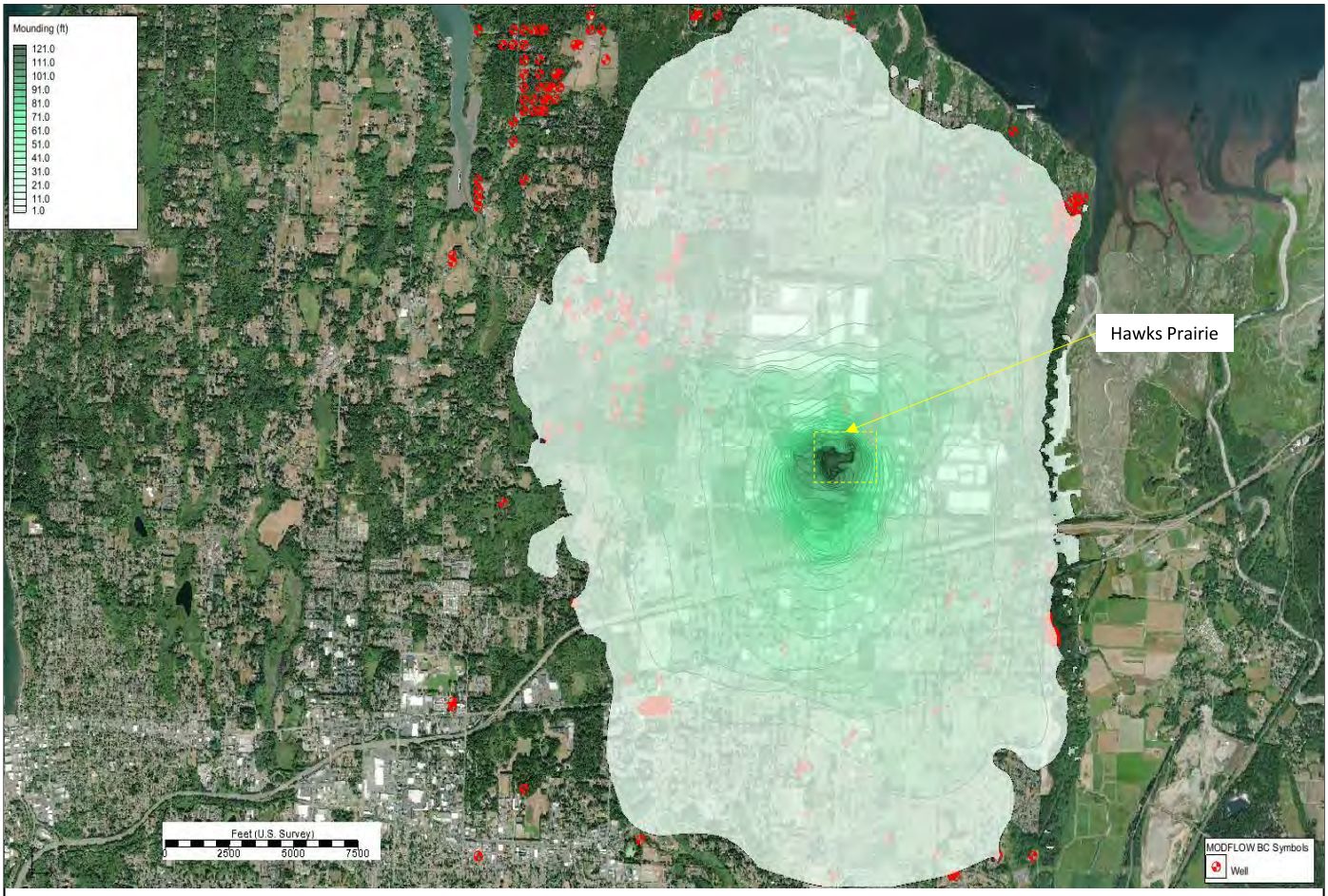

Figure D-6 Q_{va} Groundwater Mounding 2059

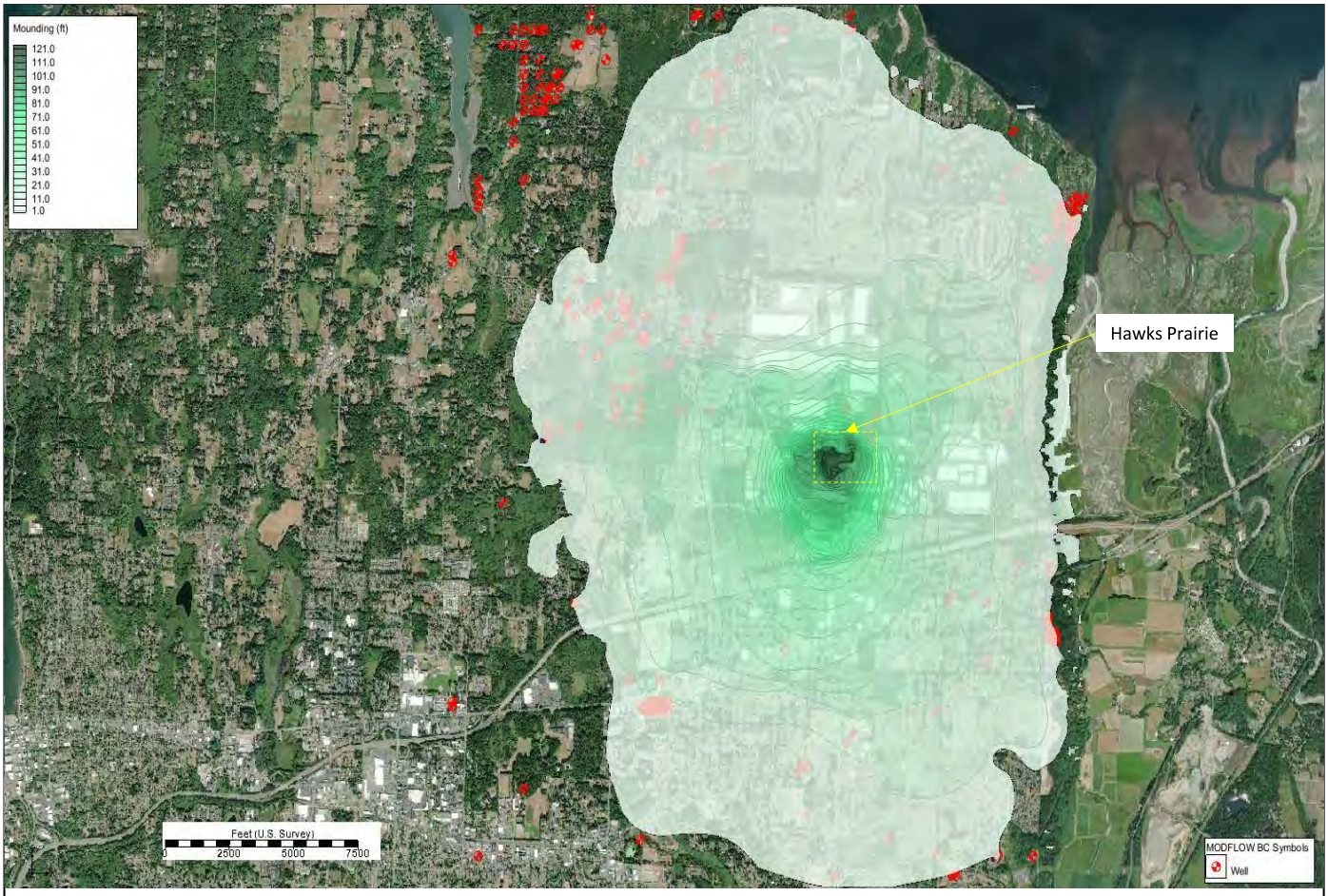

Figure D-7 Q_{va} Groundwater Mounding 2067

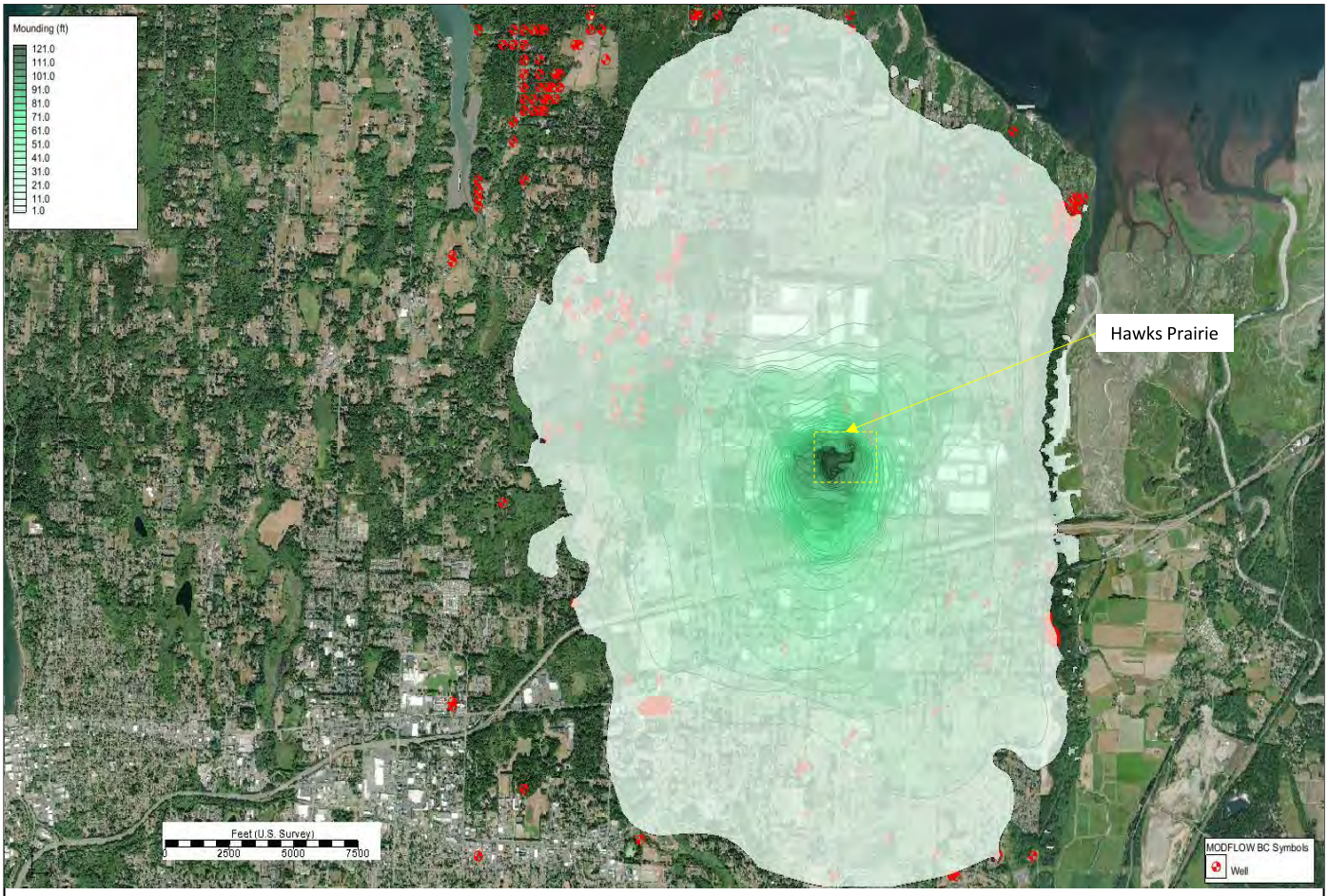

Figure D-8 Q_{va} Groundwater Mounding 2070

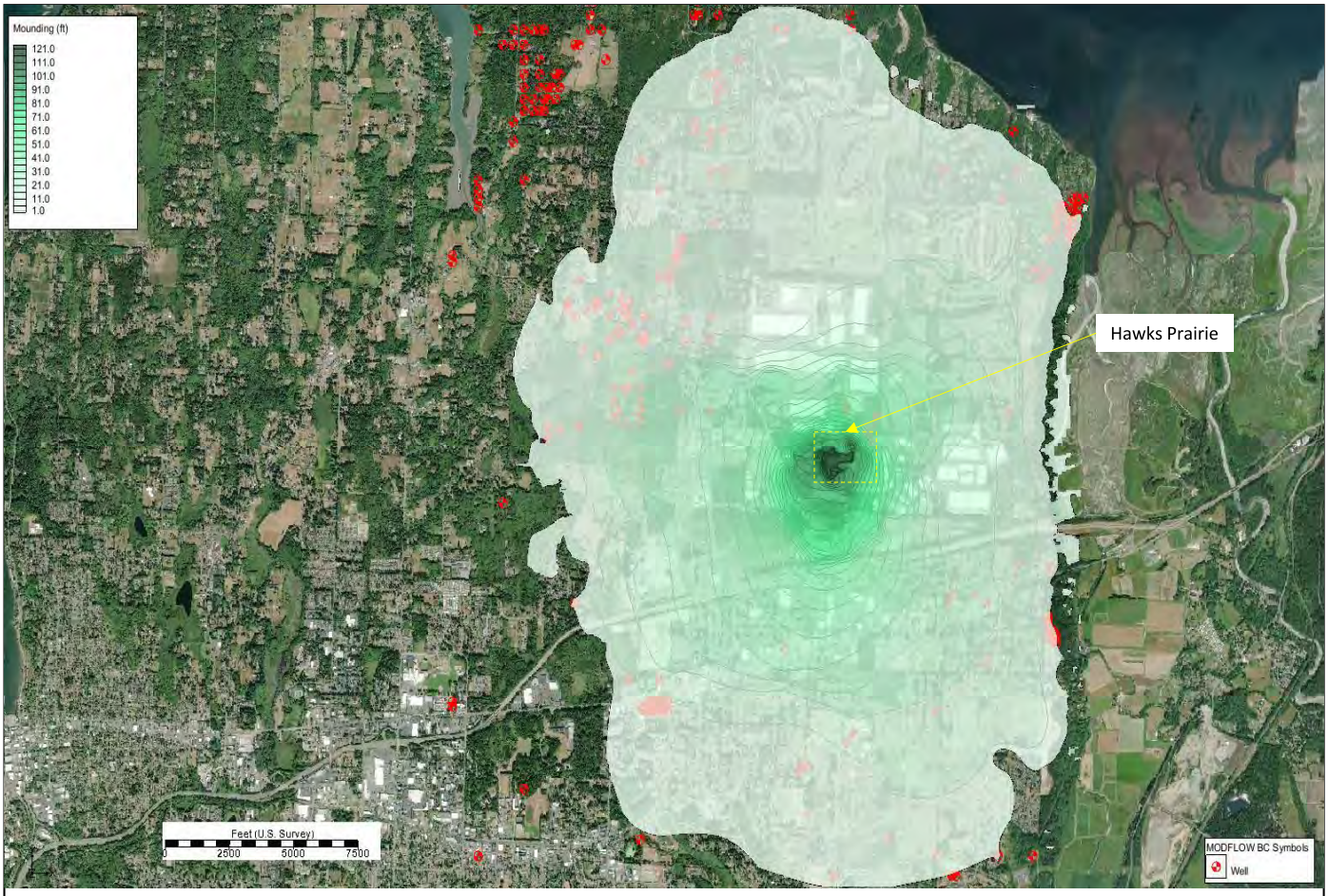

Figure D-9 Q_{va} Groundwater Mounding 2080

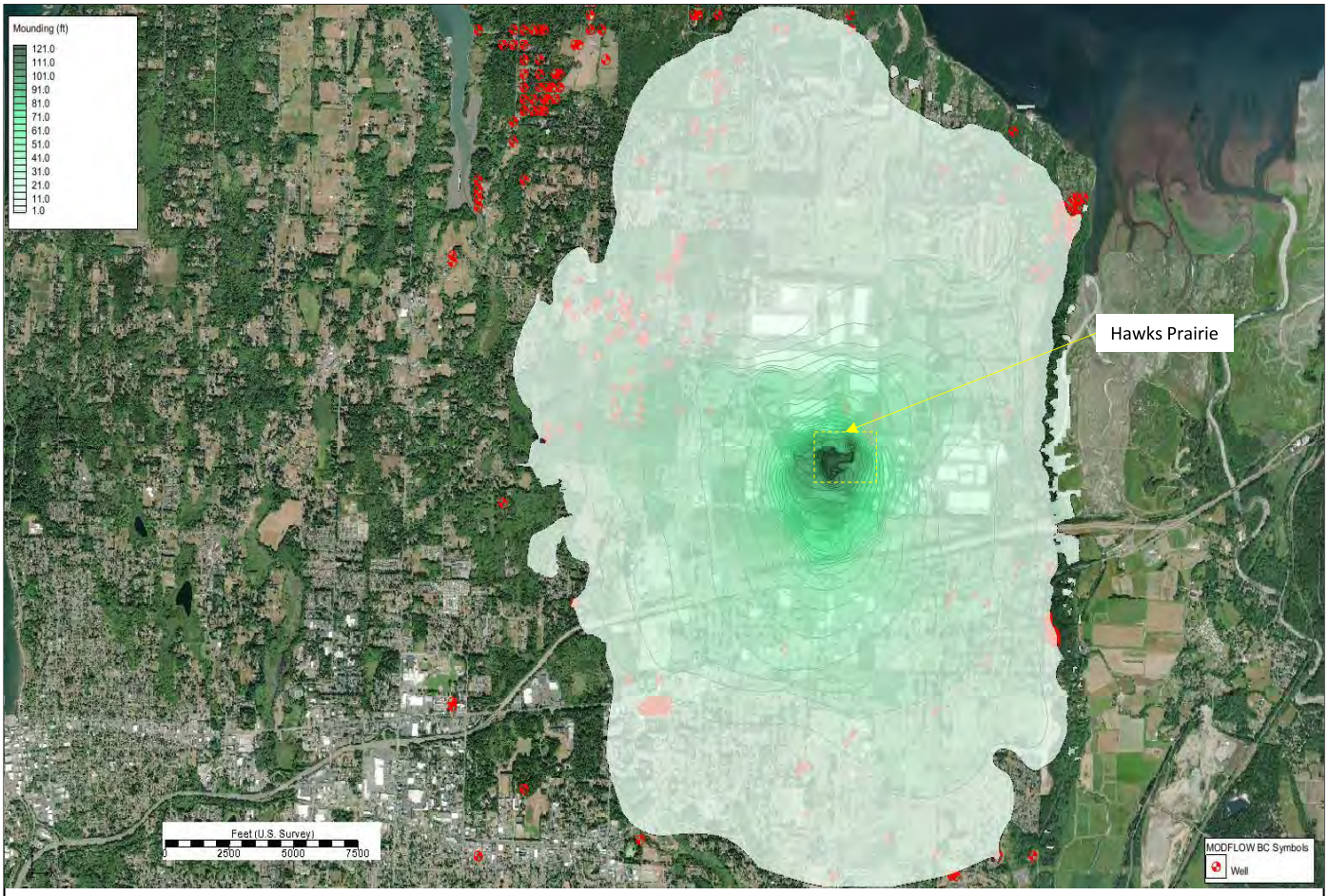

Figure D-10 Q_{va} Groundwater Mounding 2090

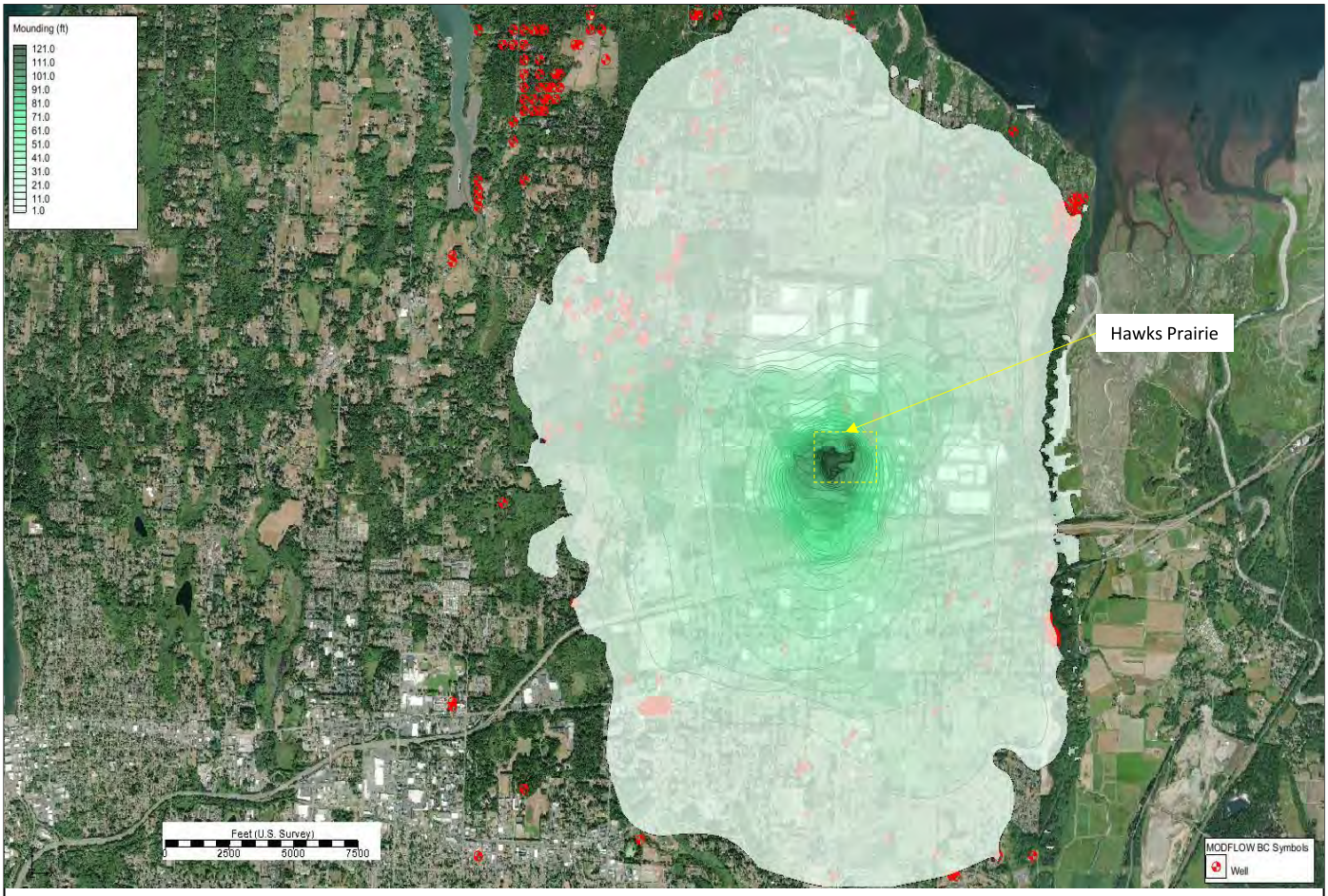

Figure D-11 Q_{va} Groundwater Mounding 2100

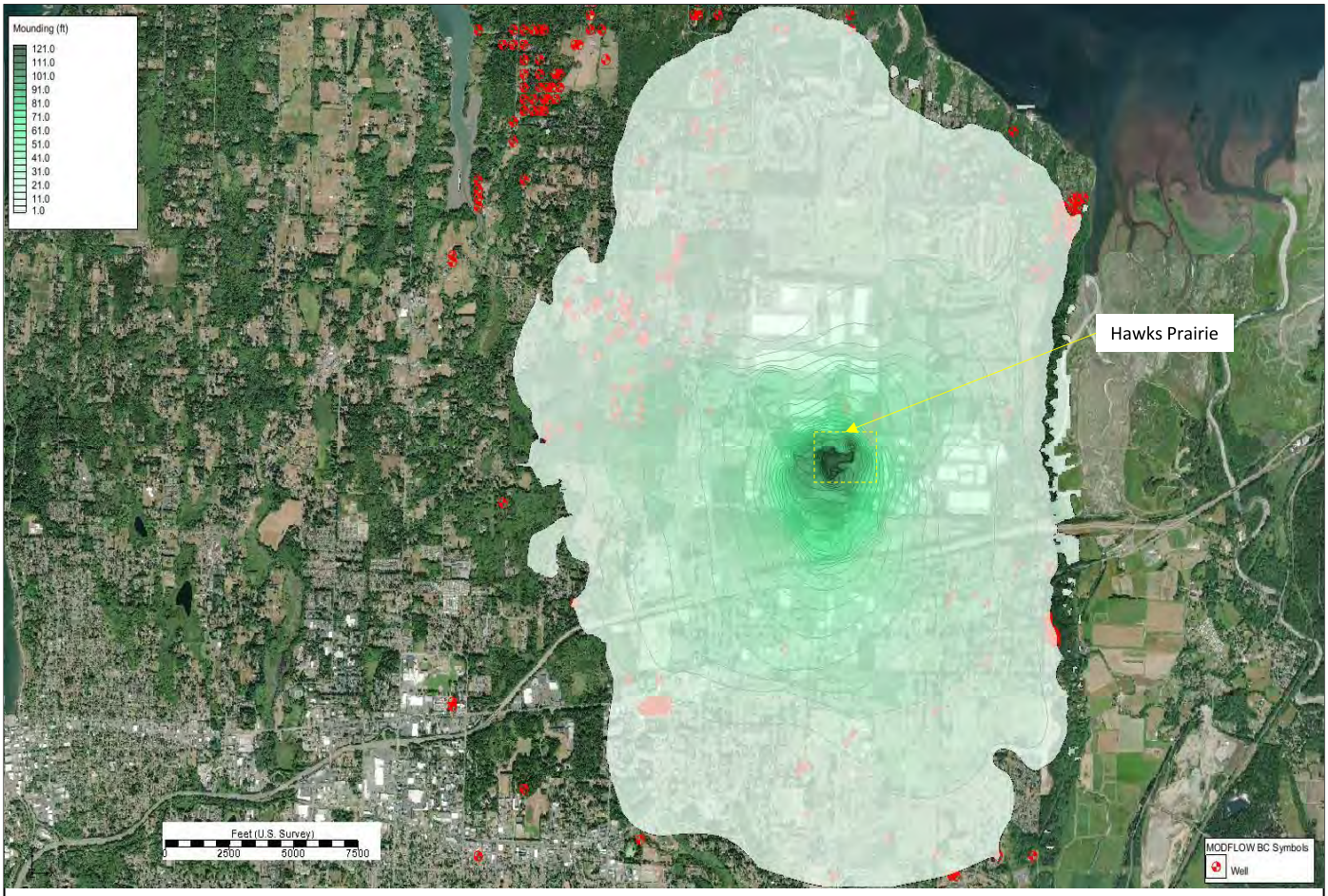

Figure D-12 Q_{va} Groundwater Mounding 2110

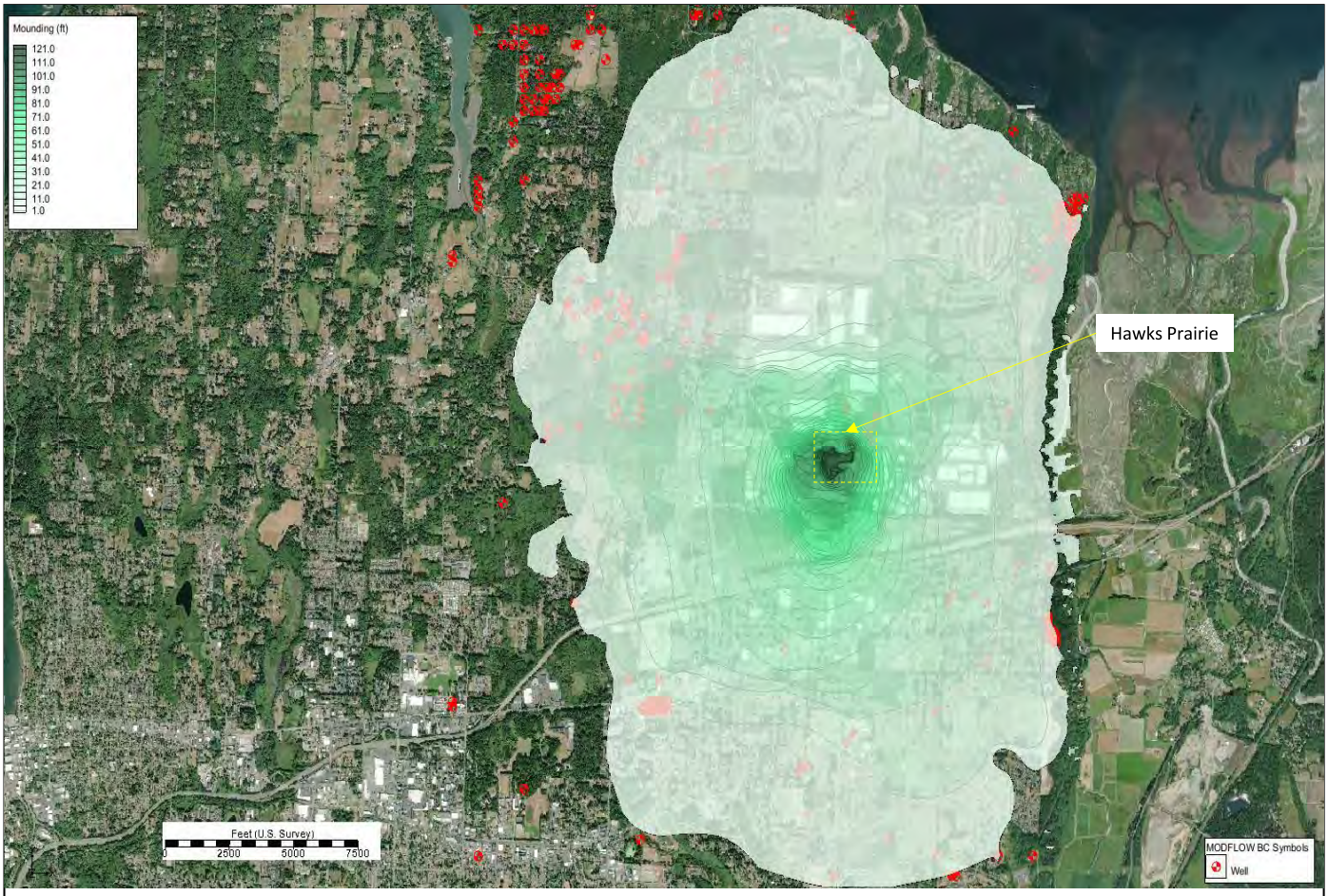

Figure D-13 Q_{va} Groundwater Mounding 2120

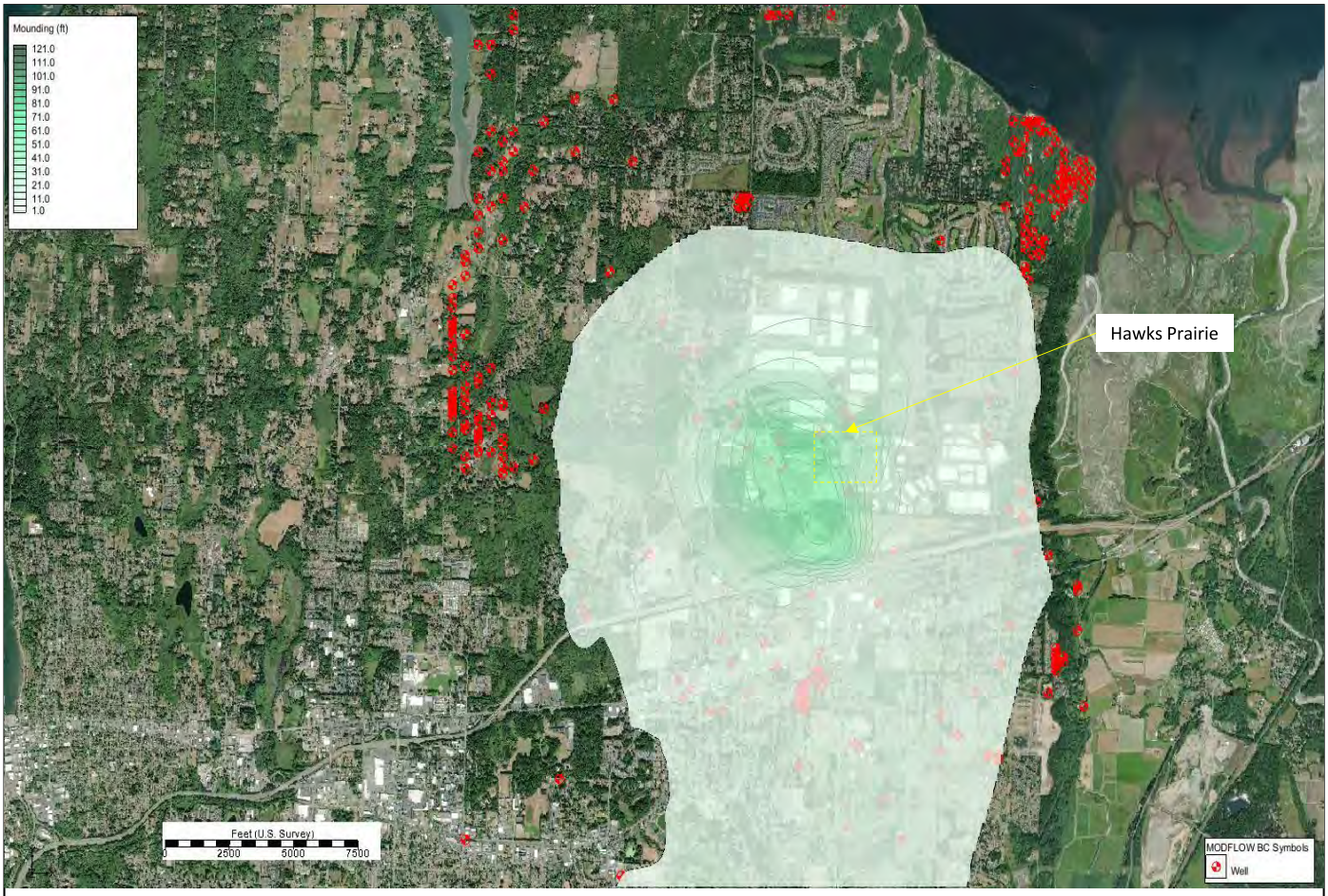

Figure D-14 Q_c Groundwater Mounding 2022

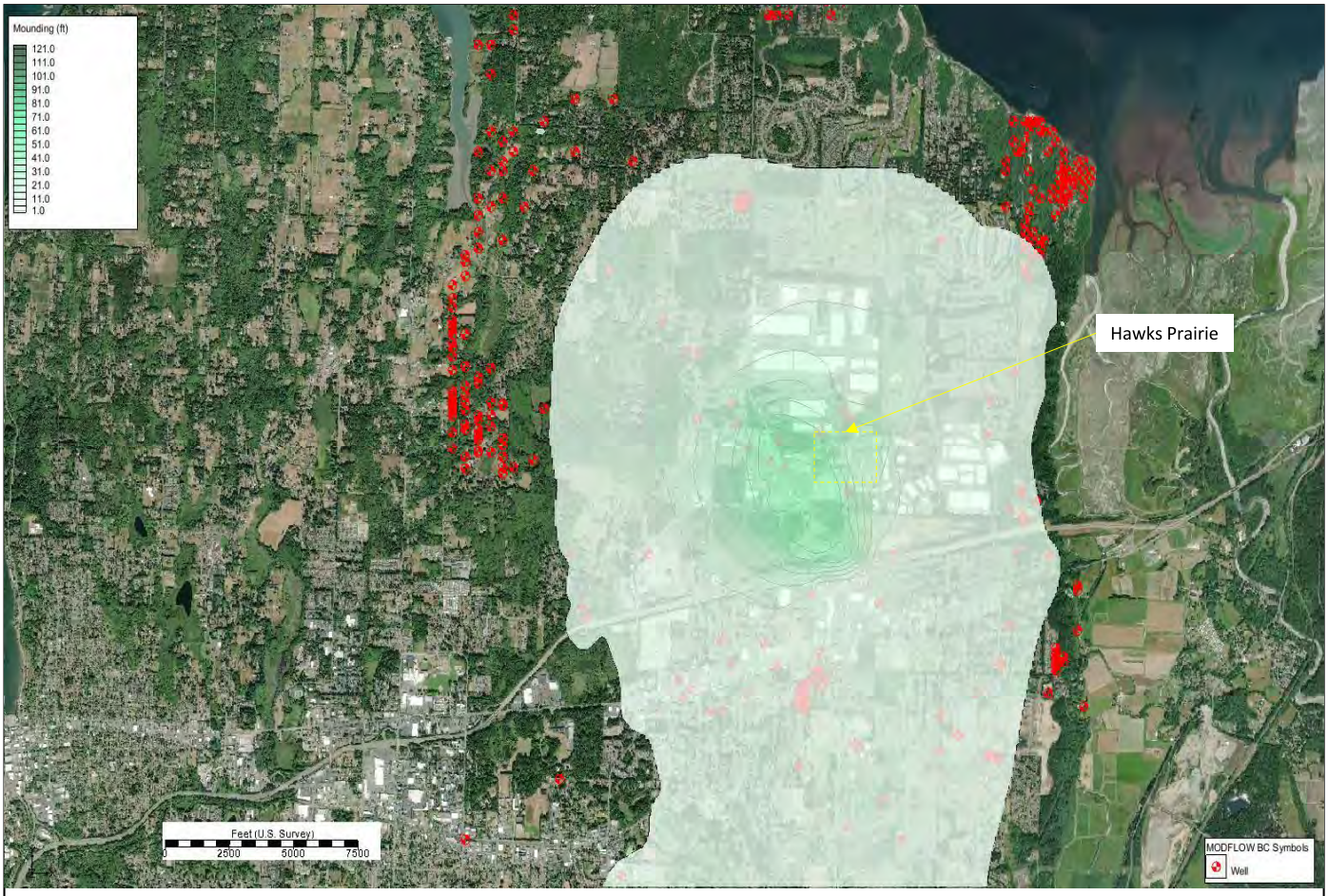

Figure D-15 Q_c Groundwater Mounding 2032

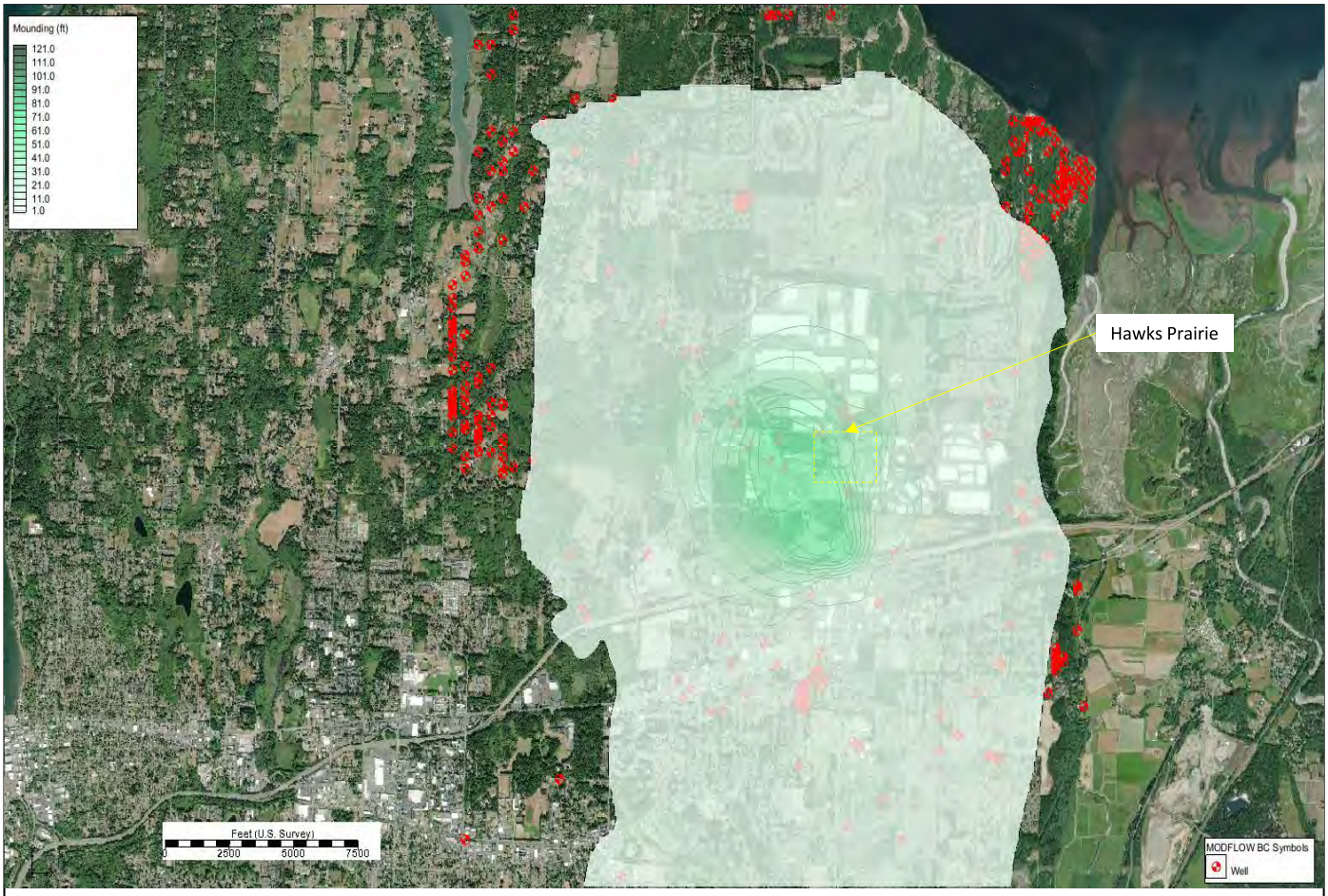

Figure D-16 Q_c Groundwater Mounding 2038

Figure D-17 Q_c Groundwater Mounding 2042

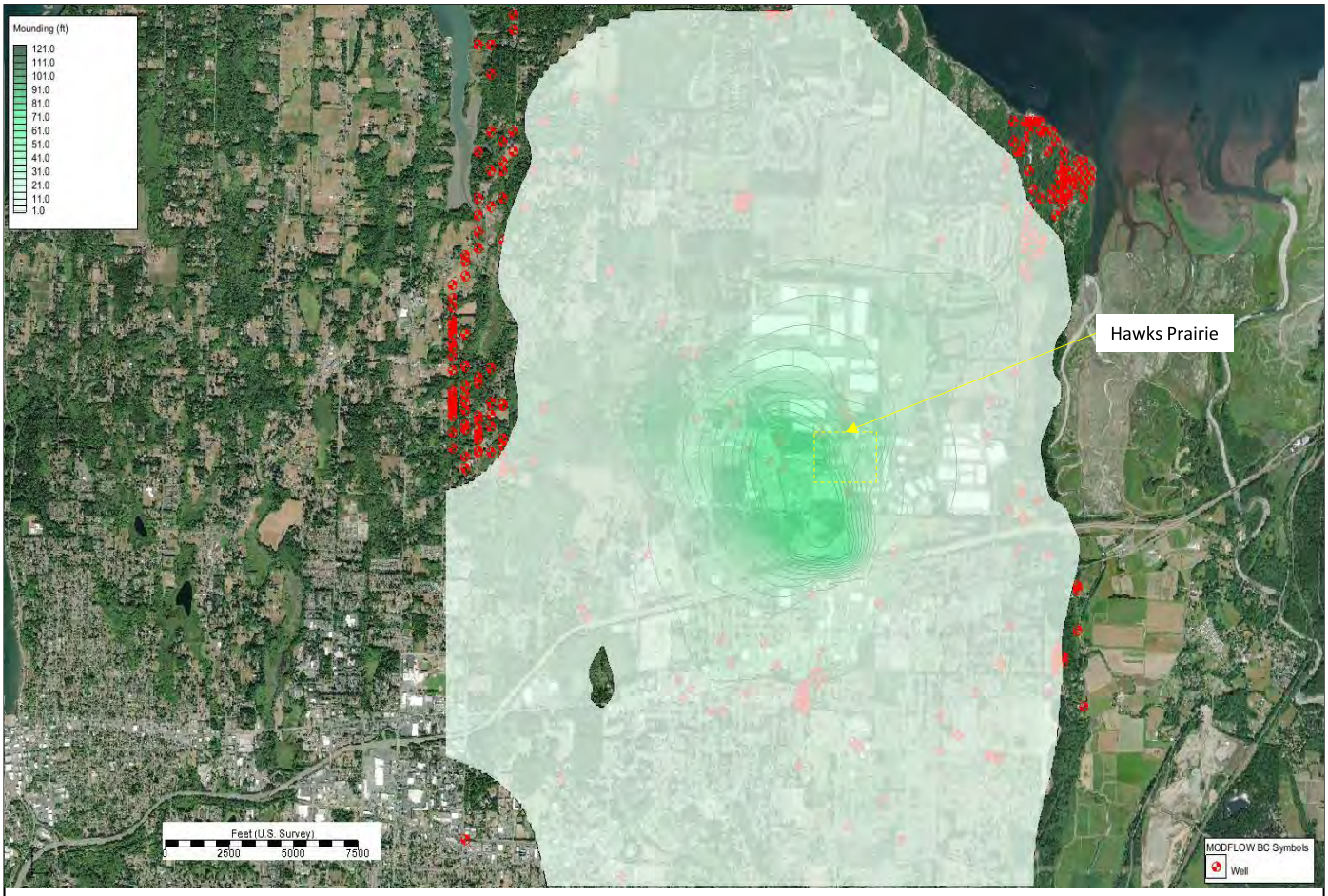

Figure D-18 Q_c Groundwater Mounding 2049

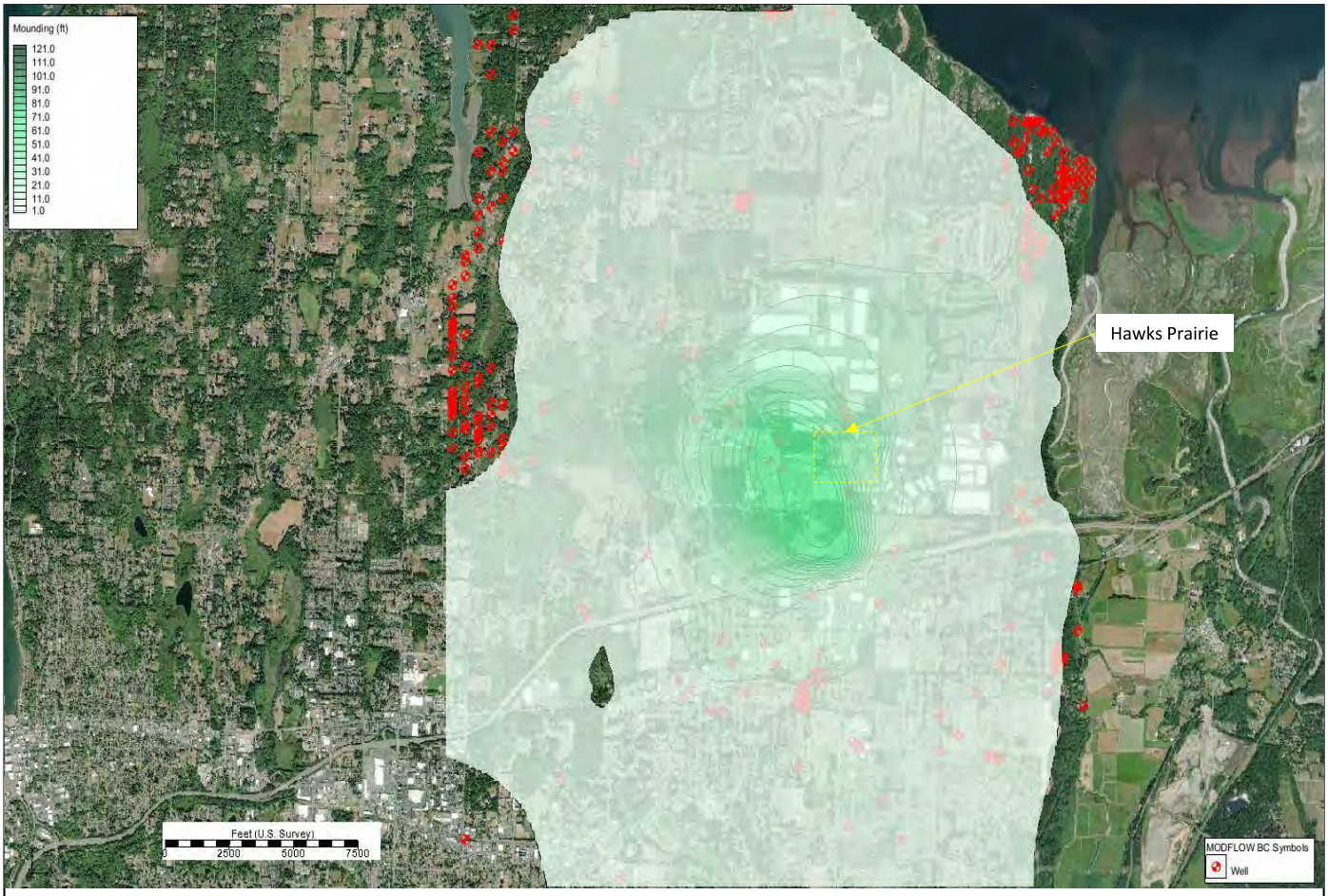

Figure D-19 Q_c Groundwater Mounding 2059

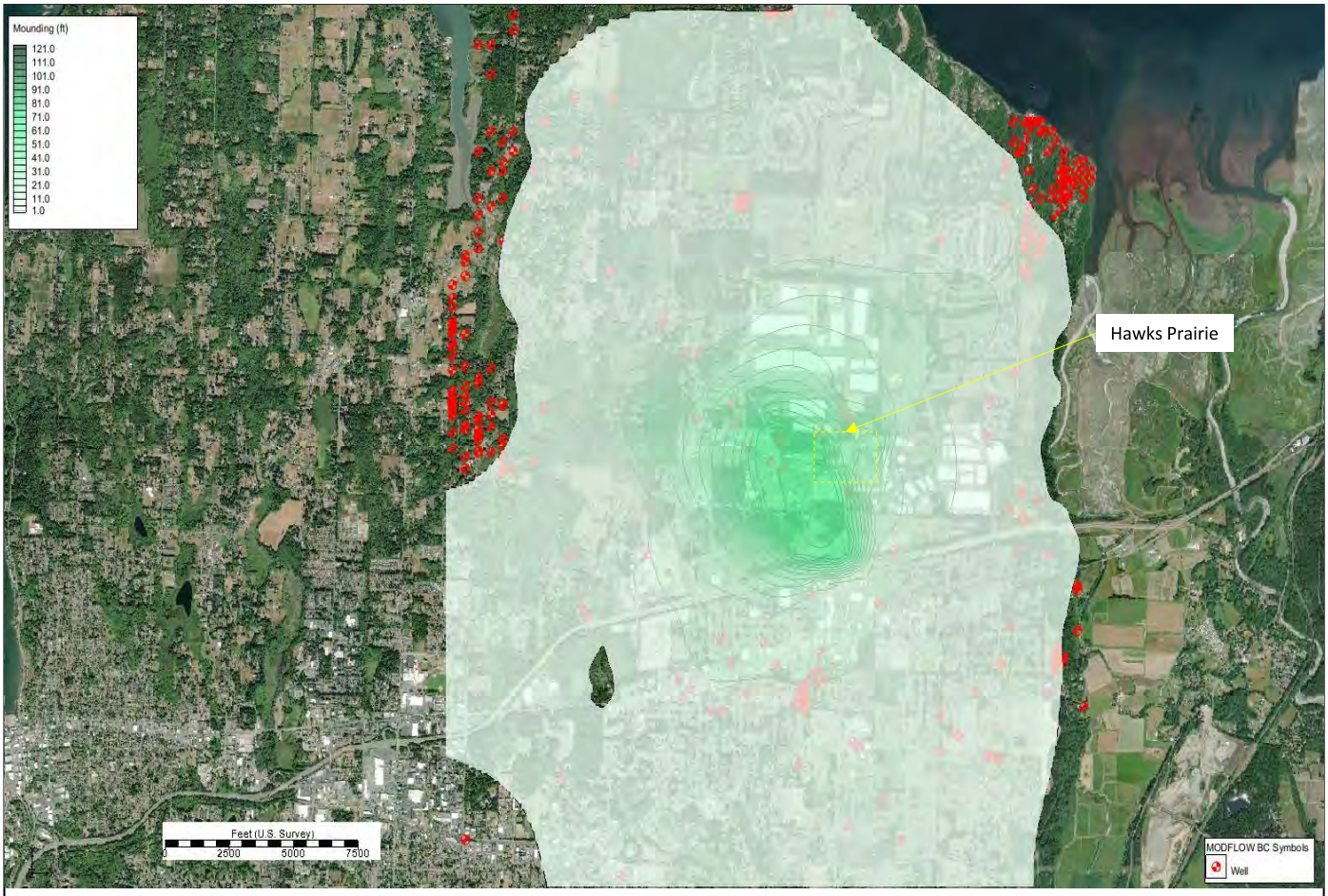

Figure D-20 Q_c Groundwater Mounding 2067

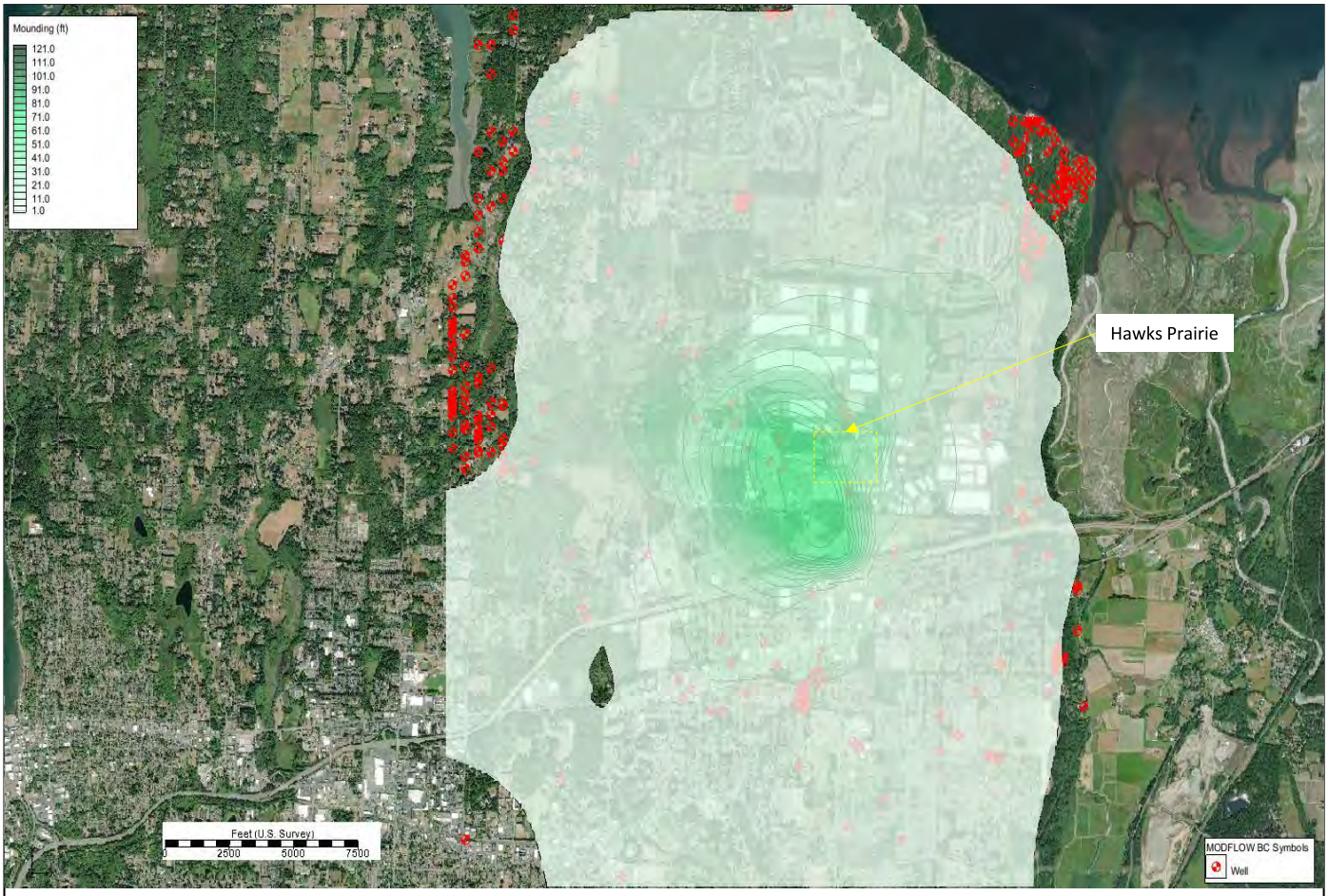

Figure D-21 Q_c Groundwater Mounding 2070

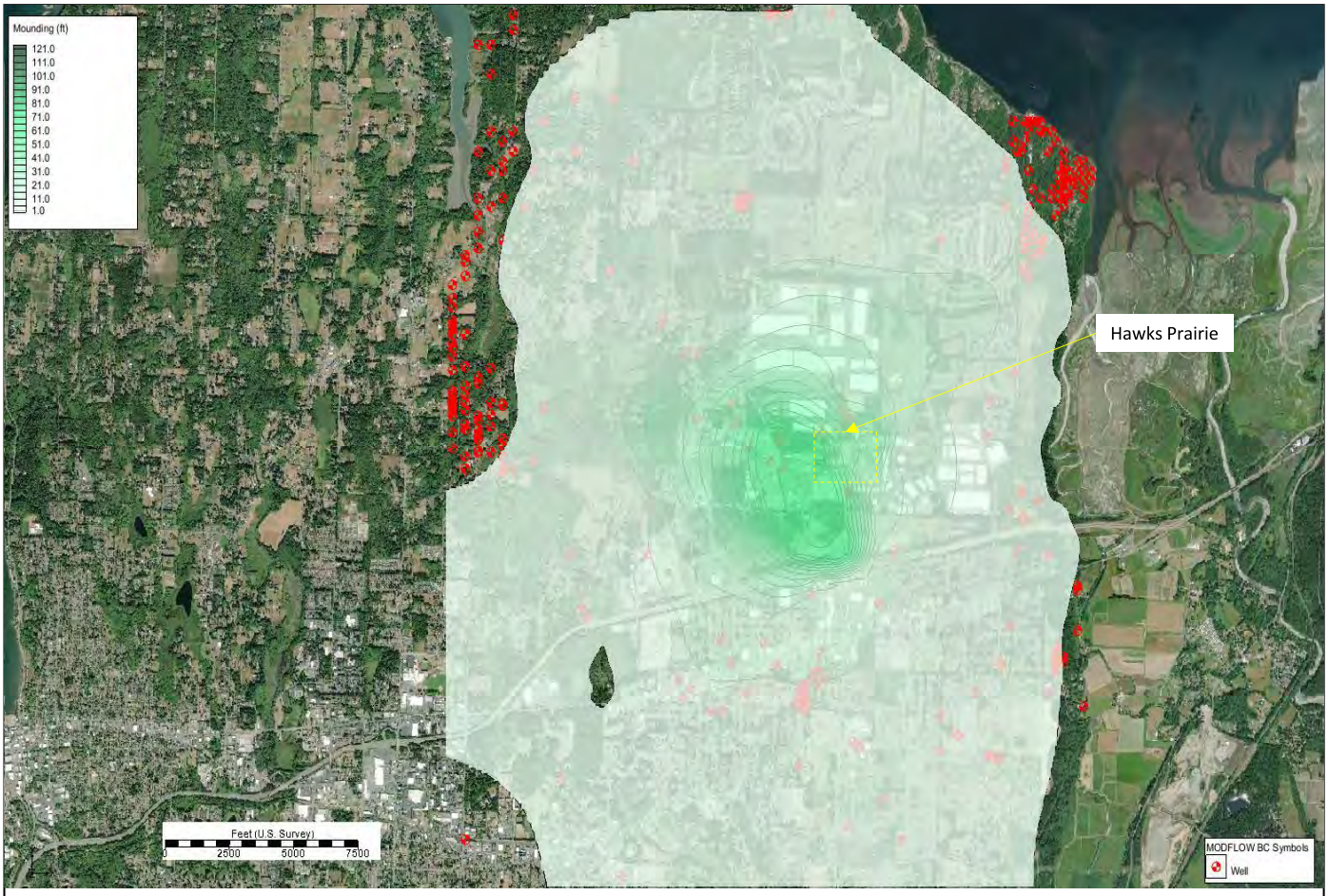

Figure D-22 Q_c Groundwater Mounding 2080

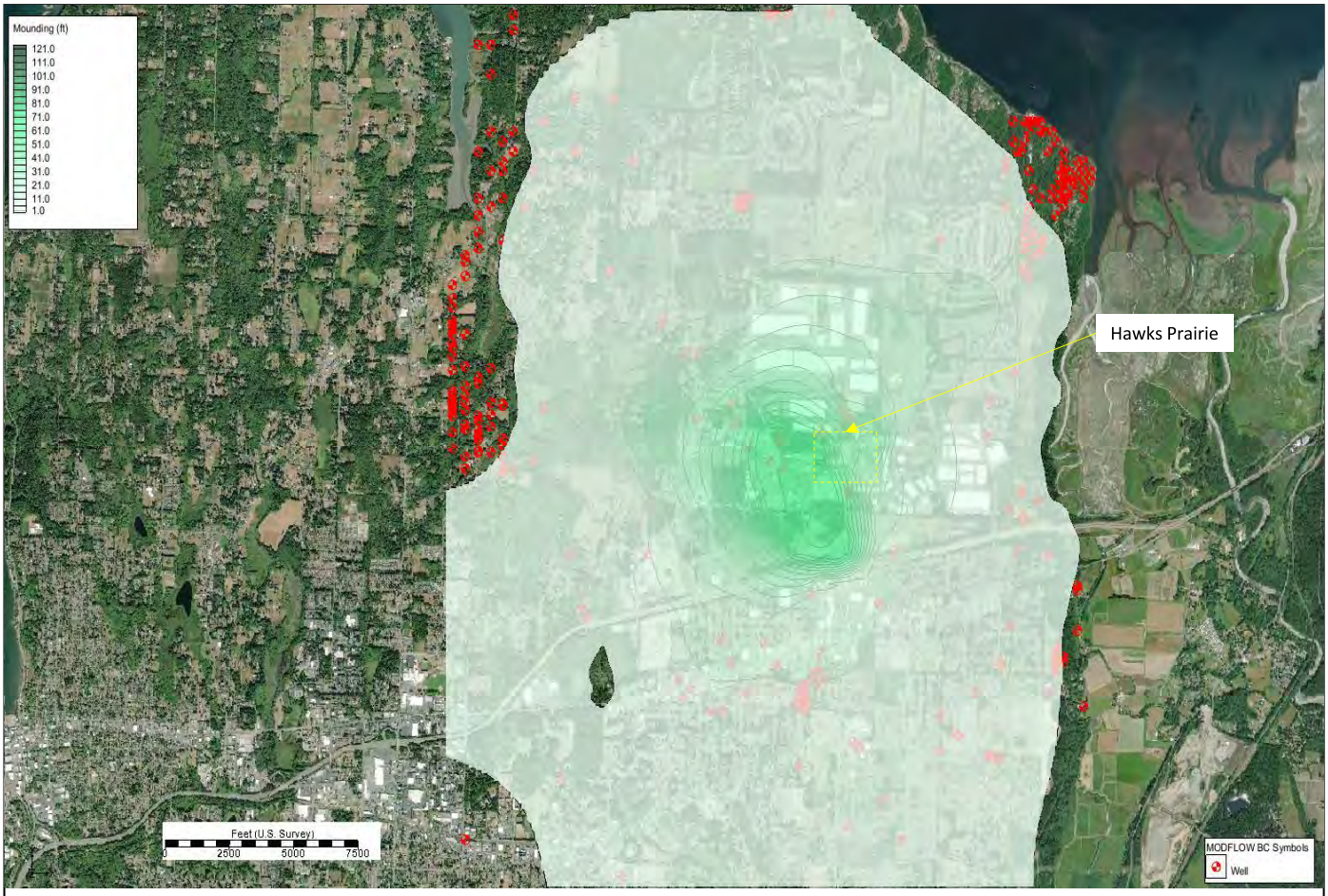

Figure D-23 Q_c Groundwater Mounding 2090

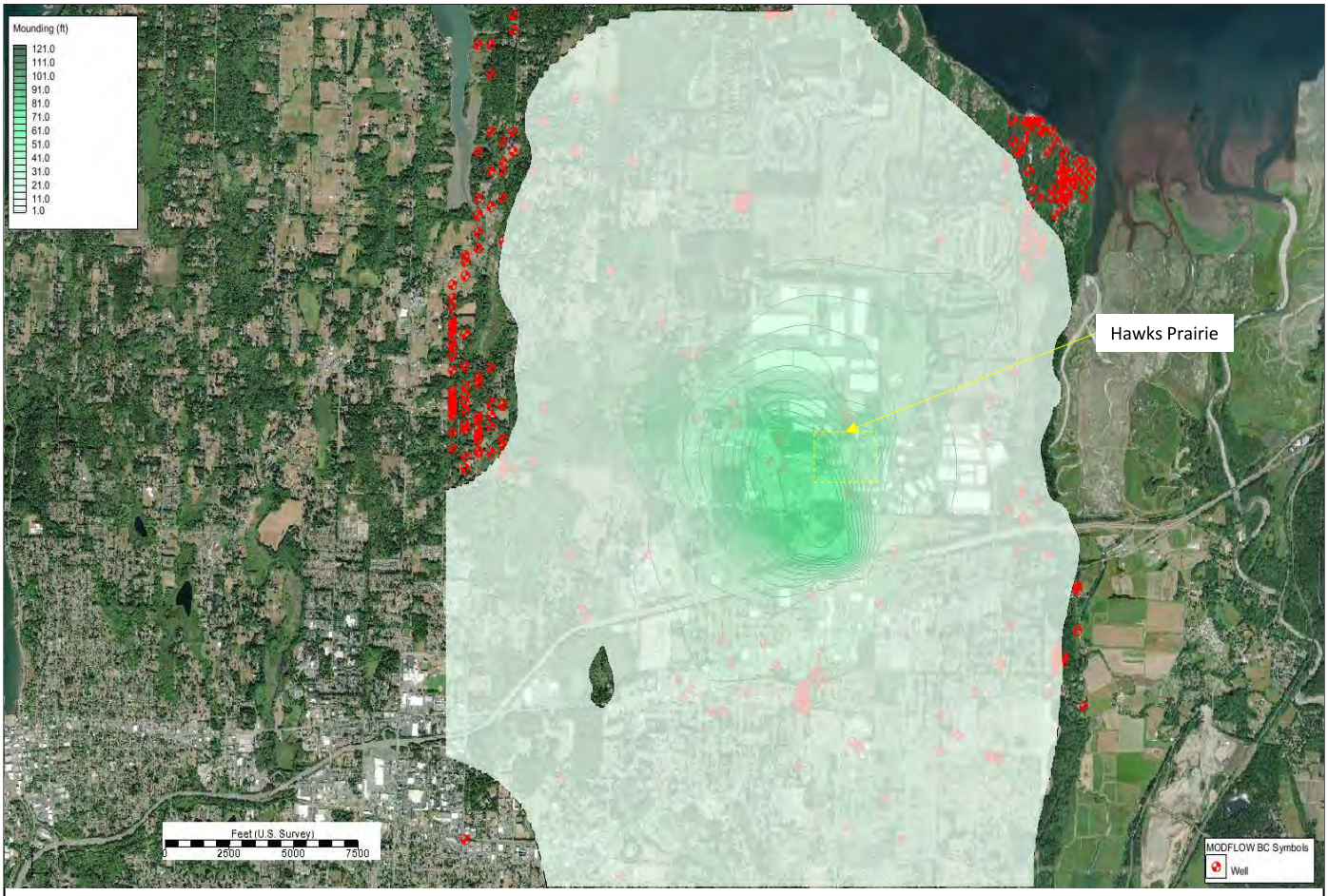

Figure D-24 Q_c Groundwater Mounding 2100

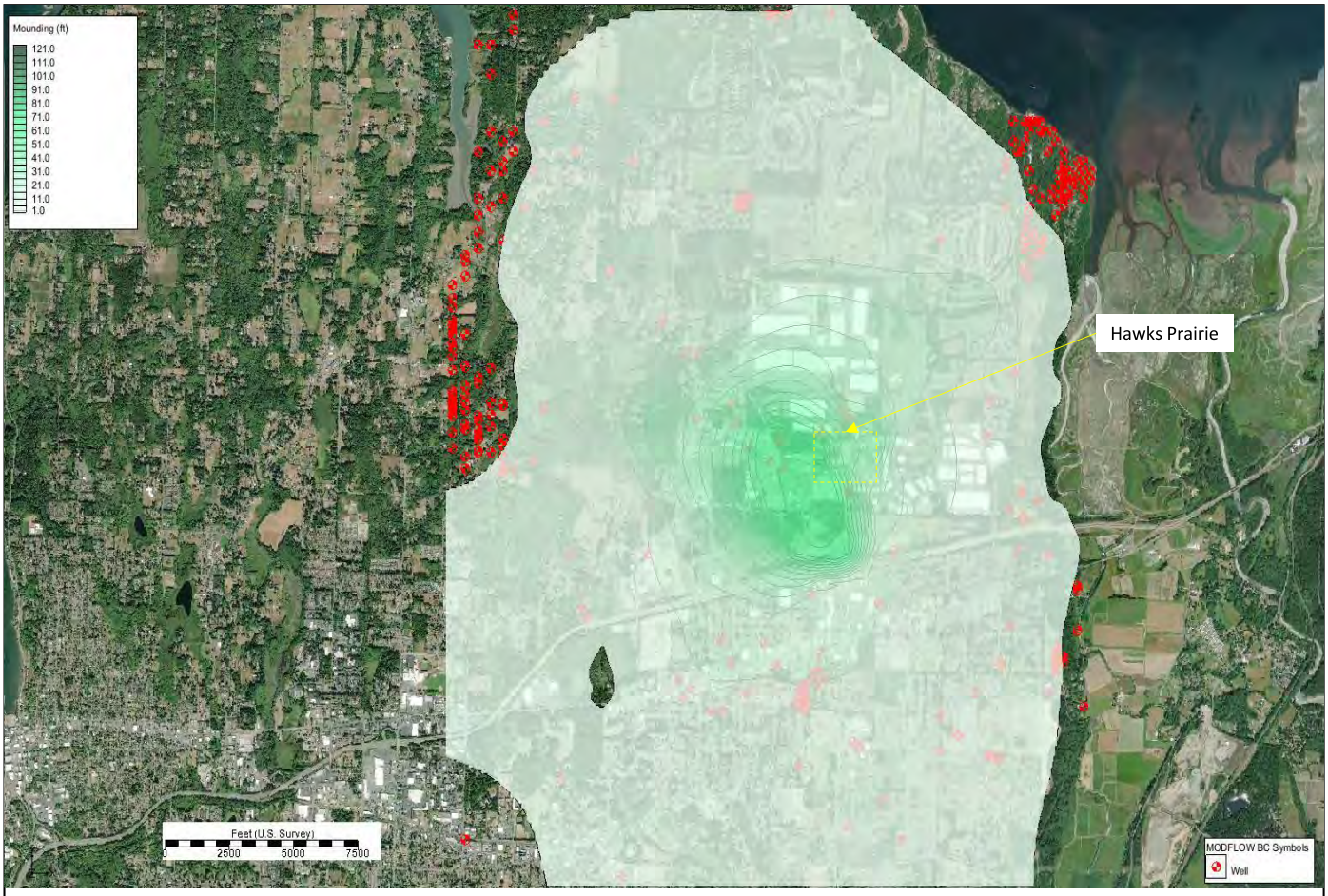

Figure D-25 Q_c Groundwater Mounding 2110

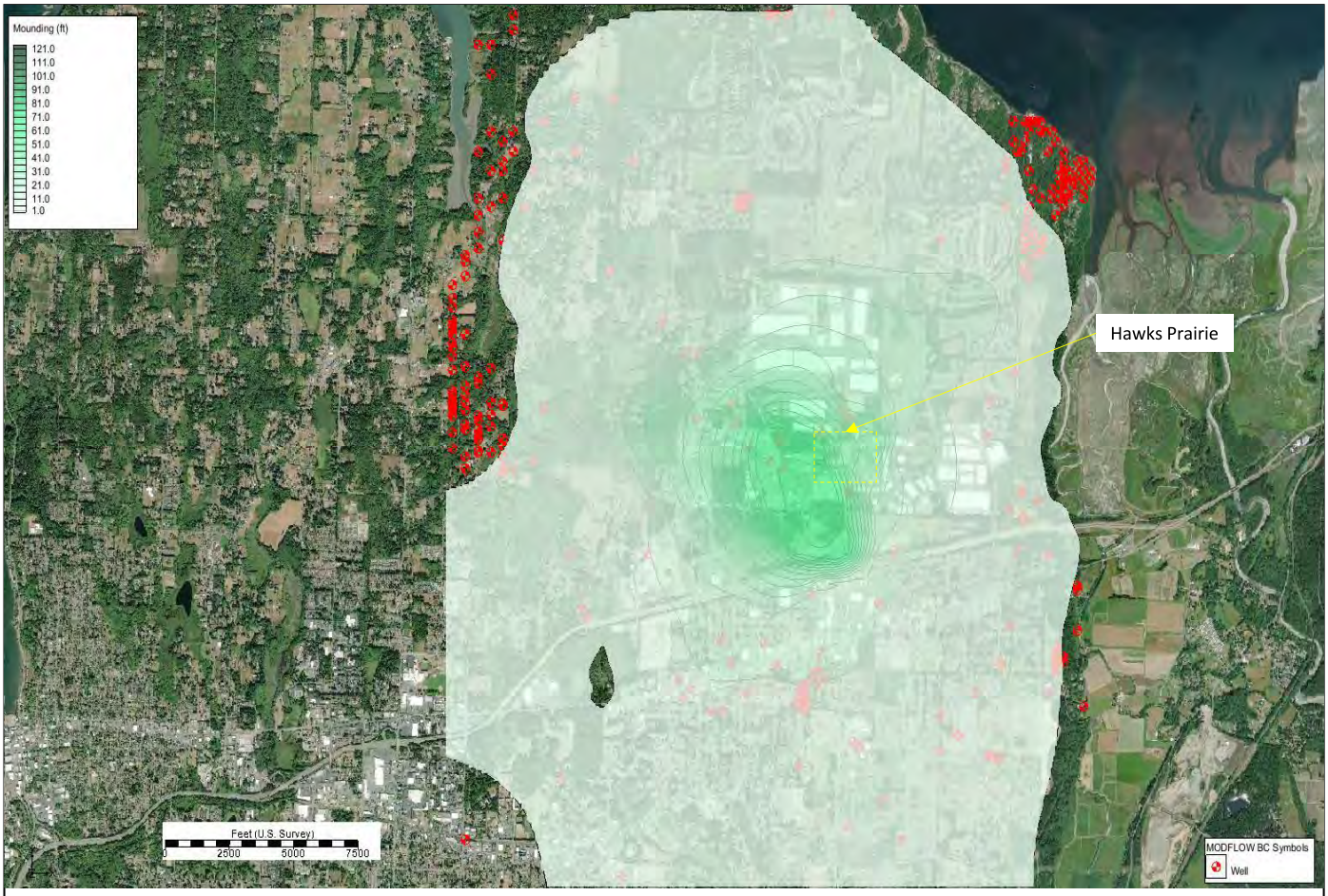

Figure D-26 Q_c Groundwater Mounding 2120

Appendix E: Model Results: Reclaimed Water Extent (2020-2120)

This page intentionally left blank.

Figure E-1 Q_{va} C/C_0 2022

Figure E-2 Q_{va} C/C_0 2032

Figure E-3 Q_{va} C/C_0 2038

Figure E-4 Q_{va} C/C_0 2042

Figure E-5 Q_{va} C/C_0 2049

Figure E-6 Q_{va} C/C_0 2059

Figure E-7 Q_{va} C/C_0 2067

Figure E-8 Q_{va} C/C_0 2070

Figure E-9 Q_{va} C/C_0 2080

Figure E-10 Q_{va} C/C_0 2090

Figure E-11 Q_{va} C/C_0 2100

Figure E-12 Q_{va} C/C_0 2110

Figure E-13 Q_{va} C/C_0 2120

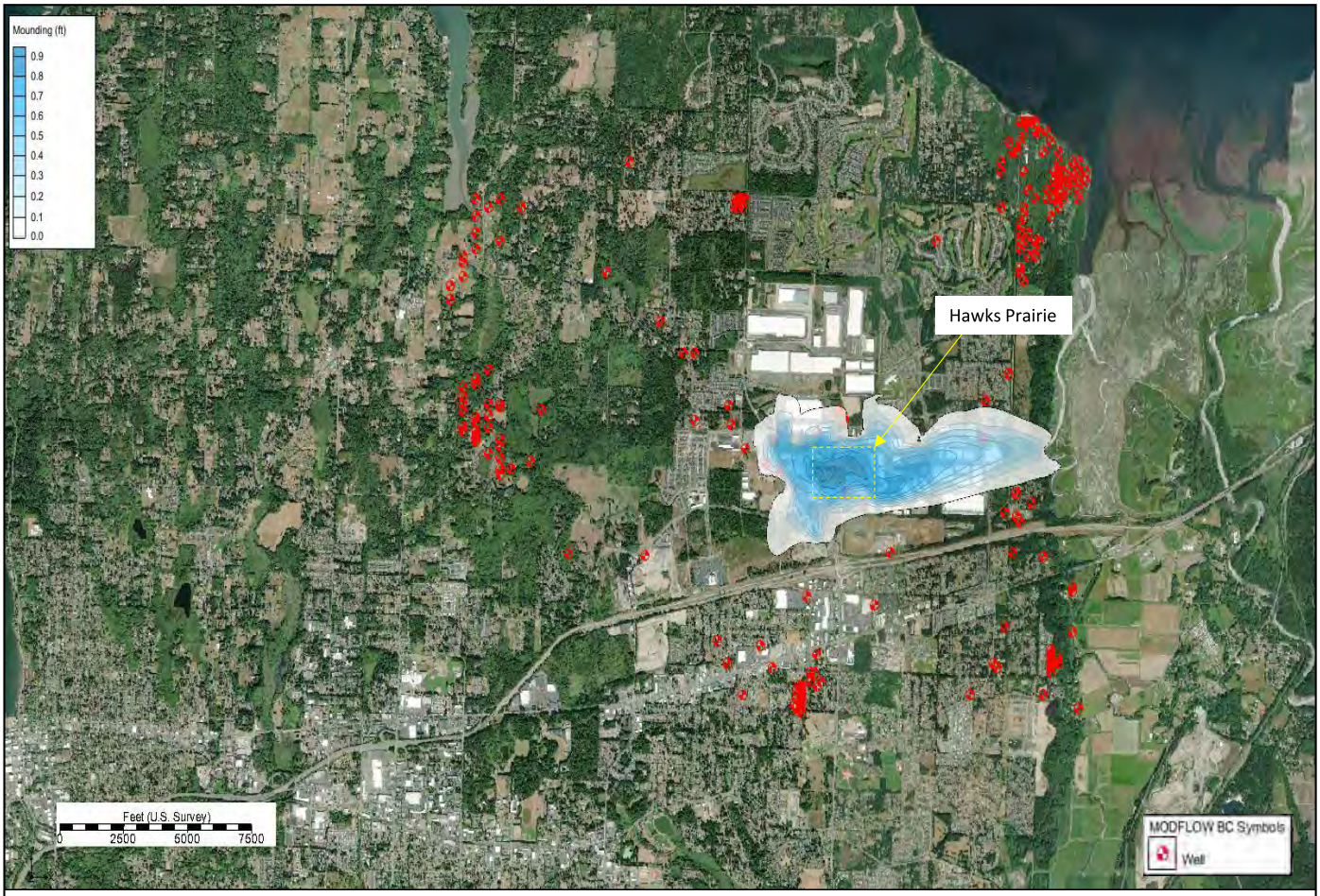

Figure E-14 Q_c C/C_0 2022

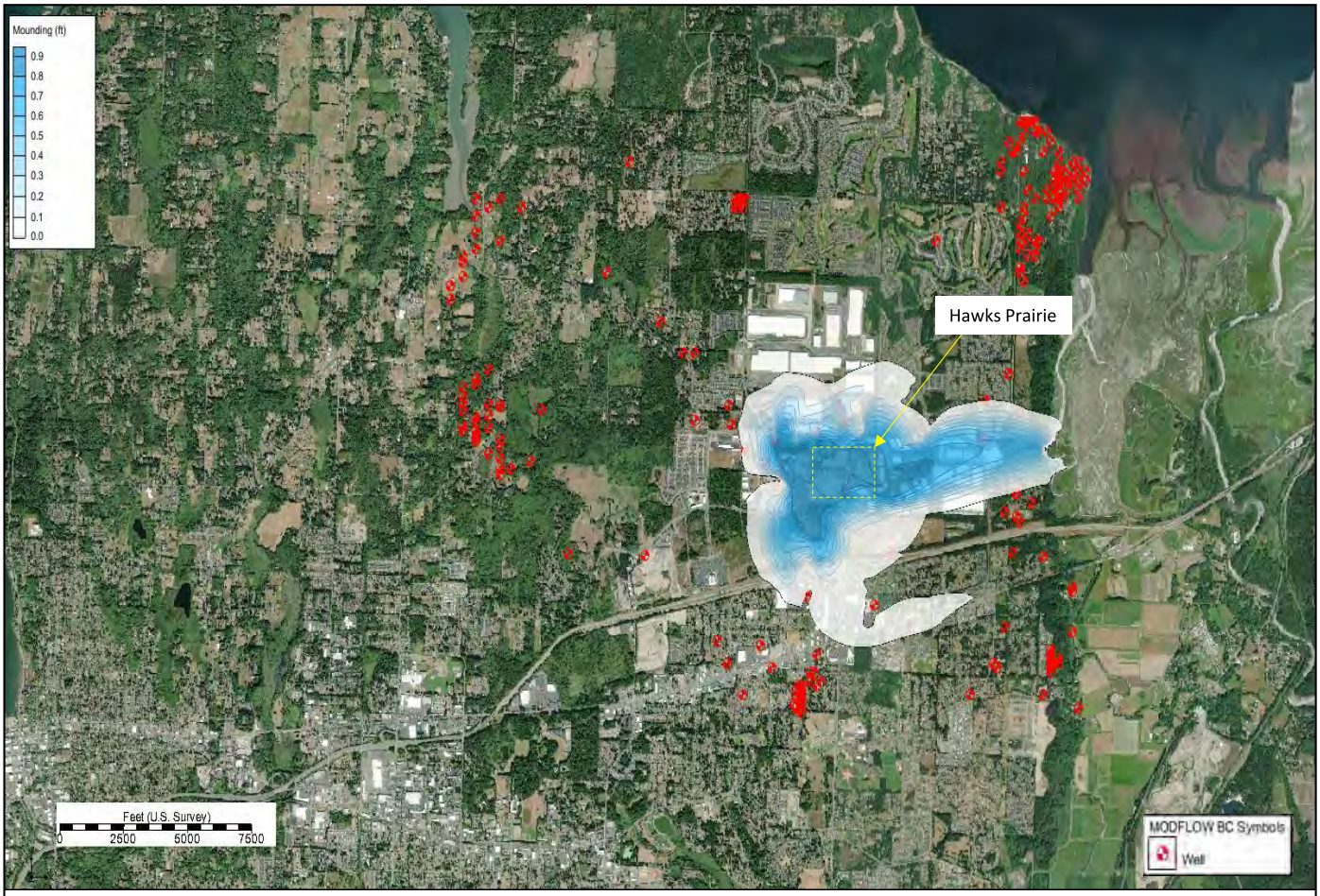

Figure E-15 Q_c C/C_0 2032

Figure E-16 Q_c C/C_0 2038

Figure E-17 Q_c C/C_0 2042

Figure E-18 Q_c C/C_0 2049

Figure E-19 Q_c C/C_0 2059

Figure E-20 Q_c C/C_0 2067

Figure E-21 Q_c C/C_0 2070

Figure E-22 Q_c C/C_0 2080

Figure E-23 Q_c C/C_0 2090

Figure E-24 Q_c C/C_0 2100

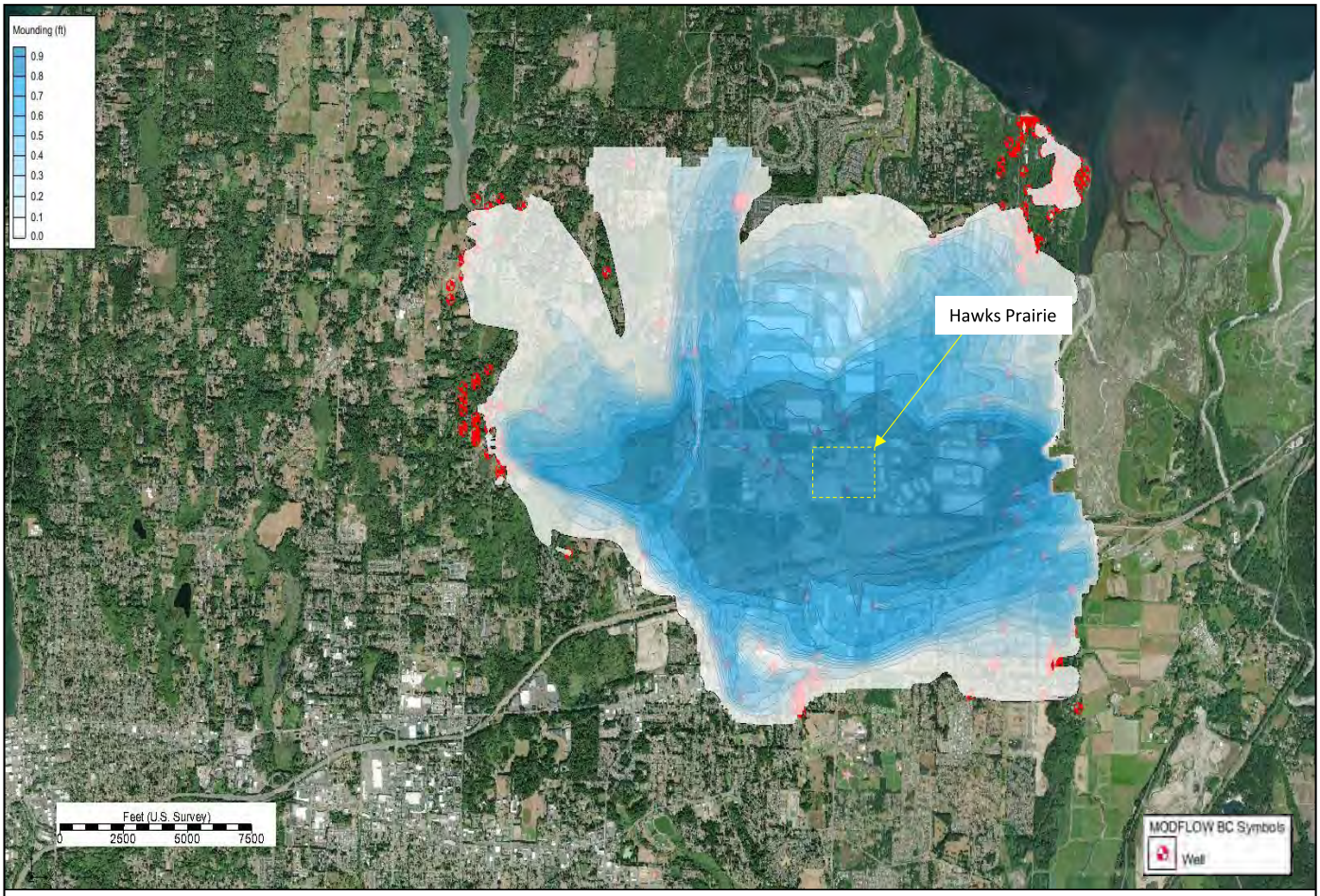

Figure E-25 Q_c C/C_0 2110

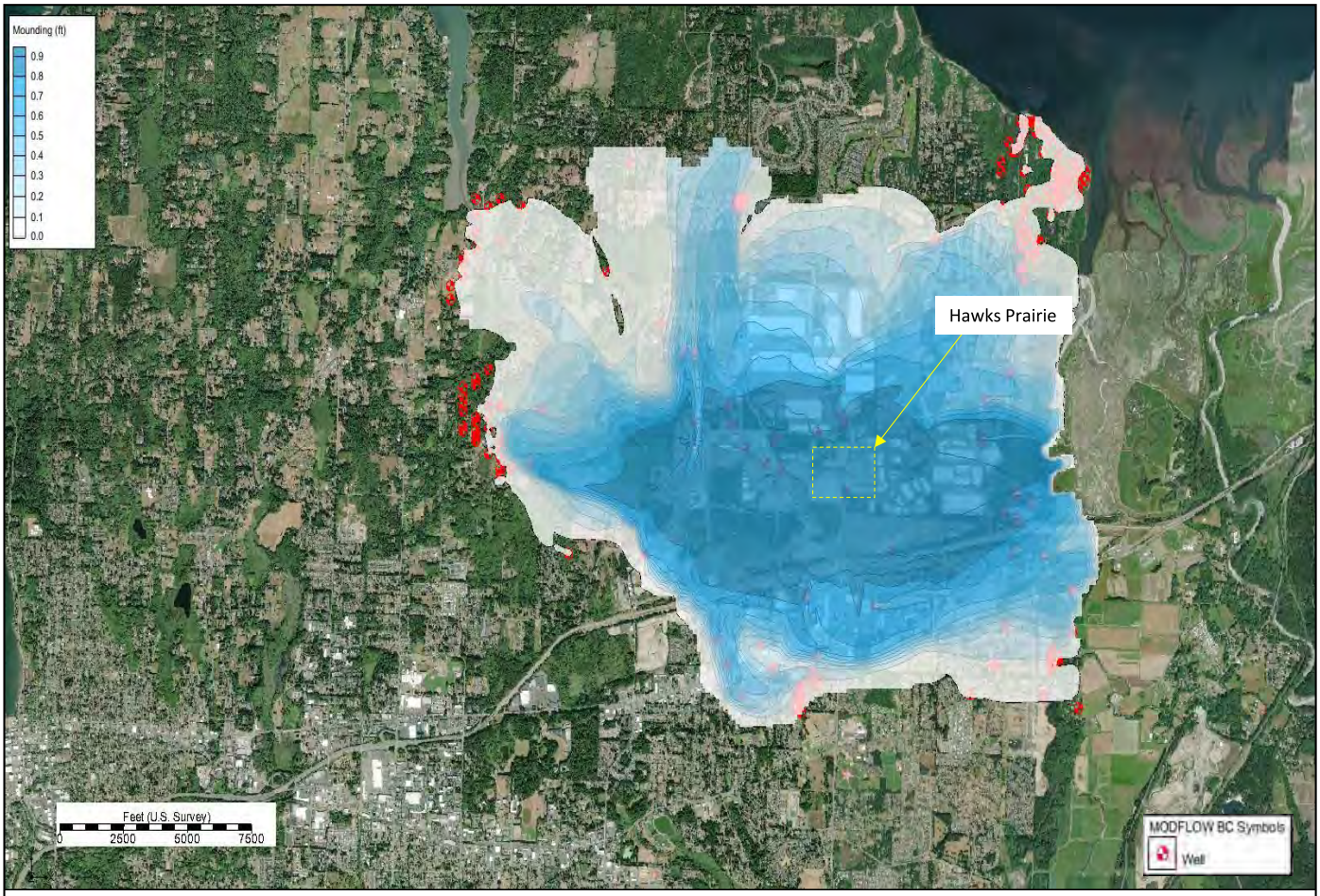

Figure E-26 Q_c C/C_0 2120

Appendix F: Attenuation Factor Data

This page intentionally left blank.

Summary of Attenuation Factor Calculation Data

				Data from Tracer Test (2018)							
				[C], ng/L unless otherwise noted				Model vs Observed Concentrations			All charts displayed as Fraction of C/Co Attenuated vs Travel Time (days)
	Aquifer	Travel Time[4] (days)	Lateral Distance from Basins	Observed [C] Q1	Q2	Q3	Q4	Model Predicted	Observed	1-(Observed/ Predicted)	(Attenuation Factor is slope of trend line. Y intercept is set at 0.)
1,4-Dioxane											
MRL: 0.07						Average RW:	**0.70**				
ug/L Reclaimed Water[2]	-	0	0	0.63	0.69	0.79	0.70	1	1		
MW-5	Qva	19	271	0.49	--	0.69	0.61	0.688	0.597	0.133	
MW-3a	Qva	27	183	0.44	0.61	0.67	0.55	0.698	0.568	0.187	
MW-9	Qva	27	564	0.39	--	0.49	0.49	0.681	0.457	0.330	
MW-8	Qva	30	692	0.4	--	0.59	0.61	0.613	0.533	0.130	
MW-27	Qva	32	838	0.26	--	0.29	0.3	0.674	0.283	0.580	
MW-16	Qva	37	-154	0.32	0.47	0.49	0.57	0.696	0.463	0.335	
MW-15	Qva	83	-119	0.43	--	--	--	0.702	0.430	0.387	
MW-25	Qva	111	1231	0.035	--	0.035	0.035	0.598	0.035	0.941	
MW-11	Qva	177	1208	0.32	--	--	--				
MW-28	Qva	987	1992	--	--	0.035	0.035				
MW-20	Qva	1316	1659	0.035	--	0.035	0.035				
Acesulfame-K											
MRL: 100						Average RW:	258				
Reclaimed Water[2]	-	0	0	440	240	165	185				
MW-5	Qva	19	271	100	110	50	250	251.86	127.50	0.49	
MW-3a	Qva	27	183	300	160	200	160	255.71	205.00	0.20	
MW-9	Qva	27	564	320	50	180	170	249.51	180.00	0.28	
MW-8	Qva	30	692	340	340	60	200	224.37	235.00	-0.05	
MW-27	Qva	32	838	290	380	170	180	246.72	255.00	-0.03	
MW-16	Qva	37	-154	50	260	280	210	254.73	200.00	0.21	
MW-15	Qva	83	-119	50	--	--	--	257.00	50.00	0.81	
MW-25	Qva	111	1231	50	71	49	64	218.95	58.50	0.73	
MW-11	Qva	177	1208	330	--	--	--				
MW-28	Qva	987	1992	--	47	50	50				
MW-20	Qva	1316	1659	37	50	50	50				
Carbamazepine											
MRL: 5						Average RW:	430				
Reclaimed Water[2]	-	0	0	145	297	570	710	Q4 only			
MW-5	Qva	19	271	350	640	760	680	694.44	680.00	0.02	
MW-3a	Qva	27	183	340	500	690	520	705.05	520.00	0.26	
MW-9	Qva	27	564	260	--	410	410	687.96	410.00	0.40	
MW-8	Qva	30	692	330	450	500	510	618.66	510.00	0.18	
MW-27	Qva	32	838	110	--	220	220	680.28	220.00	0.68	
MW-16	Qva	37	-154	210	270	360	450	702.37	450.00	0.36	
MW-15	Qva	83	-119	380	--	--	--				
MW-25	Qva	111	1231	2.5	2.5	2.5	2.5	603.71	4.12	0.99	
MW-11	Qva	177	1208	37	--	--	--				
MW-28	Qva	987	1992	--	2.5	2.5	7				
MW-20	Qva	1316	1659	2.5	2.5	2.5	2.5				
Primidone											
MRL: 5	*10*					Average RW:	346				
Reclaimed Water[2]	-	0	0	150	243	487	503				
MW-5	Qva	19	271	120	--	100	30	338.17	83.33	0.75	
MW-3a	Qva	27	183	72	52	120	68	343.34	78.00	0.77	
MW-9	Qva	27	564	90	--	79	48	335.02	72.33	0.78	
MW-8	Qva	30	692	65	--	80	67	301.27	70.67	0.77	
MW-27	Qva	32	838	48	--	24	--	342.04	36.00	0.89	
MW-16	Qva	37	-154	51	--	46	74	342.04	57.00	0.83	
MW-15	Qva	83	-119	44	--	--	--	345.07	44.00	0.87	
MW-25	Qva	111	1231	2.5	2.5	2.5	2.5	293.99	2.50	0.99	
MW-11	Qva	177	1208	49	--	--	--				
MW-28	Qva	987	1992	--	2.5	2.5	2.5				
MW-20	Qva	1316	1659	2.5	2.5	2.5	2.5				
Quinoline											
MRL: 5						Average RW:	9				
Reclaimed Water[2]	-	0	0	6	2.5	2.5	13	Only using Q4 data/RW			
MW-5	Qva	19	271	2.5	2.5	2.5	2.5	12.72	3.47	0.73	
MW-3a	Qva	27	183	2.5	2.5	2.5	2.5	12.91	3.47	0.73	
MW-9	Qva	27	564	2.5	2.5	2.5	12	12.60	12.00	0.05	
MW-8	Qva	30	692	2.5	2.5	2.5	8.2	11.33	8.20	0.28	
MW-27	Qva	32	838	2.5	2.5	2.5	2.5	12.86	3.47	0.73	
MW-16	Qva	37	-154	7.6	2.5	2.5	17	12.86	17.00	-0.32	
MW-15	Qva	83	-119	2.5	--	--	--				
MW-25	Qva	111	1231	2.5	2.5	2.5	17	11.05	17.00	-0.54	
MW-11	Qva	177	1208	2.5	--	--	--				
MW-28	Qva	987	1992	--	2.5	2.5	2.5				
MW-20	Qva	1316	1659	2.5	2.5	2.5	19				
Sucralose											
MRL: 100						Average RW:	55,867				
Reclaimed Water[2]	-	0	0	45,333	16,800	75,000	86,333				
MW-5	Qva	19	271	32,000	14,000	74,000	82,000	54642.39	50500.00	0.08	
MW-3a	Qva	27	183	40,000	16,000	69,000	61,000	55477.44	46500.00	0.16	
MW-9	Qva	27	564	24,000	38,000	49,000	54,000	54132.12	41250.00	0.24	
MW-8	Qva	30	692	31,000	21,000	61,000	72,000	48679.82	46250.00	0.05	
MW-27	Qva	32	838	22,000	15,000	27,000	32,000	55266.55	24000.00	0.57	
MW-16	Qva	37	-154	31,000	22,000	43,000	68,000	55266.55	41000.00	0.26	
MW-15	Qva	83	-119	33,000	--	--	--	55757.53	33000.00	0.41	
MW-25	Qva	111	1231	3,400	4,900	5,000	5,000	47503.53	4575.00	0.90	
MW-11	Qva	177	1208	14,000	--	--	--				
MW-28	Qva	987	1992	--	50	50	50				
MW-20	Qva	1316	1659	50	50	50	50				

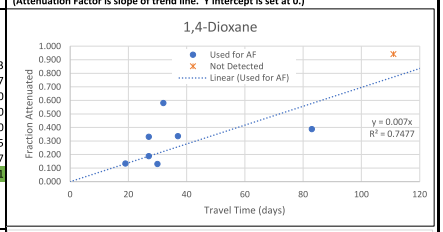

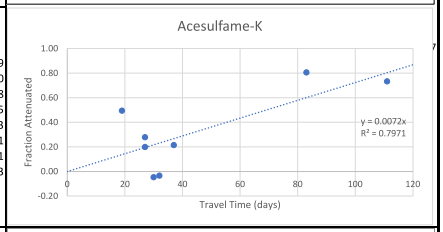

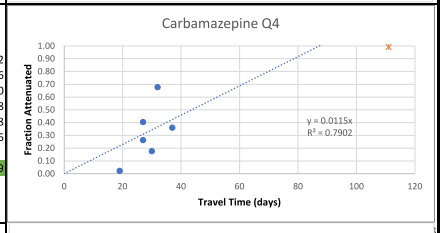

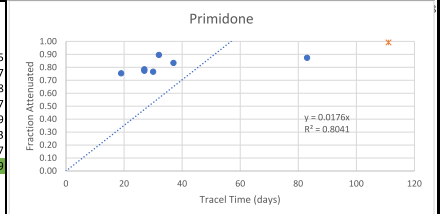

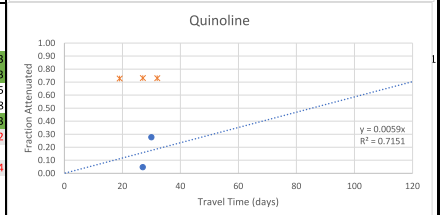

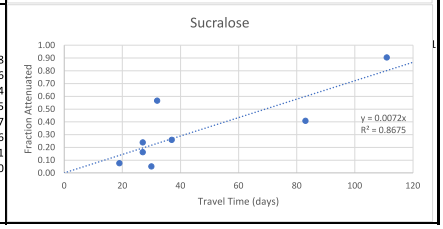

TDCPP										
MRL: 100						**Average RW:**	654	using Q1 RW value		
Reclaimed Water[2]	-	0	0	1,667	207	273	470			
MW-5	Qva	19	271	380	50	50	120	1630.14	380.00	0.77
MW-3a	Qva	27	183	260	50	110	50	1655.05	260.00	0.84
MW-9	Qva	27	564	140	50	50	50	1614.92	140.00	0.91
MW-8	Qva	30	692	280	50	50	50	1452.26	280.00	0.81
MW-27	Qva	32	838	50	50	50	50	1648.76	127.39	0.92
MW-16	Qva	37	-154	50	50	50	50	1648.76	127.39	0.92
MW-15	Qva	83	-119	50	--	--	--	1663.41	127.39	0.92
MW-25	Qva	111	1231	50	50	50	50	1417.17	127.39	0.91
MW-11	Qva	177	1208	50	--	--	--			
MW-28	Qva	987	1992	--	50	50	50			
MW-20	Qva	1316	1659	50	50	50	50			
Triclosan										
MRL: 10						**Average RW:**	66			
Reclaimed Water[2]	-	0	0	5	11	97	92			
MW-5	Qva	19	271	--	57	43	--	64.99	50.00	0.23
MW-3a	Qva	27	183	--	--	--	--			
MW-9	Qva	27	564	--	--	--	--			
MW-8	Qva	30	692	--	--	11	--	57.90	11.00	0.81
MW-27	Qva	32	838	12	--	--	--	65.73	12.00	0.82
MW-16	Qva	37	-154	5	5	5	5	65.73	5.00	0.92
MW-15	Qva	83	-119	5	--	--	--	66.31	5.00	0.92
MW-25	Qva	111	1231	5	5	5	5	56.50	5.00	0.91
MW-11	Qva	177	1208	5	--	--	--			
MW-28	Qva	987	1992	--	5	5	5			
MW-20	Qva	1316	1659	12	5	5	5			
TCEP										
MRL: 10						**Average RW:**	133			
Reclaimed Water[2]	-	0	0	94	125	97	215			
MW-5	Qva	19	271	170	170	130	120	129.84	29.93	0.77
MW-3a	Qva	27	183	5	120	5	100	131.83	11.67	0.91
MW-9	Qva	27	564	5	5	96	76	128.63	9.23	0.93
MW-8	Qva	30	692	5	130	88	98	115.67	16.29	0.86
MW-27	Qva	32	838	5	48	22	22	131.32	4.92	0.96
MW-16	Qva	37	-154	22	35	20	67	131.32	7.31	0.94
MW-15	Qva	83	-119	200	--	--	--	132.49	40.59	0.69
MW-25	Qva	111	1231	5	5	5	5			
MW-11	Qva	177	1208	5	--	--	--			
MW-28	Qva	987	1992	--	5	5	5			
MW-20	Qva	1316	1659	5	5	5	5			

Showing ND as MRL
ND, showing as 1/2 MRL
ND during TT, travel time inferred from transient MT3D model run

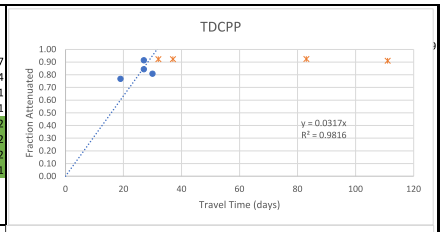

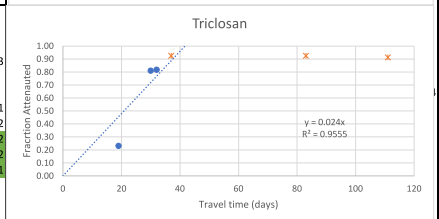

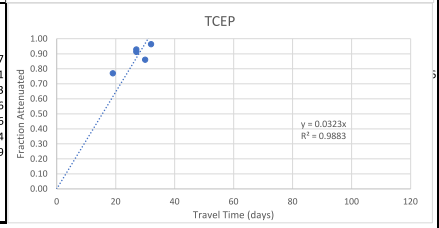

Appendix G: Sensitivity Analysis Results

This page intentionally left blank.

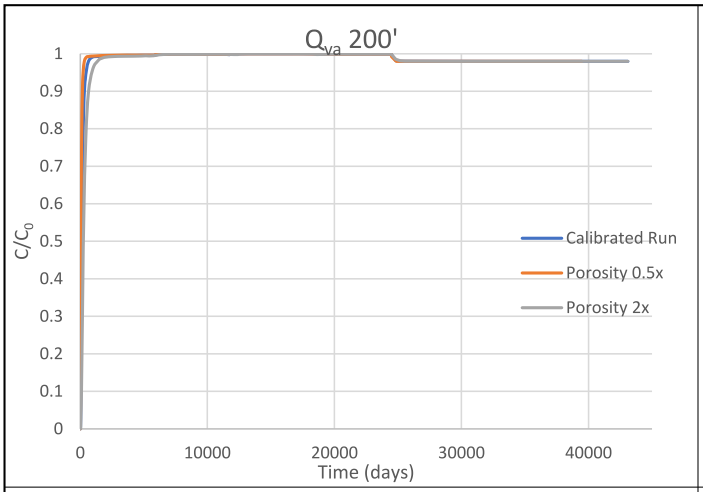

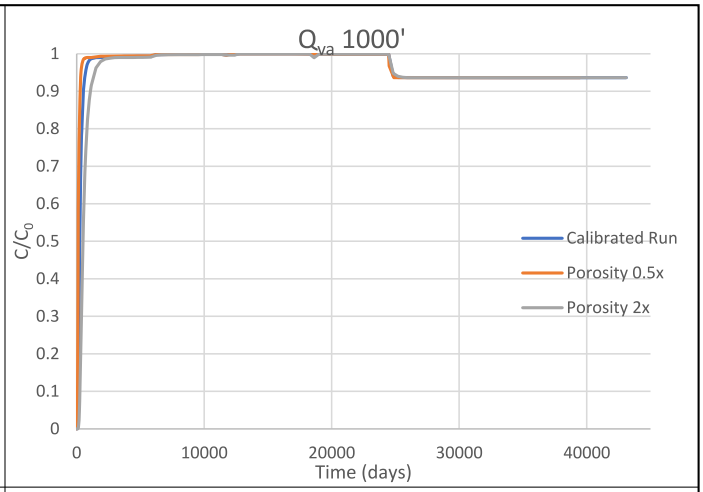

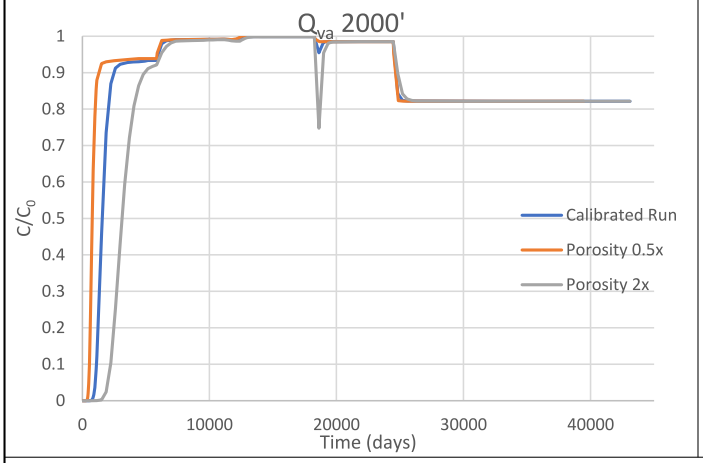

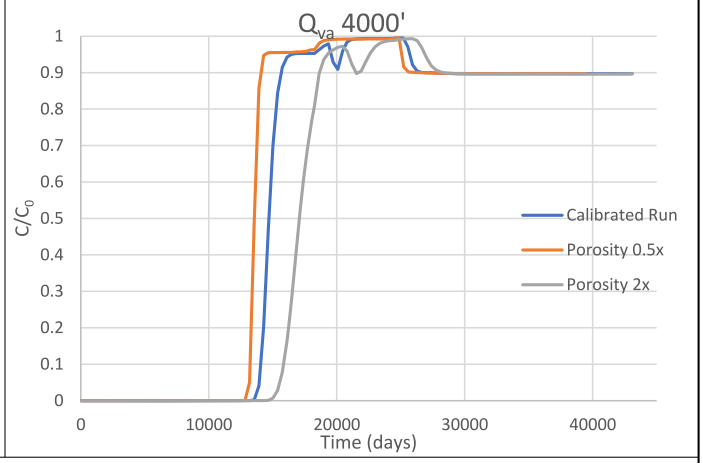

Figure G-1a: Porosity Sensitivity Analysis Q_{va}

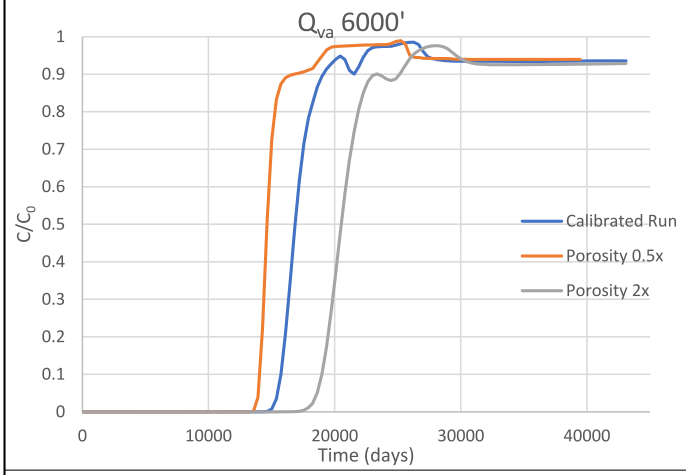

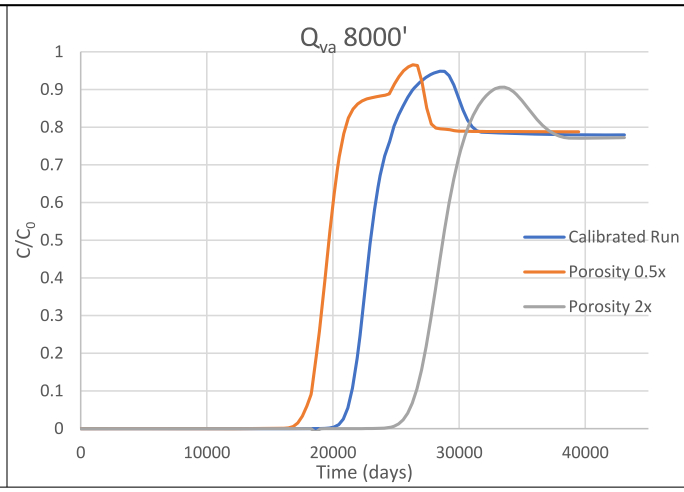

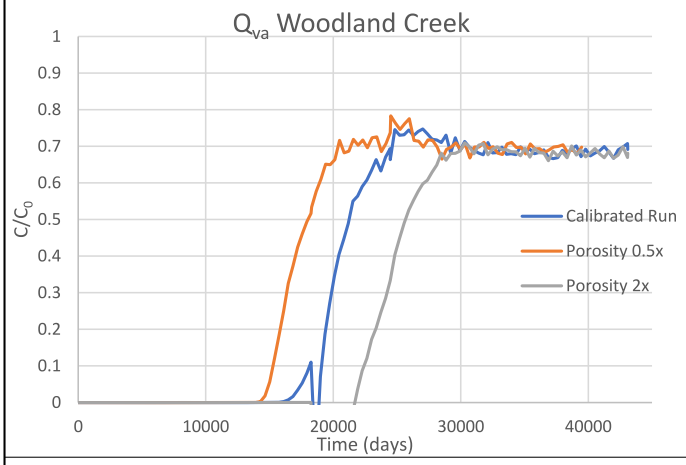

Figure G-1b: Porosity Sensitivity Analysis Q_{va}

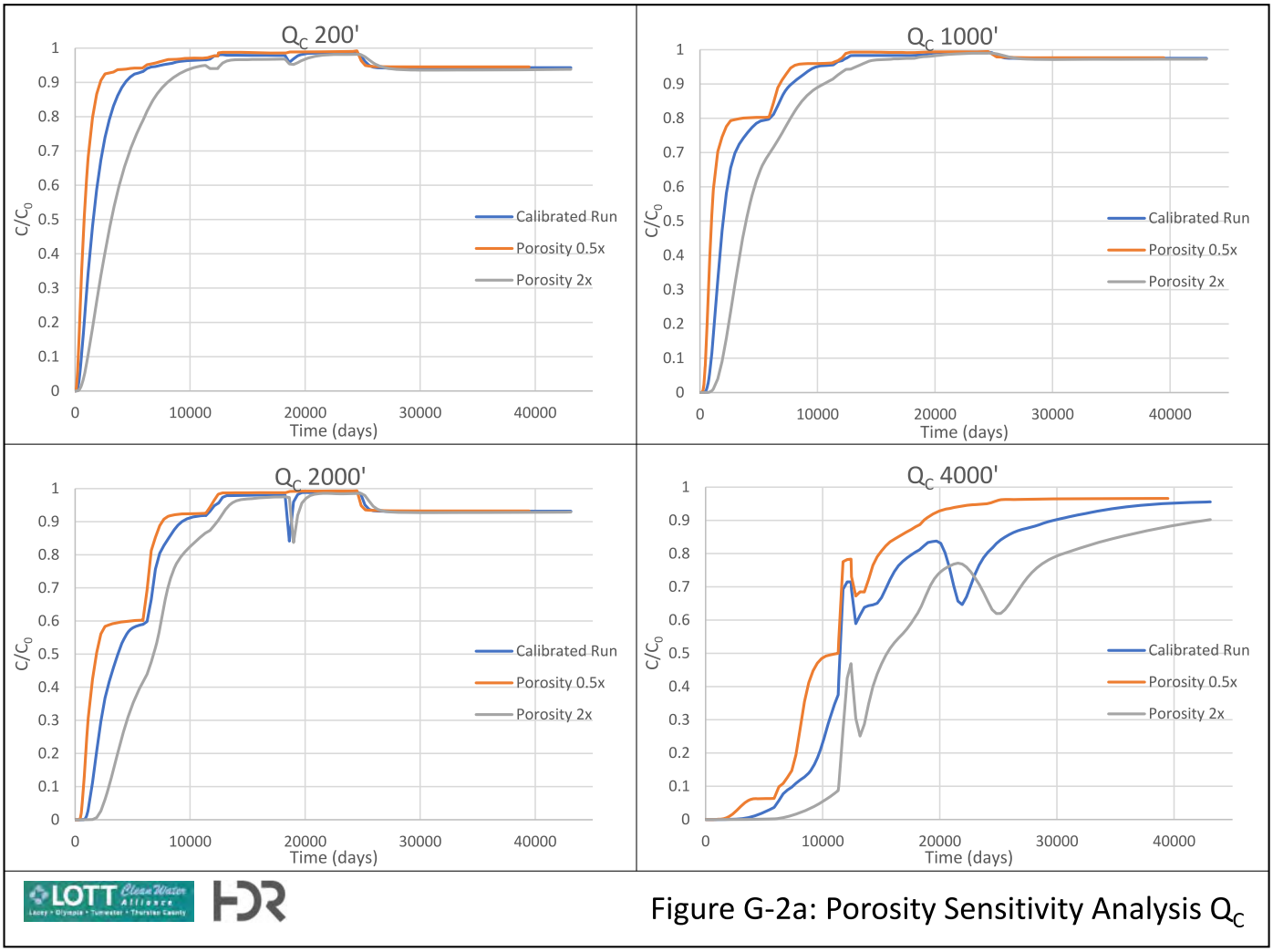

Figure G-2a: Porosity Sensitivity Analysis Q_C

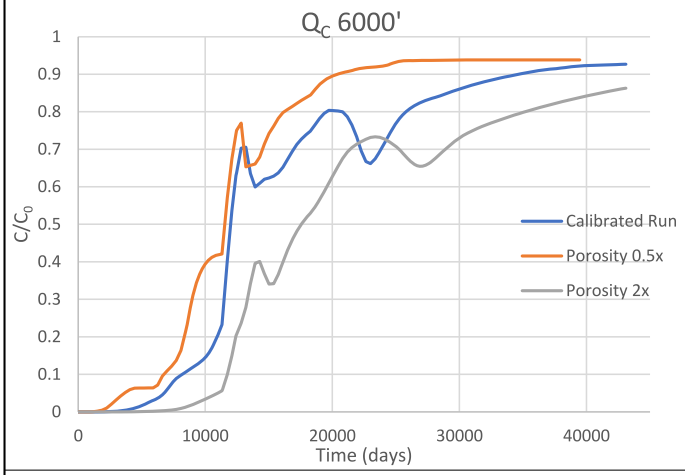

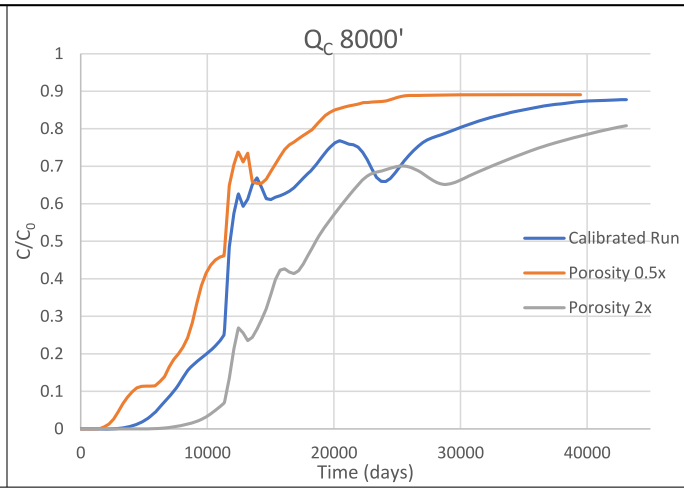

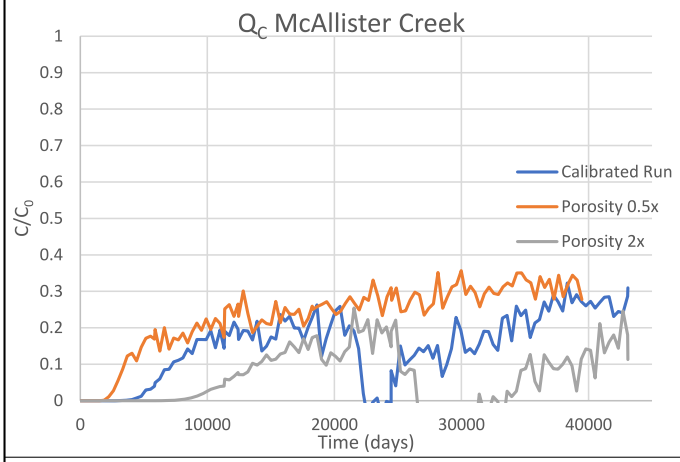

Figure G-2b: Porosity Sensitivity Analysis Q_C

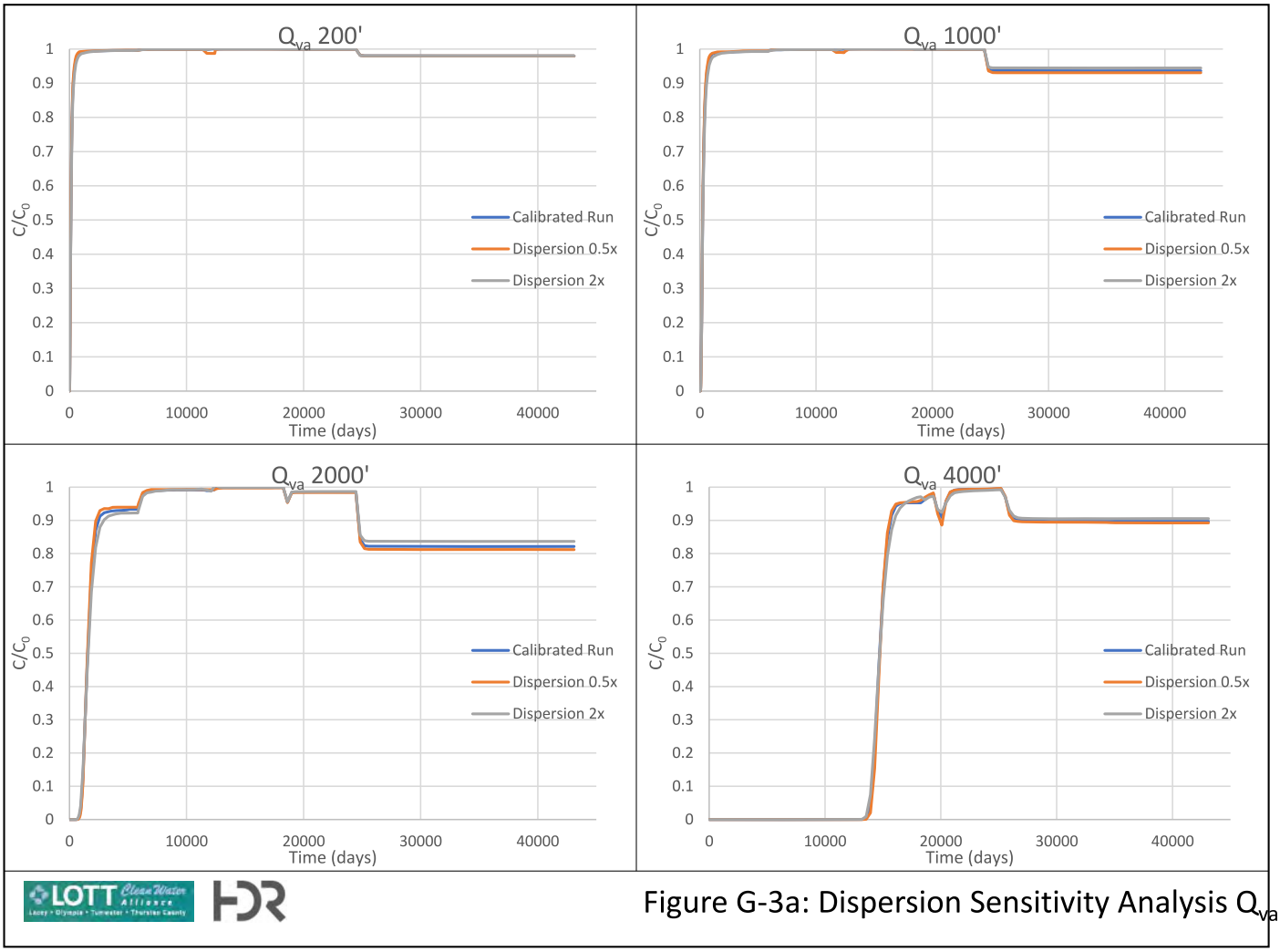

Figure G-3a: Dispersion Sensitivity Analysis Q_{va}

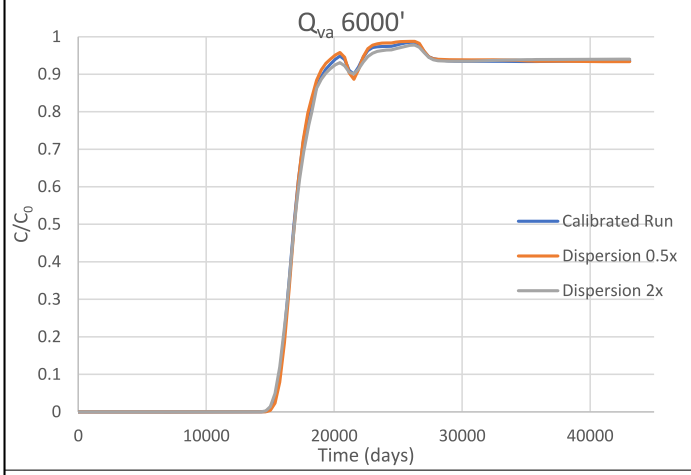

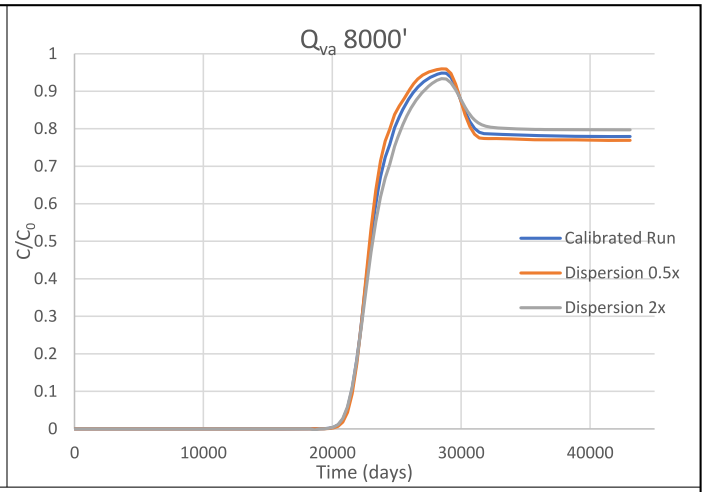

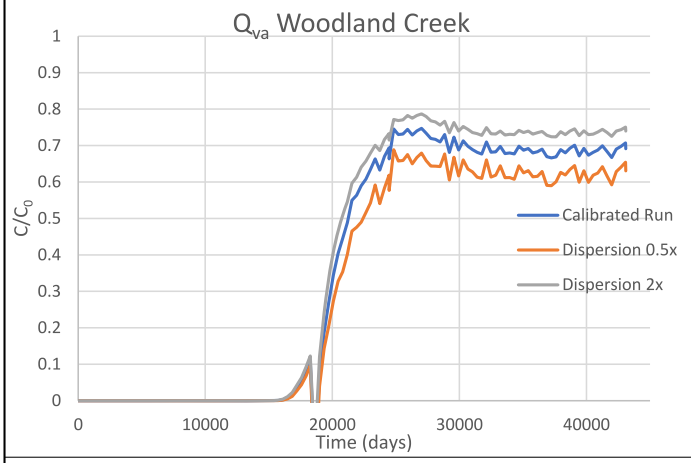

Figure G-3b: Dispersion Sensitivity Analysis Q_{va}

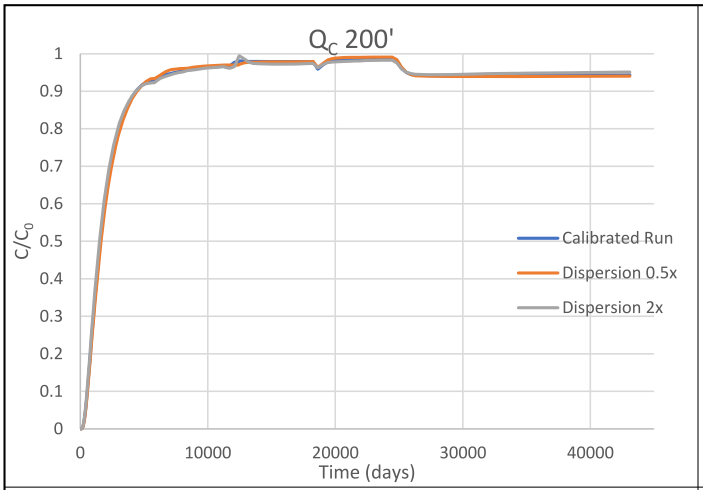

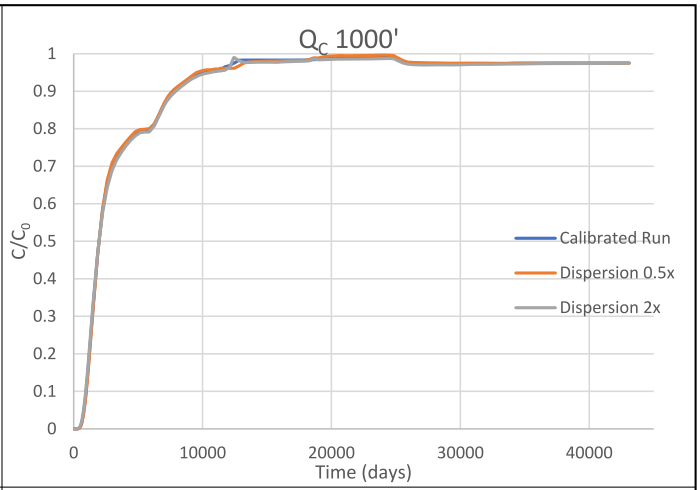

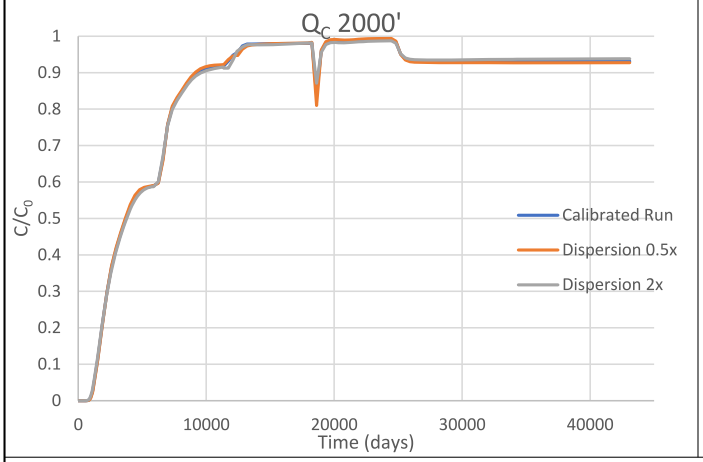

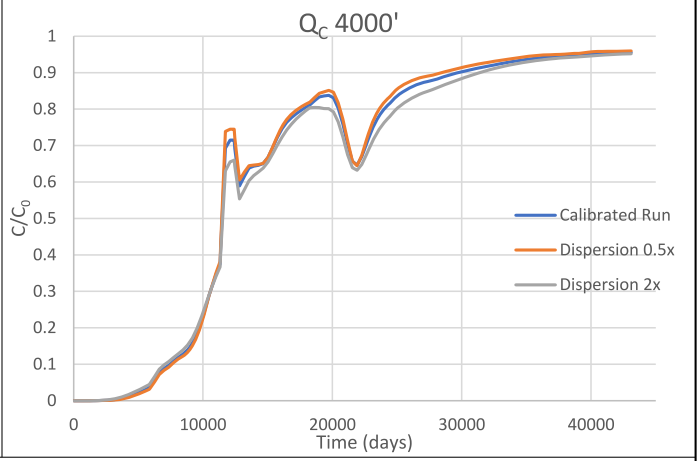

Figure G-4a: Dispersion Sensitivity Analysis Q_C

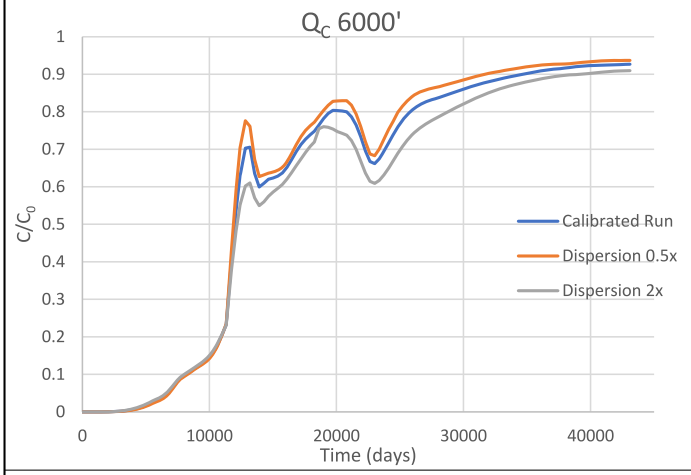

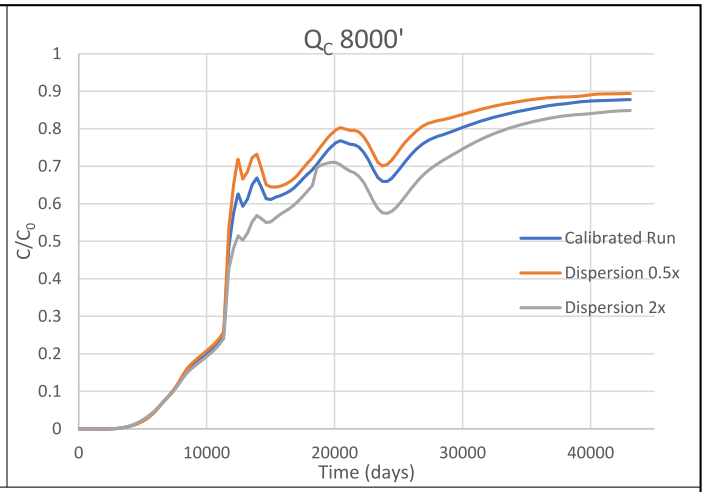

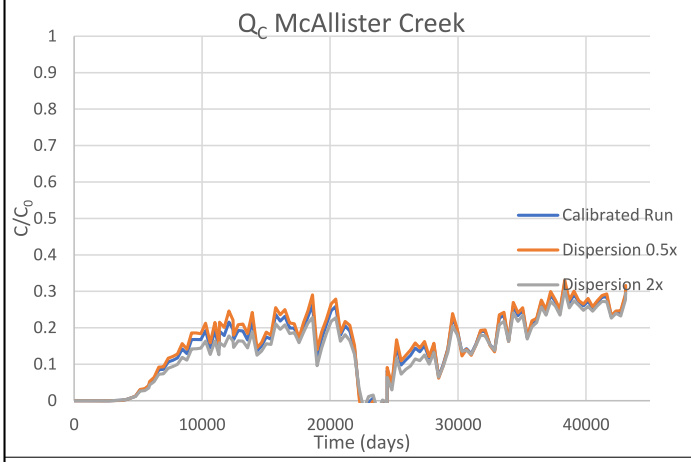

Figure G-4b: Dispersion Sensitivity Analysis Q_C

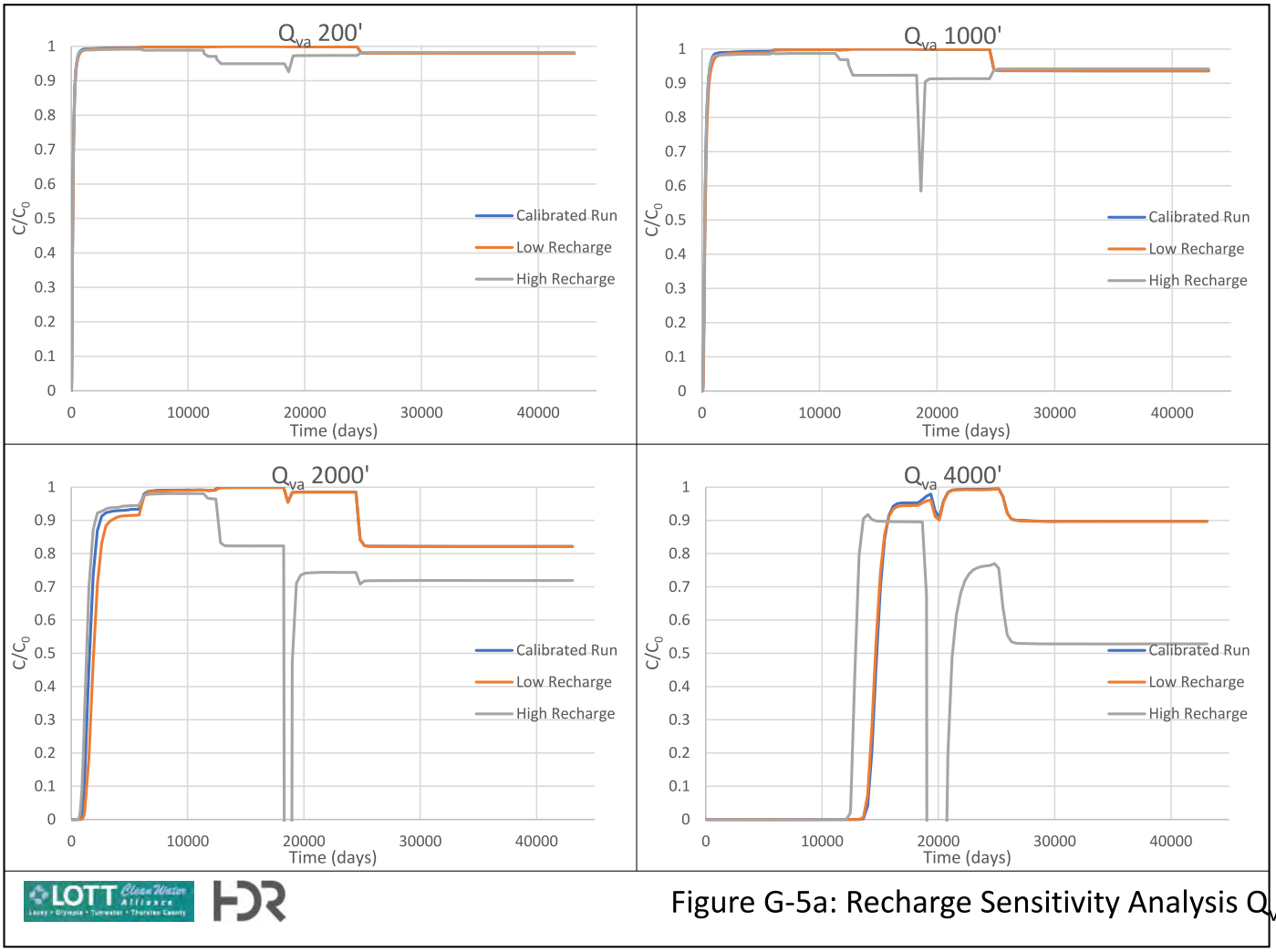

Figure G-5a: Recharge Sensitivity Analysis Q_{va}

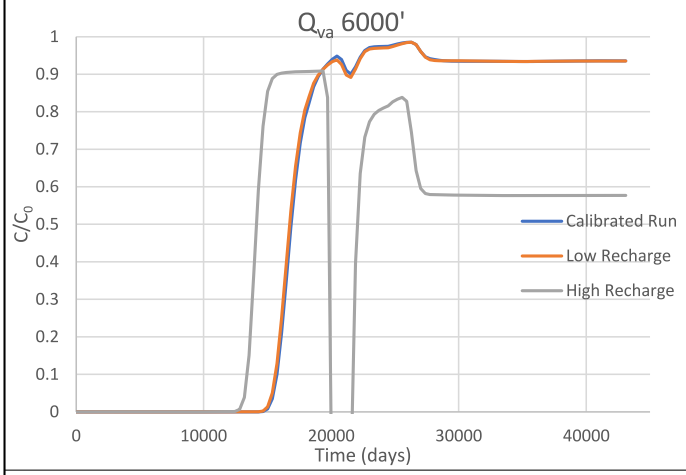

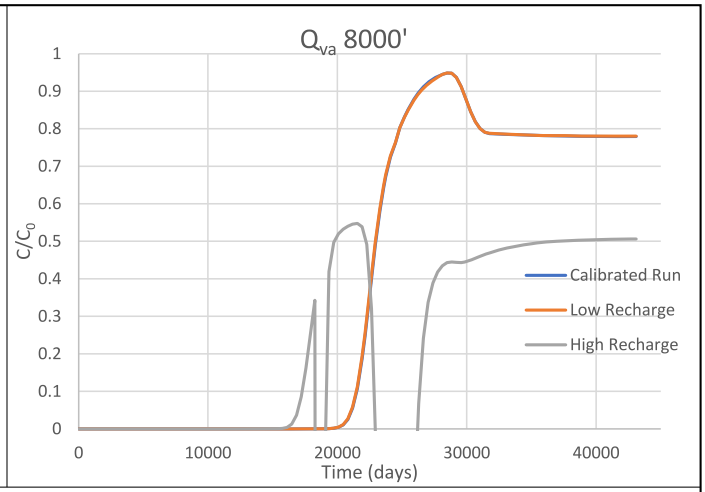

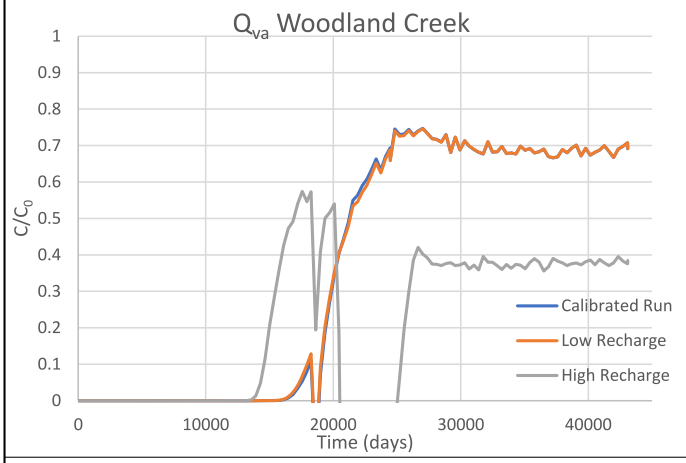

Figure G-5b: Recharge Sensitivity Analysis Q_{va}

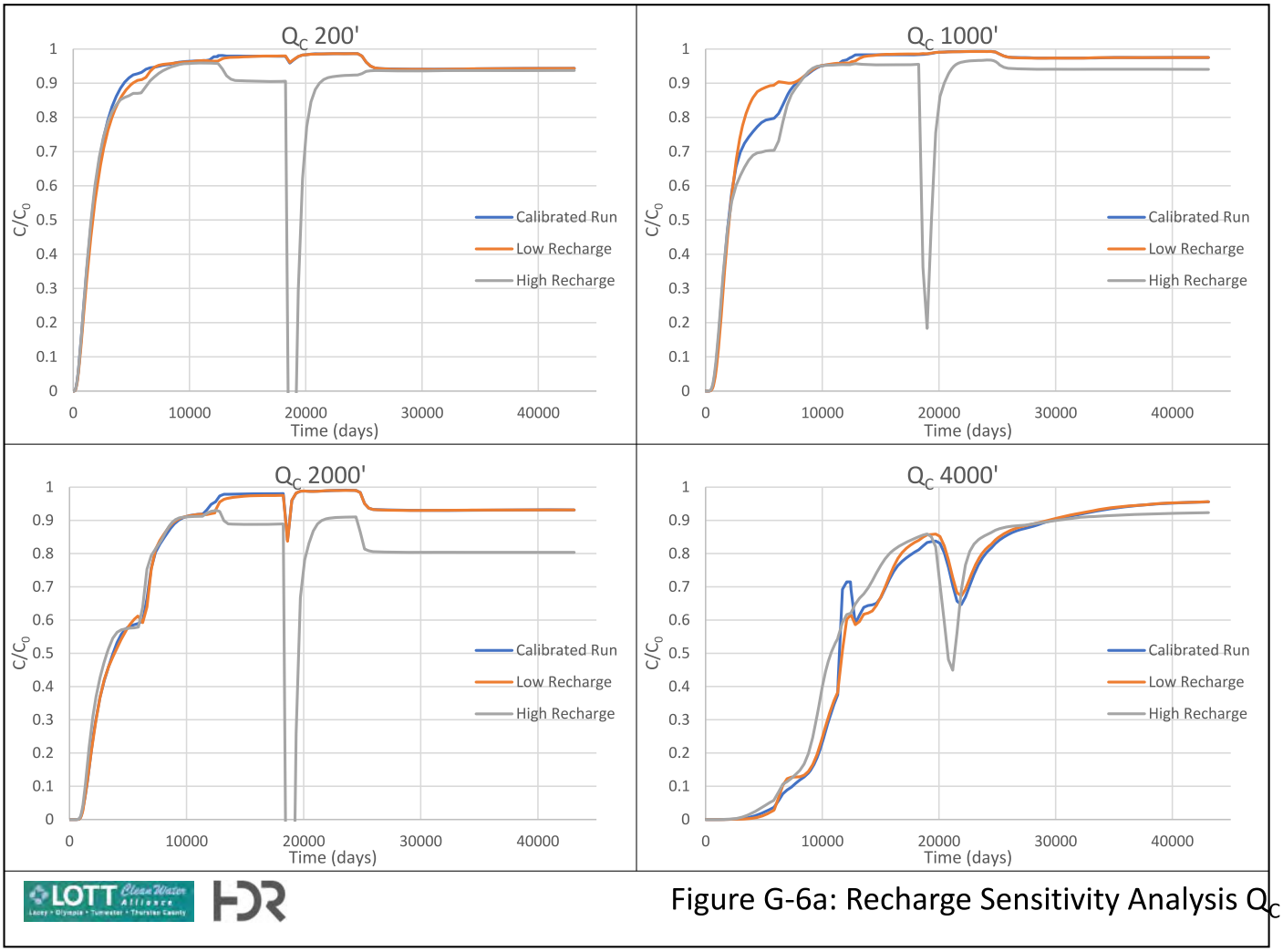

Figure G-6a: Recharge Sensitivity Analysis Q_C

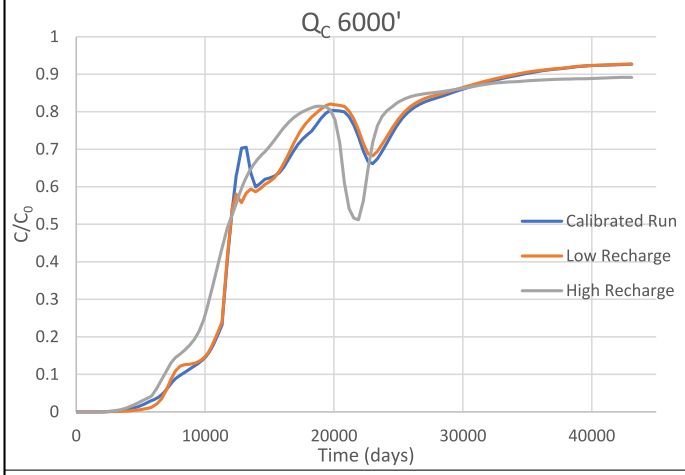

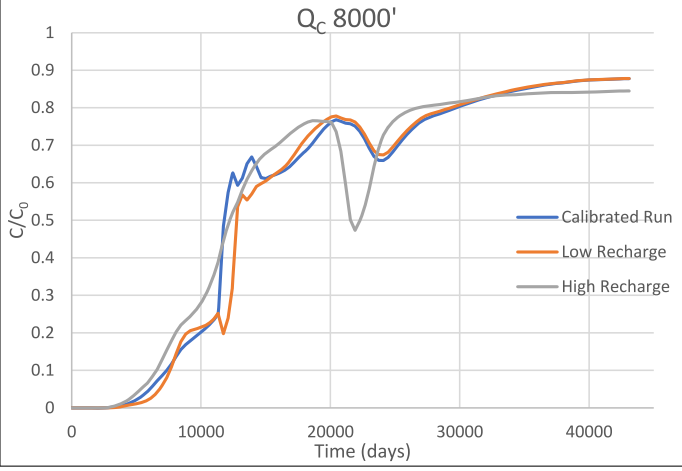

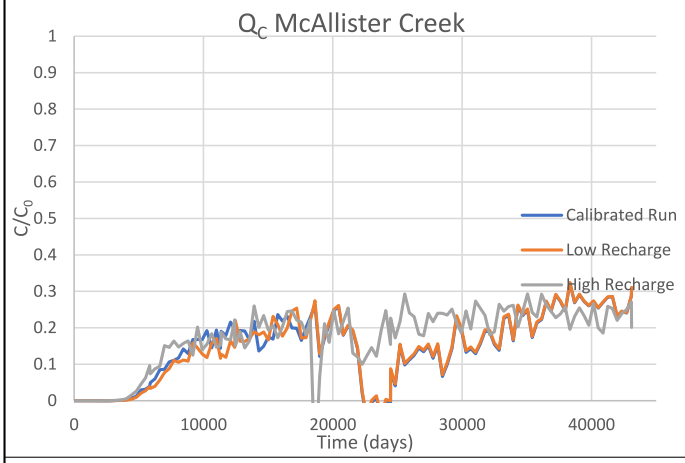

Figure G-6b: Recharge Sensitivity Analysis Q_C